JUL 30 1946

THE JOURNAL OF CHEMICAL PHYSICS

Volume 14 Number 7

JULY, 1946

Published by the

AMERICAN INSTITUTE OF PHYSICS

Lancaster, Pa. and New York, N. Y.

CHEMICAL PHYSICS

EDITORS

Editor

Editors

Terms ending December 31, 1947

CROSS

O M. FUOSS

KIRKWOOD

BERG

RICE

Terms ending December 31, 1948

CHARLES D. CORYELL

F. O. RICE

L. H. THOMAS

G. W. WHELAND

E. BRIGHT WILSON, JR.

CHEMICAL PHYSICS is published
Institute of Physics

...exponents. The solidus (/) should be used wherever possible for fractions.

All illustrations should accompany manuscript and should always be referred to in the text. Line drawings should be made with India ink on plain white paper or on tracing cloth. Coordinate paper is not desirable, but if used must be blue-lined with all coordinates to be reproduced drawn with India ink. Lettering should be of sufficient size to be legible after reduction.

Proof and all correspondence concerning papers in the process of publication should be addressed to the Publications Manager, American Institute of Physics, 57 East 55 Street, New York 22, New York.

Subscription Rates

The United States and Possessions, Canada and Mexico $10.00

Elsewhere 11.00

Back Numbers

Complete set: Vol. 1, 1933–Vol. 13, 1945 ..... $130.00

Yearly rate: $11.00

Single copies: $1.00 each.

Subscriptions and orders for single copies should be addressed to Prince and Lemon Streets, Lancaster, Pennsylvania, or to the American Institute of Physics, 57 East 55 Street, New York 22, New York.

Changes of address should be sent to the Business Manager, American Institute of Physics

...Prince and Lemon Streets, Lancaster, Pennsylvania.

...at Lancaster, Pa., under the Act of August 24, 1912. Acceptance for ..., 1923, embodied in paragraph 4, Section 538, P. L. & R.; authorized

THE JOURNAL
OF
CHEMICAL PHYSICS

VOLUME 14, NUMBER 7 JULY, 1946

Efficiency of the Electrolytic Separation of Potassium Isotopes

DWIGHT A. HUTCHISON*
Georgia School of Technology, Atlanta, Georgia
(Received May 1, 1946)

The electrolytic separation coefficient, α, has been determined for the potassium isotope separation in the electrolysis of aqueous solutions of potassium chloride at a flowing mercury cathode. Suspension of purified potassium chloride crystals in a liquid mixture of bromoform, *n*-pentanol, and *n*-hexanol served as the analytical procedure in determining the isotopic composition of samples. Densities of the liquid suspension mixture as a function of temperature were independently determined. The electrolytic separation factor for the potassium isotopes was found to be 1.0054 ± 0.0005 for the temperature range of 15°–50°C, and, within the limits of error, was independent of temperature, of the fraction electrolyzed, of the concentration of the electrolytic solution, of the current density, and of the amount of back reaction at the cathode. An empirical relation between the electrolytic separation factors of elements thus far investigated and their atomic weights is presented.

I. INTRODUCTION

THE electrolytic separation of isotopes other than those of hydrogen has received comparatively little attention. Washburn[1] showed that oxygen isotopes were noticeably separated by electrolysis and Johnston[2] determined the electrolytic separation factor, α, for O^{16} relative to O^{18} to be 1.008 ± 0.003 for the electrolysis of aqueous alkaline solutions between iron electrodes using a densimetric method of analysis.

Eucken and Bratzler[3] were the first to investigate the electrolytic separation of lithium isotopes and were able to set 1.07 as an upper limit for α in the electrolysis of aqueous lithium sulfate at a mercury cathode. Taylor and Urey[4] electrolyzed aqueous lithium hydroxide at a mercury cathode and obtained an α of 1.020 on the basis of mass spectrometer analysis by Brewer. Holleck[5] electrolyzed aqueous lithium chloride and obtained an α of 1.079 by a chemical atomic weight method of analysis. Taylor and Urey[6] reported an α of 1.039 for the electrolysis of aqueous lithium chloride. Employing a densimetric method of determining relative atomic weights, Johnston and C. A. Hutchison[7] obtained an α of 1.055 ± 0.005 for the electrolysis of aqueous and alcoholic solutions of lithium chloride at a mercury cathode. They were able to show, within their limits of observation, that the

* Research Associate, State Engineering Experiment Station, Georgia School of Technology, Atlanta, Georgia.
[1] E. W. Washburn, E. R. Smith, and F. A. Smith, Bur. Stand. J. Research **13**, 599 (1934).
[2] H. L. Johnston, J. Am. Chem. Soc. **57**, 484 (1935).
[3] Eucken and Bratzler, Zeits. f. physik. Chemie **A174**, 269 (1935).
[4] T. I. Taylor and H. C. Urey, J. Chem. Phys. **5**, 597 (1937).
[5] Holleck, Zeits. f. Elektrochemie **44**, 111 (1938).
[6] T. I. Taylor and H. C. Urey, J. Chem. Phys. **6**, 429 (1938).
[7] H. L. Johnston and C. A. Hutchison, J. Chem. Phys. **8**, 869 (1940).

α-value was independent of the cell temperature, the fraction electrolyzed, the amount of back reaction at the cathode, and within a small range, independent of current density.

Johnston and the writer,[8] employing a densimetric method of isotopic analysis, electrolyzed aqueous sodium chloride at a platinum anode and obtained an α of 1.0060 ± 0.0005 for the separation of chlorine isotopes. This work also showed no significant dependence of the α-value on the cell temperature, the fraction electrolyzed, the amount of back reaction at the anode, and the current density in the range of observation. The α-value on Acheson graphite, 1.0068 ± 0.0014, which was computed from the data of Yacouban[9] agrees with our own more precise value. The writer's recent redetermination[10] of the α-value for chlorine, with similar apparatus but by a different procedure, resulted in the value, 1.0063. The linear average of α's obtained from all the chlorine electrolyses gives $\alpha = 1.0061 \pm 0.0005$.

The purpose of the present paper is to report the results of an investigation on the electrolytic separation of potassium isotopes at a mercury cathode and to show the experimental relation between the α-values for the elements thus far investigated and their atomic masses.

II. EXPERIMENTAL DESCRIPTION

A. The Electrolysis

The apparatus used to carry out the electrolyses was similar to that of Eucken and Bratzler[3] and to that of Johnston and C. A. Hutchison.[7] The cell consisted of a four-liter round bottom Pyrex flask to the bottom of which was sealed an extension which supplied a means for a flowing mercury cathode. The cell contained a rubber stopper at its top through which passed a platinum lead to a platinum gauze anode, a thermometer for the measurement of the electrolyte temperature, and glass tubes for passage of gases from the cell which were formed during the electrolyses. These surfaces extending into the cell and the inner wall of the cell were coated with "biolloid" paraffin. The electrolyte employed was an aqueous solution of potassium chloride. The chlorine evolved during the electrolyses was swept from the cell by a stream of nitrogen and absorbed in four traps, two of which contained sodium hydroxide and the remainder, acetone. The nitrogen stream also served to give constant stirring of the electrolyte and yielded what was thought to be a uniform mixture of the solution throughout an electrolysis. The mercury for the flowing cathode was supplied from a reservoir and the rate of flow through the cell was adjusted at values varying from 2.5 to 10 liters per hour for the various electrolyses. The temperature of the cell was regulated by an external water bath. By this means the temperature of the electrolyte could be controlled to within ± 3°C. The amalgam from the electrolyses was drained from the cell into an eight-liter Erlenmeyer flask which was heavily coated with paraffin and treated as described below.

B. Preparation of Reagents

Potassium chloride employed in the electrolyses was prepared by six successive precipitations from aqueous solutions by addition of pure hydrogen chloride.[11] The purification of potassium chloride, which was used in the preparation of standard crystals of normal isotopic composition for use as comparison crystals in the densimetric analyses, was effected by a method similar to that employed by Richards and Wells[12] in their determination of the atomic weight of sodium and chlorine. The beginning material in all cases was Baker's analyzed C.P. potassium chloride. Details of the purification procedure and evidence of its effectiveness have been published elsewhere.[13]

The amalgam formed during electrolysis was placed in eight-liter Erlenmeyer flasks which had been coated with paraffin. Pure hydrochloric acid[14] was added in such quantity that its equivalent concentration was in slight excess of the concentration of the potassium ion to be liberated. Platinum foil was added to promote reaction of the amalgam. The resulting solution was boiled to dryness in a platinum container.

[8] H. L. Johnston and D. A. Hutchison, J. Chem. Phys. **10**, 469 (1942).
[9] K. V. Yacouban, Helv. Chim. Acta. **22**, 808 (1939).
[10] D. A. Hutchison, J. Chem. Phys. **13**, 536 (1945).
[11] See reference 13 for details of purification.
[12] T. W. Richards and R. C. Wells, "A Revision of the Atomic Weights of Sodium and Chlorine," Carnegie Institute of Washington, Publication No. 28 (1905).
[13] D. A. Hutchison, Phys. Rev. **66**, 144 (1944).

The residue was given two fractional crystallizations from water and then fused on platinum to eliminate traces of hydrochloric acid. The salt was then given eight more crystallizations from aqueous solutions. The material from each step of the crystallizations was centrifuged before the succeeding step. The resulting material was used in the preparation of crystals for suspension.[14,15]

The mercury used for the flowing cathode was purified by washing with dilute nitric acid and water, drying with filter paper, and finally by two successive distillations in vacuum. The purification was repeated before using the mercury again.

Water used in all reagent preparations and purification procedures was obtained by double distillation from an aqueous alkaline permanganate solution in a fused quartz still. Various water samples tested had a specific conductivity of approximately 10^{-7} ohm^{-1}.

The suspension liquid used in the densimetric analyses was a mixture of organic liquids similar to that used by H. L. Johnston and C. A. Hutchison.[7] The mixture had the following composition: bromoform, 40.00 ml; *n*-hexanol, 16.94 ml; *n*-pentanol, 16.00 ml. Baker's bromoform (boiling point range, 150°–151°C) U.S.P. IX, was washed with water, dried with calcium chloride, and distilled under vacuum. The middle third of the distillate was collected in a receiver containing a small amount of *n*-hexanol and *n*-pentanol (25 drops of each) which acted as a negative catalyst preventing decomposition. The composition was then adjusted to that of the above suspension liquid by adding drop by drop Eastman practical grade alcohols which had been double distilled. The density of this suspension mixture remained constant within the experimental limits of error ($\pm 5\times10^{-6}$ g/ml) of the density determination during the period of densimetric analyses.

C. The Isotopic Analyses and Fraction Electrolyzed

The isotopic analyses were made in an apparatus similar to that used by Johnston and the writer[8] in their work on the electrolytic separation of chlorine isotopes and that used by Johnston and C. A. Hutchison[7] in their work on the separation of lithium isotopes. Details of the isotopic analyses have previously been outlined for the work on lithium.[7] In order to get reproducible suspension temperatures, it was found necessary to anneal the crystals at a temperature 50° below their melting point for a period of four hours with gradual cooling over a period of four hours and to store them over phosphorus pentoxide under vacuum. With these precautions suspension temperatures of individual crystals were reproducible to better than ±0.002° (equivalent to 3.3×10^{-6} g/ml in the density) except in step IV of electrolysis 12.

The density of the suspension liquid, as a function of temperature, was determined by careful hydrostatic weighings of a 9.4-ml Pyrex glass bob in air, in pure water, and in the suspension medium. The necessary corrections for the buoyancy of the bob in air and the thermal expansion of Pyrex glass were applied. The experimental data and details of the weighing procedure have been described elsewhere.[13]

Eighteen determinations of the density of the suspension medium over an approximate temperature range of 25.0° to 29.3°C yielded a good straight line with a slope of $-1.883\pm0.004\times10^{-3}$ g/ml/degree. Taking into account the thermal coefficient of expansion for potassium chloride,[16] namely, α (cubical) $=113\times10^{-6}$, it is found that one degree in the ΔT of suspension corresponds to 1.659×10^{-3} g/ml in the isothermal density of the potassium chloride. This corresponds to 0.0623 unit in the atomic weight of potassium and to 3.11 percent in the distribution of the potassium isotopes. The determination of the suspension temperatures to within ±0.002°C, which is some better than the limit of reproducibility (actual reproducibility is referred to here, not the probable error of suspension temperatures) thus corresponds to 6.2×10^{-3} percent in the isotopic abundance of the potassium.

The fraction of chemical equivalents of potassium ion electrolyzed was determined by analysis of the residual electrolyte. Samples of the residual electrolyte were boiled to dryness in a

[14] See reference 13 for details of purification.
[15] See footnote 2 of reference 13.

[16] Klemm, Tilk, and Mullenheim, Zeits. f. anorg. allgem. Chemie **176**, 1 (1928).

TABLE I. Data for the separation of K isotopes in the single step electrolyses of aqueous KCL.

Run number	1	2	3	4	5	6	7	8
Average temperature (°C)	35	35	35	50	40	30	30	15
Current density (amp./cm²)	0.139	0.099	0.060	0.099	0.099	0.099	0.099	0.099
Concentration of KCl at beginning (mols/liter soln.)	0.50	0.50	0.50	0.50	0.50	0.50	1.50	0.5
Equivalents of K in starting material	1.48817	1.41512	1.38902	1.50696	1.43252	1.42860	4.14090	1.49052
Equivalents of K liberated	0.10178	0.11714	0.12310	0.11486	0.08567	0.11292	0.30930	0.09487
Fraction of equivalents of K electrolyzed	0.071266	0.082777	0.088623	0.076219	0.059803	0.079042	0.074693	0.063648
Current efficiency[b]	0.78	0.75	0.82	0.77	0.55	0.76	0.69	0.64
Suspension temperatures of different crystal fragments relative to standard crystals taken as zero[a]	0.010 0.010 0.009 0.009 0.009 *I*	0.011 0.010 0.010 0.010 0.009 *I, I, I*	0.009 0.009 0.008 0.008 0.008 *I*	0.009 0.009 0.009 0.009 0.008 *I, I*	0.010 0.010 0.010 0.009 0.009 *I, I*	0.010 0.010 0.009 0.009 0.009 *I*	0.010 0.009 0.009 0.009 0.008	0.011 0.010 0.010 0.010 0.010 *I, I, I, I*
Average suspension ΔT	0.0094	0.0100	0.0084	0.0088	0.0096	0.0094	0.0090	0.0102
Change in the atomic weight of K	−0.000586	−0.000623	−0.000523	−0.000548	−0.000598	−0.000586	−0.000561	−0.000635
α	1.0054	1.0049	1.0049	1.0050	1.0055	1.0055	1.0051	1.0058

[a] *I* indicates imperfect crystals not used to obtain the average ΔT.
[b] See p. 874 of reference 7.

platinum container. The resulting potassium chloride was then fused to remove traces of excess chloride ion. Solutions of this potassium chloride were titrated with standard silver nitrate solution. This furnished a satisfactory method of determining the number of residual equivalents of potassium ion, the whole procedure requiring about fifteen minutes. The number of equivalents electrolyzed was obtained by difference of the initial and residual number of equivalents of potassium ion.

III. EXPERIMENTAL RESULTS

Nineteen electrolyses were performed to determine the electrolytic separation factor, α.[17] Experimental conditions were varied to determine their effect on the α-value. In Table I there are presented the data for eight single step electrolyses. In the first three the current density was varied with the cell temperature held constant at 35°C. In the fourth through the eighth electrolyses, the temperature was varied from 15° to 50°C with the current density held constant at 0.099 amp./cm.² The approximate concentration of the electrolyte at the beginning of each electrolysis is recorded for the electrolyses of both Tables I and II. In order to increase the isotopic separation and thus increase the precision of the determination of α, four stepwise electrolyses were performed. The data for these electrolyses, nine through twelve, are given in Table II. The Roman numerals indicate the number of the step of a given electrolysis. The potassium chloride, obtained on reaction of the K amalgam from a given step, served as the starting material for the succeeding step. The ninth and tenth electrolyses were made in two steps, the eleventh in three steps, and the twelfth in four steps. The α's obtained here for steps other than the first are cumulative[18] α's.

With each step of the electrolyses, five crystals of potassium chloride were prepared and suspended. If the ΔT of any of the five crystals deviated by a certain amount from the closely agreeing ΔT's of remaining ones, then the non-agreeing ΔT was discarded on the basis that it was from an imperfect crystal. In this case new crystals were prepared and suspended until in all there were five crystals with ΔT's with no large differences. Crystals were excluded as imperfect

[17] α is defined by the relationship

$$d \ln K^{39} = \alpha d \ln K^{41} \qquad (a)$$

where K^{39} and K^{41} represent the numbers of atoms of the isotopes with mass 39 and 41, respectively.

[18] The cumulative α is that value taken as a constant through all steps of an electrolysis, needed to yield the experimental ΔT observed at the end of a given step.

TABLE II. Data for the separation of K isotopes in the stepwise electrolyses of aqueous KCl.

Run number	9I	9II	10I	10II	11I	11II	11III	12I	12II	12III	12IV
Average temperature (°C)	35	35	35	35	35	35	35	35	35	35	35
Current density (amp/cm²)	0.099	0.099	0.099	0.099	0.099	0.099	0.099	0.099	0.099	0.099	0.099
Concentration of KCl at beginning (mols/liter soln.)	2.50	0.50	3.00	0.50	4.00	1.00	0.33	3.94	4.14	1.82	0.61
Equivalents of K in starting material	7.25062	0.42802	9.02098	0.51808	11.8393	2.55165	0.47121	17.7480	3.63492	0.88367	0.25813
Equivalents of K liberated	0.48040	0.09152	0.58162	0.41412	2.4185	0.53201	0.10026	4.3925	1.10236	0.29831	0.10442
Fraction of equivalents of K electrolyzed	0.066256	0.21382	0.064474	0.20060	0.16963	0.20850	0.21277	0.24749	0.30327	0.33758	0.40452
Current efficiency[b]	0.62	0.74	0.63	0.56	0.69	0.79	0.83	0.57	0.59	0.91	0.91
Suspension temperatures of different crystal fragments relative to standard crystals taken as zero[a]	0.010 0.009 0.009 0.009 0.009 *I, I*	0.018 0.018 0.018 0.018 0.017 *I*	0.009 0.009 0.009 0.008 0.008 *I*	0.019 0.018 0.018 0.018 0.018 *I, I, I*	0.010 0.009 0.009 0.009 0.008 *I, I*	0.018 0.018 0.018 0.018 0.017 *I*	0.027 0.026 0.026 0.025 0.025 *I, I*	0.009 0.009 0.009 0.008 0.008 *I, I*	0.019 0.017 0.017 0.017 0.016 *I, I, I, I*	0.025 0.025 0.024 0.024 0.022 *I*	0.035 0.033 0.032 0.031 0.029 *I, I*
Average suspension ΔT	0.0092	0.0178	0.0086	0.0182	0.0090	0.0178	0.0258	0.0086	0.0172	0.0240	0.0320
Change in the atomic weight of K	−0.000573	−0.001109	−0.005358	−0.001134	−0.000561	−0.001109	−0.001607	−0.000536	−0.001072	−0.001495	−0.001 994
α	1.0052	1.0053	1.0049	1.0054	1.0055	1.0055	1.0053	1.0055	1.0056	1.0053	1.0054

[a] *I* indicates imperfect crystals not used to obtain the average ΔT.
[b] See p. 874 of reference 7.

if their ΔT differed by more than 0.006°C from the average ΔT of the closely agreeing crystals. Tables I and II record the ΔT's of all crystals suspended. Linear averages of the ΔT's were taken for the computation of α since there were no large or systematic differences for the ΔT's of any step.

α's for each step were computed from the equation,

$$\alpha=\frac{\log\left[1-F\left\{1+\frac{dM_{\mathrm{KCl}}\Delta T}{\rho_{\mathrm{KCl}}(A_{41}-A_{\mathrm{K}})}\right\}\right]}{\log\left[1-F\left\{1-\frac{dM_{\mathrm{KCl}}\Delta T}{\rho_{\mathrm{KCl}}(A_{\mathrm{K}}-A_{39})}\right\}\right]} \qquad (1)$$

in which F is the fraction of chemical equivalents of potassium ion electrolyzed in a given step of an electrolysis; M_{KCl} is the molecular weight of normal potassium chloride; A_{K} is the atomic weight of normal potassium; A_{39} and A_{41} are the mass values of K_{39} and K_{41}, respectively; ρ_{KCl} is the density of normal potassium chloride at the suspension temperature for standard normal crystals; d is the isothermal density change for a ΔT of one degree; and ΔT is the suspension temperature of crystals prepared from the potassium amalgam minus the suspension temperature of standard normal crystals. This equation is an exact solution of equation (a) of reference 17 in terms of the experimentally measured quantities, F and ΔT. Values used for the constants in Eq. (1) are: A_{39}[19]$=38.975$; A_{41}[19]$=40.974$; A_{K}[20]$=39.096$; M_{KCl}[20]$=74.553$; $d=1.659\times10^{-3}$ g/ml-deg.; and ρ_{KCl}[13]$=1.98651$ g/ml.

IV. DISCUSSION OF RESULTS

A. The Value of α and Its Dependence on Experimental Conditions

The least precisely determined quantity used in the computation of α is the ΔT of suspension. Therefore, it is worth while to consider the probable error of the ΔT's in some detail. In previous work[7, 8] the experimental uncertainty of the ΔT's was given an arbitrary assignment of ±0.002°C. Suppose, for example, in electrolysis 1 we assign an uncertainty of ±0.002°C and a weight of unity to each of the five ΔT's obtained. The value of the probable error, p_i, of the average ΔT obtained from internal consistency is

[19] E. Pollard, Phys. Rev. **57**, 1186–7 (1940).
[20] Eleventh report of the committee on atomic weights of the International Union of Chemistry, J. Am. Chem. Soc. **63**, 845 (1941).

$\pm 0.0009°$. The probable error, p_e, obtained from external consistency is $\pm 0.0002°$. The ratio, p_e/p_i, is 0.22. However, theory predicts that this ratio should not differ from unity by more than 22 percent. Thus, the arbitrary assignment of $\pm 0.002°$ to the ΔT's is too large. Let us consider the original measurement of a suspension temperature. It has been obtained in the present and previous works by the relation

$$T_S = (T_H + T_L)/2 \qquad (2)$$

where T_S is the suspension temperature, and T_H and T_L are the high and low temperatures, respectively, that define a fall or rise of a crystal in the suspension medium.[21] Relation (2) is about the best that can be assumed, especially when the difference, $(T_H - T_L)$, is of the same order of magnitude as the errors in T_H and T_L. If it is assumed that a temperature can be read with the aid of a magnifying glass from the Beckmann thermometer, which was employed, to within $\pm 0.001°$, then by taking four measurements of both T_H and T_L, as was done in the present work, the probable error of either T_H or T_L is reduced to $\pm 0.0005°$. From relation (3), there is produced a probable error of $\pm 0.00035°$ in T_S. The relation used to compute the ΔT's of suspension is,

$$\Delta T = T_A - T_N, \qquad (3)$$

where T_A is the suspension temperature of crystals prepared from the amalgam and T_N is the suspension temperature for standard normal crystals. The error produced in each ΔT of Tables I and II by relation (3) is $\pm 0.0005°$. The resulting probable error in the average ΔT for a single electrolysis is $\pm 0.00022°$ by internal consistency and $\pm 0.00017°$ by external consistency. The ratio, p_e/p_i, is then 0.77 in good agreement with that predicted by theory when no systematic errors are introduced with the temperature measurements and relation (2) is assumed correct. Certainly, because of the manner of measuring ΔT's in this work, the assignment of $\pm 0.001°$ as the error in the average ΔT's should well include all errors.

The probable error of the α-value for each electrolysis was computed on the basis of the errors associated with each quantity in the right

[21] See reference 7 for the procedure of suspending crystals.

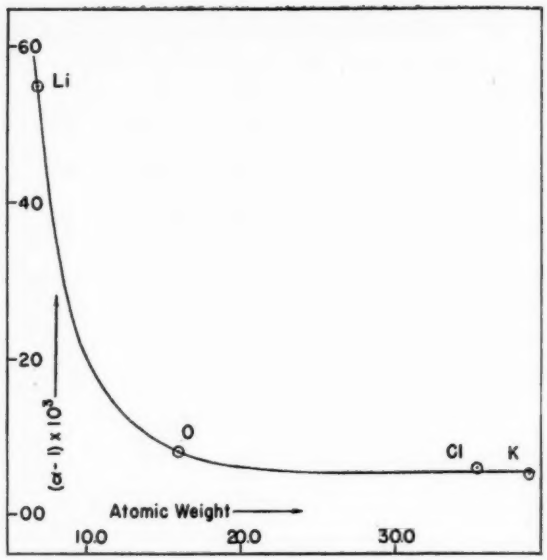

FIG. 1. Plot of $(\alpha-1)\times 10^3$ against atomic weight.

member of Eq. (1). The probable errors in these α's were used to assign weights to the nineteen α's obtained. The resulting average α is 1.0054. The ratio, p_e/p_i, for the average α is 1.48 where theory predicts its deviation from unity should be only 10 percent. Hence, systematic errors were shown to be present in one or more stages of the work, and therefore, the above assignment of weights to the α's was discarded. To obtain an average α, weights were arbitrarily assigned to each α numerically equal to the number of electrolytic steps employed in its determination, i.e., the single step α's were given a weight of one, the double step α's were given a weight of two, etc. The resulting average is 1.0054. The error limit was taken as the maximum deviation of individual α's from this average which yielded ± 0.0005.

The α-values for electrolyses 4–8 vary from 1.0058 to 1.0050 over the temperature interval of 15°–50°C. If a deviation in the average ΔT of $\pm 0.001°$ is assumed, the corresponding deviation in α is ± 0.0007 unit. It is doubtful if any significance can be attached to the above apparent variation of α with temperature since the variation is only slightly larger than that produced by an experimental uncertainty of $\pm 0.001°$ in ΔT. Likewise, no significance can be attached to the slight variation of α with change in current density recorded for electrolyses 1–3. Within the

limits of observation, the α-value is not dependent on the amount of back reaction as shown by the current efficiencies, on the concentration of the electrolyte, or on the fraction of chemical equivalents of K ion electrolyzed. The value,

$$\alpha = 1.0054 \pm 0.0005,$$

can be stated as the electrolytic separation coefficient for the separation of potassium isotopes at a mercury cathode over the temperature interval of 15°–50°C.

B. The Relation Between α and the Atomic Weight

It is of interest to note the relationship which becomes apparent when the α-value for the separation of potassium isotopes obtained in the present work is compared with the α-values given in the introduction of this paper for the elements, lithium, oxygen, and chlorine. Assuming an α-value for hydrogen of 5.000, the α's for these five elements have been plotted against their respective atomic weights. There results a good smooth curve. The actual value assumed for hydrogen, which Topley and Eyring[22] found to vary from 2.8 to 7.6 depending on the nature of the electrode, will not change the shape of the curve appreciably for atomic weights greater than 5 or 6. Figure 1 presents that part of the curve with atomic weights above 6. Since these α's have been determined at different electrodes (iron, mercury, and bright platinum) a cursory conclusion can be made that the mechanism of the separation is independent of the electrode material for elements with atomic weights greater than 5 or 6. The fact that the separation of oxygen and chlorine was effected at an anode and the separation of lithium and potassium was effected at a cathode would lead one to guess that the separation mechanism is similar at either anode or cathode, at least in its over-all effect.

The data presented in this work do not serve to distinguish among the various mechanisms[23] that have been proposed to account for the electrolytic separation of isotopes. Efforts to explain the mechanism of separation have involved two kinds of factors: (1), kinetic factors determined by processes leading to different rates of electrolysis of the different isotopic species, and (2), an equilibrium factor due to isotopic exchange between the electrolyzed material and the residual electrolyte. Sufficient precise auxiliary data are not available to test directly the various proposed mechanisms. However, the dependence of the observed α-value on temperature may be employed to make a rough conclusion as to whether a kinetic or an equilibrium factor plays the major role in the separation. Neither the proposed kinetic mechanisms, which are based on different rate determining steps, nor the isotopic exchange mechanism possesses sensible temperature dependence and such small differences in the temperature coefficient of α as are predicted could not be detected by the relatively precise method of analysis employed in this work. On first consideration, it may appear that Bell's[24] kinetic mechanism, which is a quantum-mechanical application of Gurney's[25] theory of overvoltage, refutes the latter statement. Bell's mechanism is based on the supposition that the rate limiting step in the separation is the penetration of a solvent sheath surrounding a hydrated ion by an electron. On this basis, he predicts that the temperature dependence of the $\ln \alpha$ should be equal to $-\alpha/T$. This, however, appears to be incorrect. It is believed that the temperature coefficient of $\ln \alpha$ should be equal to $-\ln \alpha/T$. When this correction is made, it is seen that the Bell-Gurney mechanism, also, does not possess sensible temperature dependence.

If the observed α represents a partial approach to an exchange equilibrium in addition to a kinetic mechanism, and if the exchange α is assumed to differ markedly from a kinetic α, it would be expected that temperature would have a noticeable effect on the observed α, by bringing about a change in the extent to which equilibrium is approached. Since α is constant within the error limits of this determination over the temperature range of 15°–50°C, it is most probable

[22] B. Topley and H. Eyring, J. Chem. Phys. **2**, 217 (1934).
[23] H. Eyring and A. Sherman, J. Chem. Phys. **1**, 345 (1933); Horiuti and Polanyi, Nature **132**, 931 (1933); R. P. Bell, J. Chem. Phys. **2**, 164 (1934); B. Topley and H. Eyring, J. Chem. Phys. **2**, 217 (1934); Fowler, Proc. Roy. Soc. **A144**, 452 (1934); Bowden and Kenyon, Nature **135**, 105 (1935); O. Halpern and Ph. Gross, J. Chem. Phys. **3**, 452 (1935); Butler, Zeits. f. Elektrochemie **44**, 55 (1938).
[24] R. P. Bell, J. Chem. Phys. **2**, 164 (1934).
[25] R. W. Gurney, Proc. Roy. Soc. (London) **A134**, 137 (1932).

that a kinetic mechanism effects the major part of the separation.

It is apparent that before any proper explanation of the mechanism of the electrolytic separation process can be forthcoming, there must be a much greater extension of the experimental material. The writer has work in progress at present on the electrolytic separation of nitrogen isotopes which is based on the discharge of the ammonium ion at a mercury cathode. The experimental curve of Fig. 1 predicts the α-value for nitrogen to be near that of oxygen. It will be of interest to check this prediction. Because of the much more rapid method of mass spectrometer analysis employed in this nitrogen work instead of the long and tedious crystal suspension method employed in previous work, much greater variation in experimental conditions of the electrolyses are made available. It is hoped that the results of the nitrogen work will furnish experimental data that can serve as a more adequate basis for interpreting the mechanism of the separation.

THE JOURNAL OF CHEMICAL PHYSICS VOLUME 14, NUMBER 7 JULY, 1946

An X-Ray Diffraction Investigation of the Thermal Decomposition of Silver Oxalate*,†

R. L. GRIFFITH
Kodak Research Laboratories, Rochester, New York

A single crystal of silver oxalate was studied by x-ray diffraction during the process of thermal decomposition. The diffraction patterns indicated that some fragmentation of the single crystal occurred early in the reaction. Except for distortion, the monoclinic structure was maintained until all trace of silver oxalate disappeared. The gradual appearance of polycrystalline silver was apparent. The diffraction patterns showed that a portion of the silver assumed preferred orientations, the ratio of oriented to unoriented silver remaining constant throughout the reaction. Four different preferred orientations were found and were defined relative to the silver oxalate lattice.

SILVER oxalate, when heated, undergoes thermal decomposition, the products being metallic silver and carbon dioxide.[1,2] The crystal structures of silver oxalate[3] and metallic silver[4] are known. It seemed quite probable, therefore, that information regarding the behavior of the silver oxalate structure during decomposition, the growth of silver, and its crystalline form and orientation with respect to the silver oxalate structure could be obtained by means of x-ray diffraction studies during the process of thermal decomposition. Such information is useful in connection with the development of photothermographic processes[5] and also in connection with the theory of photographic development.

A thick plate-like crystal of silver oxalate, prepared by slow evaporation of a concentrated ammoniacal solution,[2] was mounted on the goniometer head of a Weissenberg x-ray diffraction camera and so oriented as to rotate about its a axis. The crystal was then reduced to a cylindrical form having a diameter of approximately 0.4 mm, by rotating it against a small piece of sponge soaked in ammonium hydroxide. The goniometer head could be removed from the camera without disturbing the attached crystal.

The experimental procedure consisted in heating the crystal, still attached to the goniometer head, for a period of time in an oven at a controlled temperature ranging from 100° to 140°C for the various periods of heating. After each interval of heating, the crystal was returned to

* Paper presented before Division of Physical and Inorganic Chemistry, American Chemical Society, Atlantic City, New Jersey, April 8–12, 1946.

† Communication No. 1068 from the Kodak Research Laboratories.

[1] J. Y. Macdonald and C. N. Hinshelwood, J. Chem. Soc. 127, 2764 (1925).

[2] J. Y. Macdonald, J. Chem. Soc. 832, 839 (1936).

[3] R. L. Griffith, J. Chem. Phys. 11, 499 (1943).

[4] R. W. G. Wyckoff, *The Structure of Crystals* (Chemical Catalog Company, New York, 1931), second edition, p. 204.

[5] U. S. Patent, 1,976,302, S. E. Sheppard and W. Vanselow (assigned to Eastman Kodak Company).

TABLE I. Diffraction patterns of silver oxalate during thermal decomposition.

Photograph No.	Type	Heat treatment Time (Hr.)	Temp. °C	Remarks Silver oxalate pattern	Silver pattern
3	*R*	1½	100	Normal single crystal.	None.
4	*R*	3	100	Normal pattern plus ten weak spots just off 0 and ±1 layer lines.	None.
5	*R*	5½	100	Normal pattern. Extra spots slightly stronger.	Three weak powder lines.
6	*R*	4	100	Normal pattern slightly diffuse at large angles. About 50 extra spots.	Six silver lines. Maxima on lines.
7	*R*	5	100	Normal pattern same as in No. 6. Extra spots stronger.	Pattern considerably stronger.
8	*W*	None		Normal pattern. Spots at large angles slightly diffuse.	One line visible. Maxima on line.
9	*R*	6	100	Normal pattern becoming more diffuse. No additional extra spots.	Same as No. 7.
10	*W*	None		Same as No. 8.	Two silver lines with distinct maxima.
11	*R*	15	100	About same as No. 9.	Lines much stronger.
12	*W*	None		Spots diffuse.	Four lines present. All have maxima.
13	*R*	21	100	Normal pattern and extra spots becoming weaker and more diffuse.	Intensity greater.
14	*W*	None		Same as No. 12.	Intensity greater than No. 12.
15	*R*	17½	110	Same as No. 13.	Same as No. 13.
16	*R*	17	125	Normal pattern and extra spots are weaker.	Stronger. Eight lines. Maxima at same points on lines.
17	*W*	None		Same as No. 14.	Six lines visible. Same maxima present.
18	*W*	43	125	Pattern considerably weaker.	Seven lines visible. Maxima on all.
19	*R*	None		Much weaker. All extra spots present.	Pattern stronger.
20	*R*	39	130	Weaker. Spots quite diffuse.	Same as No. 19.
21	*W*	None		Spots quite diffuse.	Same as No. 18.
22	*W*	42	140	No evidence of pattern.	Eight lines. Maxima not as sharp as on No. 18.
23	*R*	None		No evidence of pattern.	Maxima not as sharp as on No. 20.

the camera where rotation and usually zero-layer Weissenberg photographs were obtained, using filtered copper *K* radiation. By this procedure the effect of thermal decomposition on the silver oxalate diffraction pattern and the appearance and growth of the diffraction pattern of the thermally produced silver could be observed.

The photographs obtained and the observations concerning these photographs are summarized in Table I. Column 1 gives the number of the photograph; Column 2 indicates the type of photograph, *W*, indicating Weissenberg and *R*, rotation photograph. Columns 3 and 4 give the thermal treatment received since the previous photograph. Notes concerning the silver oxalate and silver patterns are in Columns 5 and 6. Typical photographs are shown in Figs. 1–7, these figures representing the photographs listed in Table I as 3, 7, 20, 23, 8, 18, and 22, respectively.

Figure 1, which is photograph No. 3 of Table I, is the diffraction pattern obtained by rotating a single crystal of silver oxalate about its *a* axis. The pattern consists of sharp spots, all distributed along straight lines across the pattern, the so-called layer-lines. There is no evidence of the silver diffraction pattern on this photograph. That silver was undoubtedly present was indicated by the darkening of the crystal, but the amount was too small to give a detectable diffraction pattern. Figure 2, photograph No. 7, contains, in addition to the pattern for rotation of a single crystal of silver oxalate, spots which are not on layer-lines. These spots can be accounted for by assuming that the crystal has undergone fragmentation in which small portions

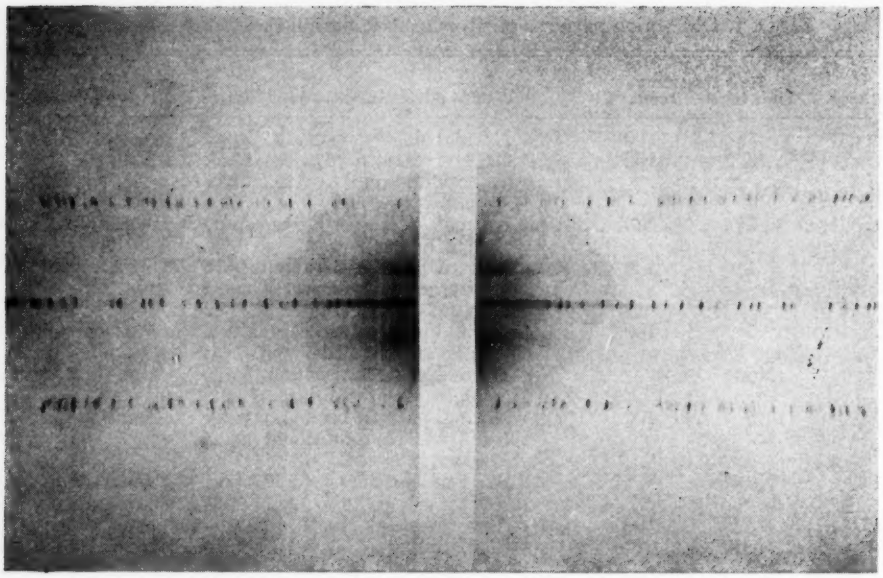

FIG. 1. Rotation photograph. Heat treatment: 1½ hr. at 100°C.

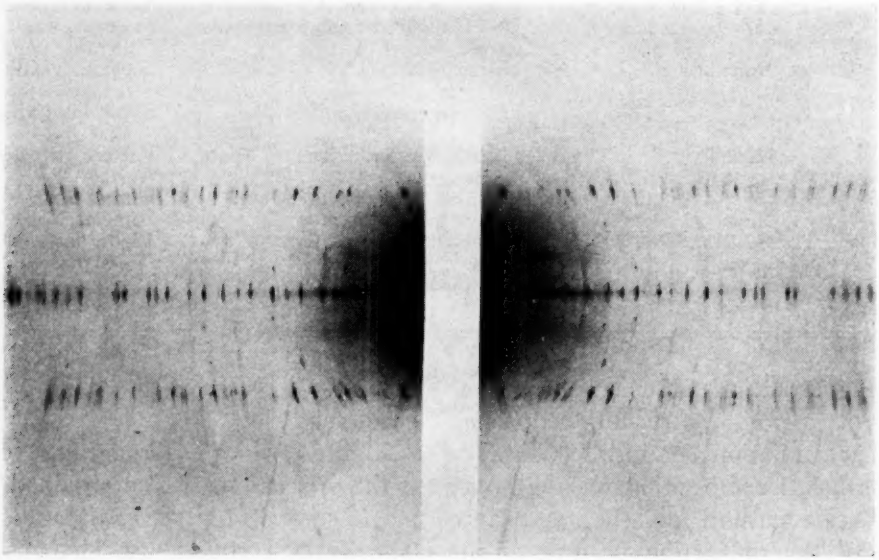

FIG. 2. Rotation photograph. Heat treatment: 19 hr. at 100°C.

of the original single crystal break away and assume orientations in which their *a* axes are not parallel to that of the parent crystal. These extra spots first appear on photograph No. 4 and increase in number and intensity on going from No. 4 to No. 7. All rotation photographs following No. 7 up to and including No. 20, Fig. 3, show the same extra spots at about the same intensity relative to that of the normal silver oxalate pattern. Beyond photograph No. 20, as is shown in Fig. 4, there is no evidence of the silver oxalate pattern nor of the extra spots. Examination of the series of photographs shows that as the reaction progresses, the silver oxalate pattern and the extra spots become gradually weaker and more diffuse. This is caused by disappearance of silver oxalate and the distortion of the structure of the remaining silver oxalate.

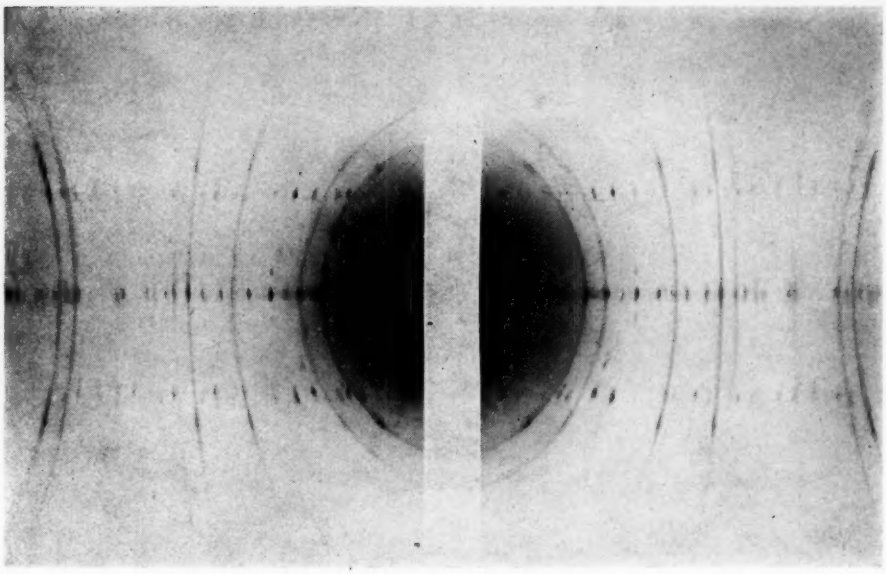

FIG. 3. Rotation photograph. Heat treatment:
61 hr. at 100°C 60 hr. at 125°C
17½ hr. at 110°C 39 hr. at 130°C

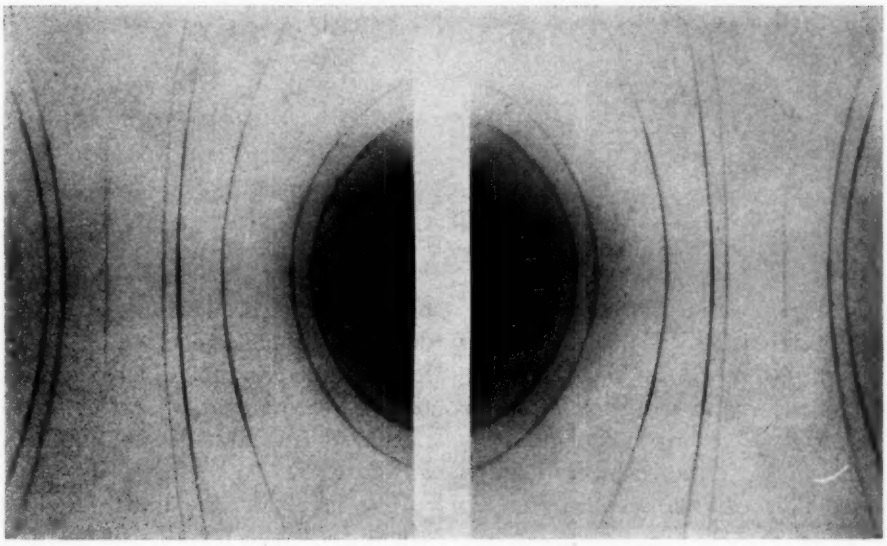

FIG. 4. Rotation photograph. Heat treatment:
61 hr. at 100°C 39 hr. at 130°C
17½ hr. at 110°C 42 hr. at 140°C
60 hr. at 125°C

Apparently, the time required for the decomposition to occur in the parent crystal and in the fragments which split off is about the same. The increase in number and intensity of the extra spots between photograph No. 4 and No. 7 may be caused by the growth and increased perfection of the fragments which split off from the parent silver oxalate crystal. The extra spots do not appear on the Weissenberg photographs because of the presence of the layer-line screen in the camera when the photographs were taken.

The first photograph exhibiting any evidence of the diffraction pattern of silver is No. 5, on which three weak powder lines are visible. These

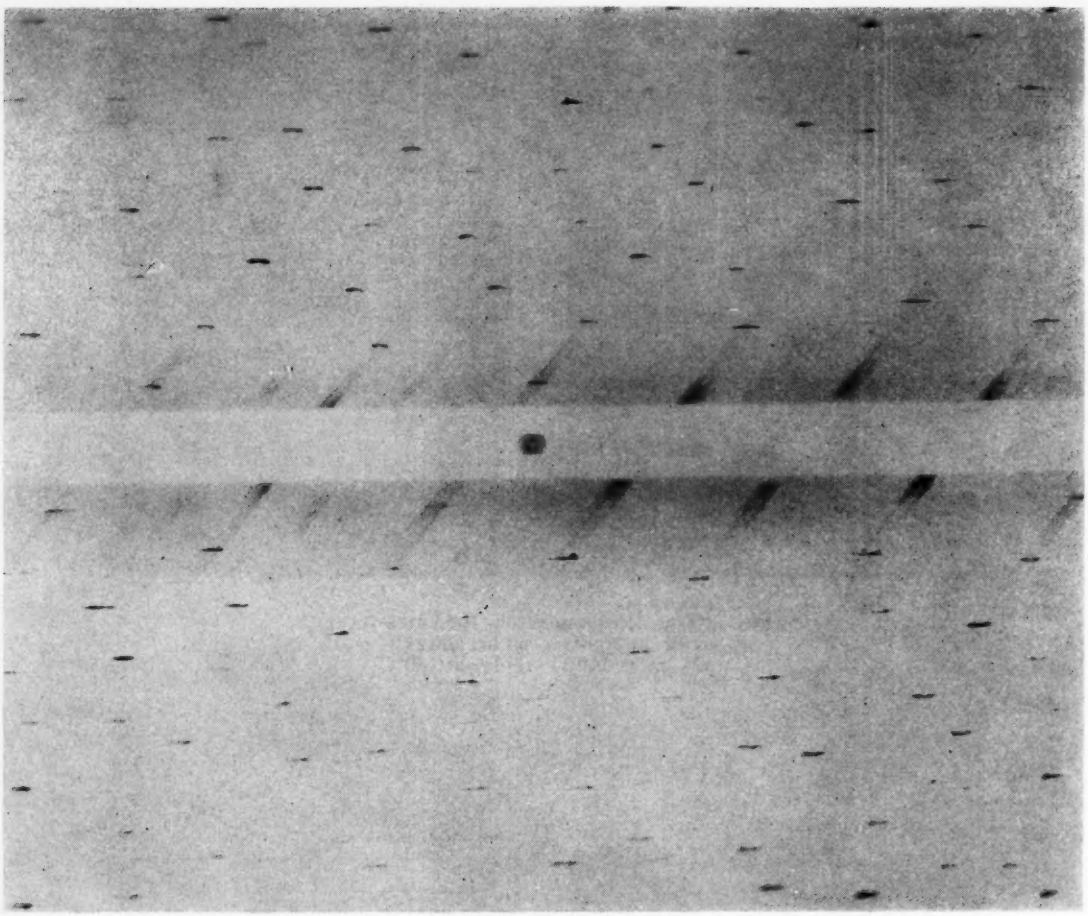

FIG. 5. Weissenberg photographs. Heat treatment: 19 hr. at 100°C.

lines and those on succeeding photographs are caused by face-centered cubic, polycrystalline silver. On photograph No. 6, the silver pattern is considerably stronger and close examination shows that the powder lines are not of uniform density over their length but exhibit definite density maxima. This can be seen in Fig. 2, which is photograph No. 7. Fig. 5, photograph No. 8, a Weissenberg photograph, shows one powder line for silver. This line exhibits density maxima. As the decomposition progresses, the lines on the diffraction pattern increase in intensity and number. Density maxima are present on the lines at the same points in all photographs. Comparison of Figs. 3 and 4 shows that the density maxima are less pronounced on Fig. 4—the photograph taken after all the silver oxalate pattern had disappeared—than on Fig. 3, which was taken before the disappearance of the oxalate pattern. This may be caused by the orienting influence exerted on the silver crystallites by the residual silver oxalate lattice. Continued heating at 130°C after the silver oxalate pattern disappeared did not diminish the maxima any further.

The fact that the lines due to silver are of about the same breadth on all patterns, allowance being made for differences in exposure, is consistent with the view that when the growth of a small crystal is initiated it rapidly grows to final size, the over-all process taking place by the initiation and growth of new crystals rather than by the simultaneous growth to a large size of a small number of crystals. The mass of polycrystalline silver left at the completion of the reaction was a pseudomorph of the original crystal.

All the maxima on the diffraction lines of the

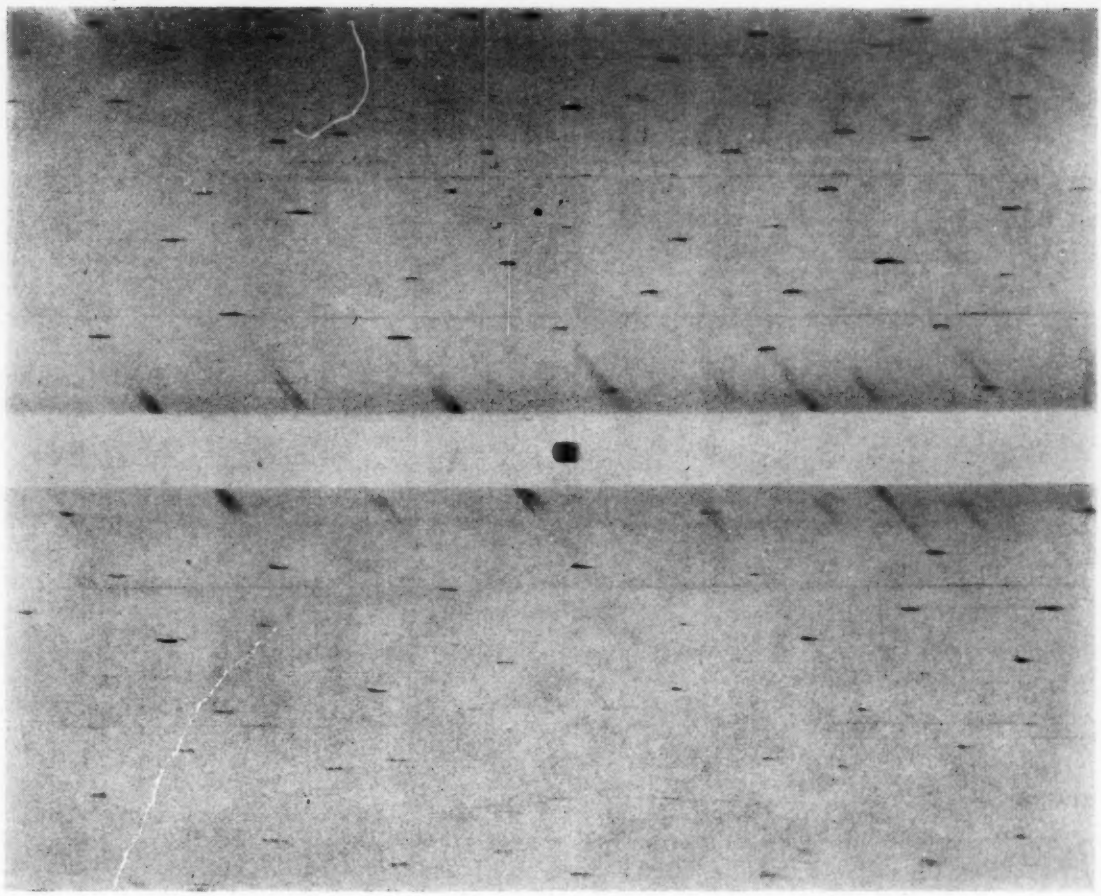

FIG. 6. Weissenberg photograph. Heat treatment:
61 hr. at 100°C 60 hr. at 125°C
17½ hr. at 110°C

silver pattern on the rotation photographs can be accounted for both as to position and relative intensity by assuming that a portion of the polycrystalline silver which is formed assumes a preferred orientation with respect to the silver oxalate lattice such that the [011] direction of the silver structure is parallel to the *a* axis of silver oxalate. The fact that the intensity maxima are arcs rather than spots indicates a range of orientations. From the lengths of these arcs one may conclude that the orientation of nearly all of those crystallites which are oriented lies within ±4° of that described here.

Having established that the [011] direction of the oriented silver structure is parallel to the *a* axis of the silver oxalate structure, we can define completely the relative orientation in space of the two structures by determining the angle between some direction in the silver oxalate lattice which is normal to its *a* axis, for example, the *b* axis, and a direction in the lattice of the oriented silver which is normal to its [011] direction, for example, the [01$\bar{1}$] direction. The angle between these directions can be determined by well-established methods[6] from the zero-layer Weissenberg photographs shown in Figs. 6 and 7. From these patterns it was determined that there are at least four different preferred orientations of silver with respect to the silver oxalate structure. In all four cases the [011] direction of silver is parallel to the *a* axis of silver oxalate. The four orientations are then completely defined by the angles between the [01$\bar{1}$] directions and the *b* axis of the silver oxalate structure. These

[6] M. J. Buerger, *X-Ray Crystallography* (John Wiley and Sons, New York, 1942).

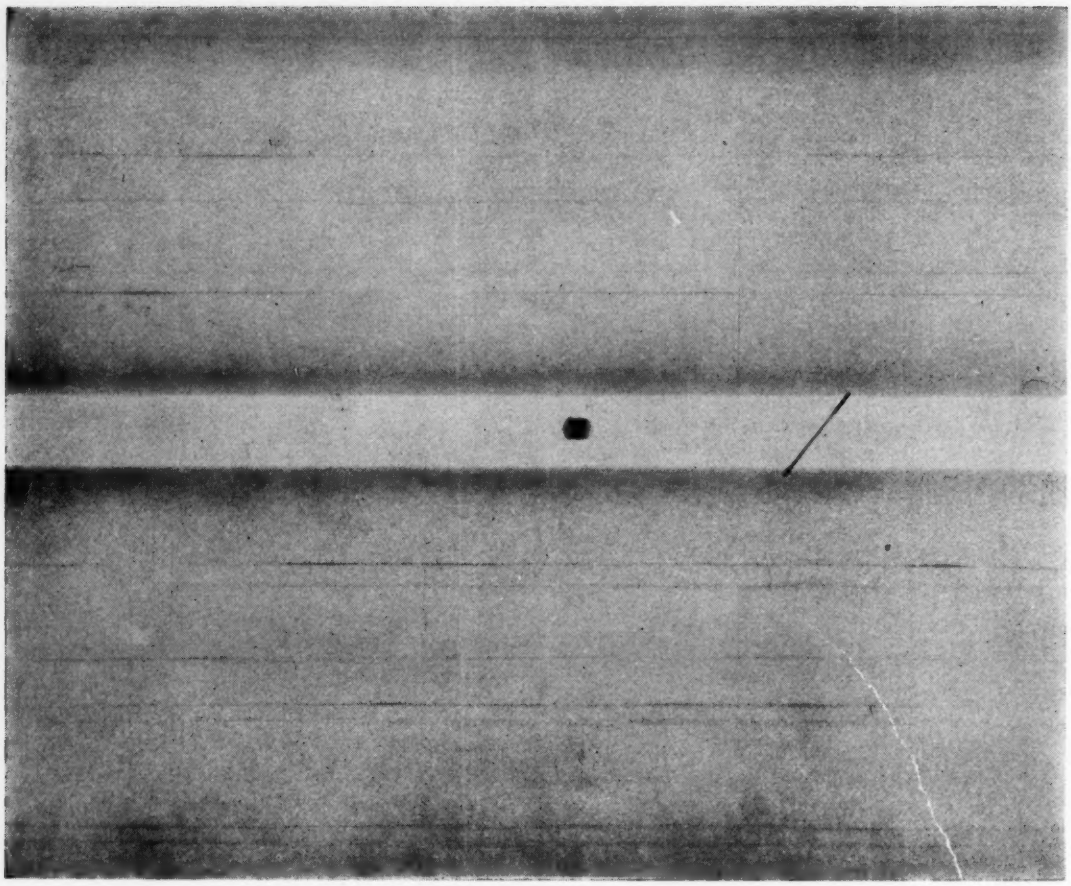

FIG. 7. Weissenberg photograph. Heat treatment:
61 hr. at 100°C 39 hr. at 130°C
17½ hr. at 110°C 42 hr. at 140°C
60 hr. at 125°C

angles are −30°, 35°, 75°, and 100°, with a range of ±5°. These four preferred orientations of silver account for all the density maxima which appear on the diffraction lines of silver in the photographs shown in Figs. 6 and 7.

The preferred orientation of silver with respect to the silver oxalate structure probably arises from the attempt of the silver crystals to grow in such a fashion that at the interface between silver and silver oxalate there will be as nearly as possible a correspondence in direction and magnitude of the silver-silver distances. There are no close silver-silver distances in these two structures which agree in magnitude. The closest distances in metallic silver are 2.88A and 4.08A. Those in silver oxalate are 3.34A, 3.35A, and 3.58A. The process of crystal growth must involve a considerable adjustment of silver-silver distances. The oriented silver probably grows in such a fashion as to produce a minimum of readjustment of distances. The probability that a silver crystal will be in a position of preferred orientation is about the same as the probability that it will have a random orientation, since, as is shown by the diffraction patterns, a considerable portion of the silver is randomly oriented. The ratio of oriented to unoriented silver remains about the same throughout the process of thermal decomposition. Continued heating of the mass of silver after decomposition is complete does not change the ratio of oriented to unoriented silver.

CONCLUSIONS

In the crystal of silver oxalate which was investigated, thermal decomposition is accom-

panied by fragmentation of the crystal, the fragments produced being slightly disoriented with respect to the original crystal. The undecomposed silver oxalate maintains its structure until the reaction is complete, except for distortion produced by removal of carbon dioxide from the lattice. The silver formed by the decomposition exists in the form of face-centered cubic crystals having a final size of approximately 10^{-5} cm. Some of the crystals of silver assume preferred orientations with respect to the silver oxalate lattice, the ratio of oriented to unoriented silver remaining approximately constant during and after the reaction. The explanation of the particular preferred orientations assumed is probably to be found in the structures of the two crystals but it is not immediately evident.

ACKNOWLEDGMENT

The author wishes to thank Dr. S. E. Sheppard for suggesting this investigation and for helpful discussions concerning the interpretation of the results obtained. Thanks are also due Dr. M. L. Huggins for helpful advice and criticism.

THE JOURNAL OF CHEMICAL PHYSICS VOLUME 14, NUMBER 7 JULY, 1946

The Behavior of Macromolecules in Inhomogeneous Flow

H. A. KRAMERS
Institute for Theoretical Physics, University of Leiden, Leiden, Holland
(Received March 6, 1946)

Following up the ideas of W. Kuhn's skein theory, J. J. Hermans has recently elaborated a theory of the properties of dilute solutions of highly polymerized molecules. Hermans describes the behavior of linear molecules by the diffusion of their end points. He finds that the contribution of a single molecule to the viscosity coefficient as well as to the double refraction of the solution is proportional to the square of the degree of polymerization, in agreement with the experiments. In the present article we investigate the statistical behavior of the individual links of the solved molecules. In this way we arrive at results equivalent with those of Hermans. Our method, however, can also be applied to molecules which possess branching points and rings.

1. INTRODUCTION

IN connection with Kuhn's skein theory, Hermans[1] developed a simplified method to describe the influence of macromolecules on viscosity and double refraction. In this method the behavior of the molecule is characterized by the diffusion of the end points. This can be described as if two mass points which exert a fictive elastic force upon each other are diffusing in the liquid. The equilibrium distribution of the vector joining the end points, showing spherical symmetry in a liquid at rest, is deformed under the influence of the flow. It is assumed that this flow does not alter the elastic force. By means of a relatively simple calculation Hermans shows that the contributions of a molecule both to the viscosity and to the birefringence of flow are proportional to the *square* of the number of elementary links, in conformity with experiment (Staudinger, Signer).

In the following we attempt to develop a more detailed theory. Our method also enables us to give a treatment of macromolecules which possess branching points and rings.

2. THE BEHAVIOR OF A SYSTEM OF MUTUALLY CONNECTED PARTICLES IN A FLOW DERIVED FROM A VELOCITY POTENTIAL

Let the systematic force which the liquid exerts on the ith particle be $-\zeta_i \mathbf{v}_i$, where $\mathbf{v}_i$ is the velocity of the particle with respect to the liquid. This velocity can be written $-\mathbf{v}_i'+\mathbf{v}_i''$, if $\mathbf{v}_i'$ represents the velocity of the liquid and $\mathbf{v}_i''$ that of the particle. If the streaming is irrotational and stationary and if its velocity potential is $\Psi(\mathbf{r})$, we have $\mathbf{v}_i' = -\nabla\Psi(\mathbf{r}_i)$. Consequently,

[1] J. J. Hermans, Physica **10**, 777 (1943).

the force which the liquid exerts on the ith particle can be written

$$X_i=-\frac{\partial U}{\partial x_i}-\zeta_i\dot{x}_i+X_i', \quad (y), \quad (z), \tag{1}$$

$$U=\sum_i \zeta_i\Psi(\mathbf{r}_i). \tag{2}$$

Here X_i' is a random force of such a nature that for a free particle it would maintain the equipartition. The influence of the pressure-forces which has here been neglected will be considered in Section 6.

The equations of motion are the same as those which would apply to our system in a liquid at rest if it were subject to a field of force with potential energy U. Introducing generalized coordinates q^1, $q^2\cdots q^s$ and conjugated momenta p_1; p_s and writing

$$T=\tfrac{1}{2}a_{kl}\dot{q}^k\dot{q}^l=\tfrac{1}{2}a^{kl}p_kp_l, \quad (p_k=a_{kl}\dot{q}^l) \tag{3}$$

for the kinetic energy T, the molecules will be distributed in p, q-space according to Boltzmann:

$$W\prod_k dp_kdq_k=\text{const. } e^{-(T+U)/\theta}\prod_k dp_kdq_k, \tag{4}$$

where U must be regarded as a function of the q's. Boltzmann's constant times the absolute temperature has been called θ.

Average values of functions of $\dot{q}$ and q can now be calculated in principle. A function which is linear in the $\dot{q}$'s (or p's) will on the average be zero. The average value of a function which is quadratic in $\dot{q}$ can simply be found by first reducing it to the average value of a function $F(q_1\cdots q_s)$ of the q's alone by means of the relation

$$\langle\dot{q}^k\dot{q}^l\rangle_{Av}=a^{kl}\theta. \tag{5}$$

Averaging a function $F(q_1\cdots q_s)$ of the q's alone amounts, as is well known,[2] to computing the ratio

$$\langle F(q_1\cdots q_s)\rangle_{Av}$$

$$=\int Fe^{-U/\theta}(A)^{\frac{1}{2}}\prod_k dq^k\Big/\int e^{-U/\theta}(A)^{\frac{1}{2}}\prod_k dq^k, \tag{6}$$

where A is the determinant of the coefficient a_{kl}:

$$A=\text{Det }|a_{kl}|. \tag{7}$$

[2] W. Gibbs, *Principles of Statistical Mechanics*, Chap. 6.

3. PEARL-NECKLACE MODEL OF A MACROMOLECULE

As a model for a macromolecule we consider a number of particles with coordinates $\mathbf{r}_1(x_1y_1z_1)\cdots\mathbf{r}_i\cdots\mathbf{r}_N$, in which every two successive particles are connected by a weightless rod of length L. Let the mass m and the frictional constant ζ be the same for all these particles. The direction cosines of the ith "link," i.e., of the rod which connects the ith particle with the $(i+1)$st particle, will be called α_i, β_i, γ_i (vector $\boldsymbol{\omega}_i$). If x, y, z ($\mathbf{r}$) are the coordinates of the center of gravity of our model, one has

$$x_i=x+\frac{L}{N}(\alpha_1+2\alpha_2+\cdots i\alpha_i-[N-i-1]\alpha_{i+1}$$
$$-[N-i-2]\alpha_{i+2}\cdots-\alpha_{N-1}), \tag{8}$$

$$\sum_1^N\dot{x}_i^2=\frac{L^2}{N}\sum_{\mu\nu}g_{\mu\nu}\dot{\alpha}_\mu\dot{\alpha}_\nu+N\dot{x}^2, \tag{9}$$

$$g_{\mu\nu}=\begin{cases}\mu(N-\nu) & \nu\geqslant\mu\\ \nu(N-\mu) & \nu\leqslant\mu\end{cases} \tag{10}$$

$$T=\frac{mL^2}{2N}\sum_{\mu\nu}g_{\mu\nu}(\dot{\boldsymbol{\omega}}_\mu\dot{\boldsymbol{\omega}}_\nu)+\tfrac{1}{2}Nm(\dot{x}^2+\dot{y}^2+\dot{z}^2). \tag{11}$$

The simplest model is obtained if it is assumed that the two rods which meet in a particle are completely free to rotate with respect to each other; a link would then be more or less analogous to W. Kuhn's "statistical chain-element." In that case we introduce, for instance, in addition to x, y, z, the polar angles ϑ_μ, φ_μ:

$$\alpha_\mu=\cos\vartheta_\mu=c_\mu,$$
$$\beta_\mu=\sin\vartheta_\mu\cos\varphi_\mu=s_\mu C_\mu,$$
$$\gamma_\mu=\sin\vartheta_\mu\sin\varphi_\mu=s_\mu S_\mu.$$

The total number of coordinates is $2N+1$. The coefficients a_{kl} in the kinetic energy are easily derived from (11) using the following formulas:

$$(\dot{\boldsymbol{\omega}}_\mu\dot{\boldsymbol{\omega}}_\nu)=(s_\mu s_\nu+c_\mu c_\nu C_{\mu\nu})\dot{\vartheta}_\mu\dot{\vartheta}_\nu+s_\mu s_\nu C_{\mu\nu}\dot{\varphi}_\mu\dot{\varphi}_\nu$$
$$+c_\mu s_\nu S_{\nu\mu}\dot{\vartheta}_\mu\dot{\varphi}_\nu+s_\mu c_\nu S_{\mu\nu}\dot{\varphi}_\mu\dot{\vartheta}_\nu$$
$$\begin{pmatrix}C_{\mu\nu}=\cos(\varphi_\mu-\varphi_\nu)\\ S_{\mu\nu}=\sin(\varphi_\mu-\varphi_\nu)\end{pmatrix}. \tag{12}$$

With 2, 3, 4, 5 links, these formulas lead to the following expressions for the determinant A of the coefficients a_{kl} (the angle between the μth and the $(\mu+1)$st link is denoted by ψ_μ):

$$
\begin{array}{ll}
N-1 & A \text{ (apart from a numerical factor).} \\
2 & s_1^2 s_2^2 (1-\tfrac{1}{4}\cos^2\psi_1), \\
3 & s_1^2 s_2^2 s_3^2 (1-\tfrac{1}{4}[\cos^2\psi_1+\cos^2\psi_2]), \\
4 & s_1^2 s_2^2 s_3^2 s_4^2 (1-\tfrac{1}{4}[\cos^2\psi_1+\cos^2\psi_2+\cos^2\psi_3]+\tfrac{1}{16}\cos^2\psi_1\cos^2\psi_3), \\
5 & s_1^2 s_2^2 s_3^2 s_4^2 s_5^2 (1-\tfrac{1}{4}[\cos^2\psi_1+\cos^2\psi_2+\cos^2\psi_3+\cos^2\psi_4] \\
 & \qquad +\tfrac{1}{16}[\cos^2\psi_1\cos^2\psi_3+\cos^2\psi_1\cos^2\psi_4+\cos^2\psi_2\cos^2\psi_4]).
\end{array} \tag{13}
$$

For $N-1=5$ we have calculated A only for the special case that all links are lying in the same plane; for $N-1=2$, 3, 4, however, the formulas (13) are of general applicability. We have not yet succeeded in deriving a general expression for A holding for arbitrary values of N, but its form can be surmised.

In a liquid at rest the probability that ϑ_μ and φ_μ have values between ϑ_μ and $\vartheta_\mu+d\vartheta_\mu$, and φ_μ and $\varphi_\mu+d\varphi_\mu$, respectively, is

$$\text{const. } A^{\frac{1}{2}} \prod_\mu d\vartheta_\mu d\varphi_\mu. \tag{14}$$

From the formulas (13) it is seen how the orientations of the various links are correlated: The correlation is strongest between successive links. The probability that they are perpendicular to each other is somewhat larger than that they are parallel or antiparallel; in the case of two links these probabilities are in the ratio $(4/3)^{\frac{1}{2}} \leqq 1.15$.

A somewhat less artificial model would be one in which a given constant value ψ_0 (for instance the supplement of the tetrahedron angle 109.5°) is assigned to the angle between two successive links. The number of degrees of freedom in that case amounts to $3+2+N-2=N+3$, but it is now difficult to introduce generalized coordinates in a simple manner. If desired, however, one can start from the former case, i.e., retain the complete number of $2N+1$ degrees of freedom, but complete this by introducing a potential energy

$$U'=\tfrac{1}{2}K\{(\psi_1-\psi_0)^2+(\psi_2-\psi_0)^2 + \cdots (\psi_{N-2}-\psi_0)^2\}. \tag{15}$$

We would thus introduce explicitly the bending vibrations of the valence bonds instead of replacing these by rigid bonds. It is clear that the incomplete freedom of rotation of a link with respect to another link from which it is separated by one neighbor could, if desired, also be accounted for by a suitable potential energy.

4. INTERNAL FRICTION IN A NON-UNIFORM FLOW

In a volume element of sufficiently small size the Poiseuille flow which occurs in the experiments is of the well-known laminar type

$$u=\kappa y, \quad v=0, \quad w=0. \tag{16}$$

This flow, however, is not irrotational and we will rather replace it by

$$
\begin{aligned}
u &= -\partial\Psi/\partial x = \tfrac{1}{2}\kappa y, \\
v &= -\partial\Psi/\partial y = \tfrac{1}{2}\kappa x, \\
w &= -\partial\Psi/\partial z = 0, \\
\Psi &= -\tfrac{1}{2}\kappa x y.
\end{aligned} \tag{17}
$$

Superposing a uniform rotation $u=\frac{1}{2}\kappa y$, $v=-\frac{1}{2}\kappa x$ on this flow, one obtains the laminar flow (16). If κ is not too large, the effect of this rotation can be neglected, as will be shown in Section 6.

According to the considerations of Section 2, the effect of the flow (17) can be described by a potential energy U (compare Eq. (2)):

$$U=-\tfrac{1}{2}\zeta\kappa\sum_1^N x_i y_i. \tag{18}$$

Omitting the coordinates of the center of gravity, this becomes

$$U=-\frac{\kappa\zeta L^2}{2N}\sum_{\mu\nu} g_{\mu\nu}\alpha_\mu\beta_\nu,$$

since it is clear that the coefficients $g_{\mu\nu}$ which occur in the dependency of $\sum xy$ on the α's and β's are the same as those which occur in the dependency of $\sum\dot{x}^2$ on the $\dot{\alpha}$'s (see Eq. (9)).

The influence of the flow is described by the Boltzmann factor $\exp(-U/\theta)$ which for sufficiently small κ can be replaced by

$$e^{-U/\Theta} \leqq 1-U/\Theta. \tag{19}$$

If $P_{xx}P_{xy}\cdots$ represents the stress tensor in the liquid, the coefficient of internal friction η is

defined by

$$P_{xy}=\eta\left(\frac{\partial u}{\partial y}+\frac{\partial v}{\partial x}\right)=\kappa\eta.$$

We will now calculate the average contribution δP_{xy} of a single macromolecule per unit volume to the value of P_{xy}. The contribution $\delta\eta$ per molecule to the viscosity will then be given by

$$\delta\eta=\frac{1}{\kappa}\delta P_{xy}. \tag{20}$$

Two effects contribute to δP_{xy}, the motion of the particles and the tension in the links. The former amounts to

$$\delta_I=-m\sum\langle\dot{x}_i\dot{y}_i\rangle_{Av},$$

because the probability that in unit time a plane of unit area perpendicular to the y axis is traversed by the ith particle in the direction of the negative y axis is $-\dot{y}_i$, and the momentum transferred in this process is $m\dot{x}_i$.

The second contribution results from the tensions in the links. If S_μ is the tension in the μth link, this tension contributes an amount $S_\mu\alpha_\mu$ to δP_{xy} if the link intersects the plane mentioned. The probability for the occurrence of such an intersection is $L\beta_\mu$ per molecule; hence

$$\delta_{II}=L\sum_\mu\langle S_\mu\alpha_\mu\beta_\mu\rangle_{Av}.$$

If the total force on the ith mass point resulting from the tensions is called X_i'', Y_i'', Z_i'', we have

$$X_i''=\sum_j S_i^{(j)}\alpha_i^{(j)},\quad Y_i''=\sum_j S_i^{(j)}\beta_i^{(j)}, \tag{21}$$

where the sum extends over all links j which meet in the ith particle. Usually there will be only two of such links, but in a ramified molecule —for which this calculation also holds good— there can be three or more. Considering now the virial-like expression

$$V=\sum_i X_i''y_i(=\sum_i Y_i''x_i),$$

in which we sum over all the particles, and substituting (21), each $S_i^{(j)}\alpha_i^{(j)}$ will occur twice, *viz.*, for those two particles which form the ends of the links concerned, but in these two cases the $\alpha_i^{(j)}$'s are of opposite sign. Consequently we may write

$$V=\sum_\mu S_\mu\alpha_\mu(y_i-y_i')=-\sum_\mu S_\mu\alpha_\mu\cdot L\beta_\mu,$$

where y_i and y_i' characterize the two ends of the μth link, and where α_μ is the direction cosine of the link $i\to i'$. Now, if X_i represents the force which the ith particle experiences from the liquid, we have according to Eq. (1):

$$X_i''=m_i\ddot{x}_i-X_i=m_i\ddot{x}_i+\frac{\partial U}{\partial x_i}+\zeta_i\dot{x}_i-X_i'.$$

In the average value of $\sum_i X_i''y_i$ in Boltzmann's distribution the contributions of the last two terms in the third member vanish, and we finally obtain

$$\delta_{II}=-\sum_i\langle X_i''y_i\rangle_{Av}=-m\sum_i\langle\ddot{x}_iy_i\rangle_{Av}-\sum_i\left(\frac{\partial U}{\partial x_i}y_i\right)_{Av},$$

$$\delta P_{xy}=\delta_I+\delta_{II}=-m\sum_i(\langle\dot{x}_i\dot{y}_i\rangle_{Av}+\langle\ddot{x}_iy_i\rangle_{Av})-\sum_i\left(\frac{\partial U}{\partial x_i}y_i\right)_{Av}. \tag{22}$$

The sum of the first two terms in the third member represents the derivative with respect to time of the average value of $-m\sum_i\dot{x}_iy_i$, and therefore contributes nothing. For the remaining expression one can write $\sum_i\langle X_i'''y_i\rangle_{Av}$, if X_i''' represents the systematic force resulting from the streaming liquid. That this expression is equal to $\kappa\delta\eta$ also follows immediately from the considerations given by J. M. Burgers[3] in connection with Einstein's work. Burgers studied the changes which forces acting on the liquid in a certain region (here $-X_i'''$) will bring about in the flow of the liquid outside that region, and arrived at a formula which is equivalent to ours.

With the aid of (18) and (20) it follows from (22) that

$$\delta\eta=\tfrac{1}{2}\zeta\sum_i\langle y_i^2\rangle_{Av}=\tfrac{1}{6}\zeta\sum_i\langle(x_i^2+y_i^2+z_i^2)\rangle_{Av}=\frac{\zeta L^2}{6N}\sum_{\mu\nu}g_{\mu\nu}\langle(\mu\nu)\rangle_{Av}. \tag{23}$$

To a sufficient approximation we may here take the average over the Boltzmann distribution *in the liquid at rest* ($U=0$ in Eq. (4)). In the third member we have introduced the abbreviated notation

$$(\omega_\mu\omega_\nu)=(\mu\nu)$$

[3] J. M. Burgers, "Viscosity report. II," Proc. Roy. Acad. Amsterdam [1] **16**, 128 (1938).

for the cosine of the angle between the μth and the νth link.

An accurate calculation of the expression (23) would require a precise knowledge of the correlation between the orientations of two different links. Now, in the free pearl necklace these correlations are small for neighboring links and negligible for more remote links. Moreover, in those cases with a small number of links where the calculation was carried out, the correlation only depends on the second power of the cosine of the angle between the two links, which means that $\langle(\mu\nu)\rangle_{Av}$ becomes zero. It would seem that this also applies to arbitrary N-values. Since $\langle(\mu\mu)\rangle_{Av}=1$, we may therefore write

$$\delta\eta=\frac{\zeta L^2}{6N}\sum_{\mu=1}^{N-1} g_{\mu\mu}=\frac{\zeta L^2}{6N}\sum \mu(N-\mu)$$

$$=\frac{\zeta L^2}{6N}\frac{(N-1)N(N+1)}{6},$$

or, if N is assumed to be large:

$$\delta\eta\cong(1/36)\zeta L^2N^2. \tag{24}$$

As in the analogous formula derived by Hermans, this equation shows $\delta\eta$ to be proportional to the square of the number of links, in conformity with Staudinger's viscosity rule.

If the free rotation of the links is of a nature such as that known from organic chemistry, i.e., if two successive links always enclose a given angle α, we get

$$\langle(\mu\mu)\rangle_{Av}=1,\quad \langle(\mu,\mu\pm1)\rangle_{Av}=\cos\alpha,$$
$$\langle(\mu,\mu\pm2)\rangle_{Av}=\cos^2\alpha,\quad \langle(\mu\nu)\rangle_{Av}=\cos^{|\mu-\nu|}\alpha.$$

To a sufficient approximation we may then write

$$\delta\eta\cong\frac{1}{36}\zeta L^2N^2\operatorname{ctg}^2\frac{\alpha}{2}. \tag{25}$$

If the links are connected by ordinary C–C bonds, α is the supplement of the tetrahedron angle, $\cos\alpha$ amounts to $\frac{1}{3}$, $\operatorname{ctg}^2\alpha/2$ equals 2, and the influence on the viscosity becomes, therefore, twice as large as in the case of the free pearl necklace.

5. DOUBLE REFRACTION IN NON-UNIFORM FLOW

The birefringence is described by a dielectric tensor ϵ_{xx}, $\epsilon_{xy}=\epsilon_{yx}$, etc., which is related to the polarization tensor $\bar{p}_{xx}$, $\bar{p}_{xy}$ resulting from the influence of a single molecule per unit volume according to the formulas

$$\epsilon_{xx}=\epsilon_0+4\pi G\bar{p}_{xx},\quad \epsilon_{xy}=4\pi G\bar{p}_{xy},\quad \text{etc.} \tag{26}$$

Here $\bar{\epsilon}^{\frac{1}{2}}_0$ is the refractive index of the liquid and G represents the number of macromolecules in unit volume. To simplify matters, we assume that the contribution of each link to the polarization tensor shows cylindrical symmetry round the direction of the link and can therefore be written

$$p_\lambda=a\begin{pmatrix}1&0&0\\0&1&0\\0&0&1\end{pmatrix}+b\begin{pmatrix}\alpha_\lambda^2-\frac{1}{3}&\alpha_\lambda\beta_\lambda&\alpha_\lambda\gamma_\lambda\\ \beta_\lambda\gamma_\lambda&\beta_\lambda^2-\frac{1}{3}&\beta_\lambda\gamma_\lambda\\ \gamma_\lambda\alpha_\lambda&\gamma_\lambda\beta_\lambda&\gamma_\lambda^2-\frac{1}{3}\end{pmatrix}. \tag{27}$$

The total polarization tensor of the molecule becomes

$$p=\sum_1^{N-1} p_\lambda.$$

To a first approximation the average contribution resulting from a is independent of κ and simply amounts to

$$(N-1)a\begin{pmatrix}1&0&0\\0&1&0\\0&0&1\end{pmatrix}.$$

The average contribution which results from the anisotropy constant b will to a first approximation be proportional to κ and originate from the term $-U/T$ in the expression (19).

From considerations of rotational invariance it is at once obvious that only the xy component of p in (27) gives a contribution which differs from zero. Its average value per molecule per unit volume will be

$$\bar{p}_{xy}=b\sum_1^{N-1}\langle\langle\alpha_\lambda\beta_\lambda\rangle_{Av}\rangle_{Av},$$
$$=b\frac{\kappa\zeta L^2}{2\theta N}\langle(\textstyle\sum_\lambda\alpha_\lambda\beta_\lambda)(\sum_{\mu\nu}g_{\mu\nu}\alpha_\mu\beta_\nu)\rangle_{Av}. \tag{28}$$

The angular brackets enclosing the product in the third member of (28) means that we are to integrate over a Boltzmann distribution $\exp(-T/\theta)\Pi dpdq$. Since no $\dot{q}$ occurs, we can at

once average over the q's, with $A^{\frac{1}{2}}$ as weight factor:

$$\langle F\rangle_{Av}=\int FA^{\frac{1}{2}}\prod dq\Big/\int A^{\frac{1}{2}}\prod dq. \qquad (29)$$

It is suitable first to use the following formula which follows immediately from rotational invariance and in which the choice of the coordinate system no longer plays a part:

$$\tfrac{1}{2}\langle\alpha_\lambda\beta_\lambda(\alpha_\mu\beta_\nu+\alpha_\nu\beta_\mu)\rangle_{Av} =(1/15)\langle\{\tfrac{3}{2}(\lambda\mu)(\lambda\nu)-\tfrac{1}{2}(\mu\nu)\}\rangle_{Av}. \qquad (30)$$

We thus obtain for the polarization tensor per molecule:

$$\bar{p}_{xx}=\bar{p}_{yy}=\bar{p}_{zz}\backsimeq Na,\quad \bar{p}_{xz}=\bar{p}_{yz}=0,\quad \bar{p}_{xy}\backsimeq C\kappa b, \qquad (31)$$
$$C=\frac{\zeta L^2}{60\theta N}\sum_{\lambda\mu\nu}g_{\mu\nu}\{3\langle(\lambda\mu)(\lambda\nu)\rangle_{Av}-\langle(\mu\nu)\rangle_{Av}\}.$$

This shows that the polarization tensor is deformed as a result of the flow; it has become "tri-axial." For electrical oscillations parallel to z the polarization has remained Na, as in the liquid at rest. In the directions perpendicular to z which make angles of 45° and −45° with the x and y axis, however, the polarization has respectively increased and decreased by an amount $C\kappa b$.

The constant C is proportional to ζ, and therefore to the viscosity of the liquid, and inversely proportional to the absolute temperature. Above all, however, we are interested in its dependence on the number of links in the molecule. To discuss this dependence, we note that according to (31) everything depends on the correlation between the orientations of different links, in as far as λ, μ, and ν are different. For links which are far apart, this correlation is practically negligible. In the model of completely free rotation of neighboring links with respect to each other only the correlation between two adjacent links differs perceptibly from zero. The main terms are then doubtless those for which μ and ν in (31) are exactly or almost equal. In this case the average value of $3(\lambda\mu)(\lambda\nu)$ practically cancels that of $(\mu\nu)$ if λ differs perceptibly from μ, and the sum in formula (31) becomes approximately

$$2\sum_{1}^{N-1}g_{\mu\mu}\backsimeq\tfrac{1}{3}N^3,$$

while for the constant C we obtain the approximate expression

$$C\backsimeq\frac{\zeta L^2}{180\theta}N^2. \qquad (32)$$

If in (28) we had only retained the term with $\lambda=\mu=\nu$, we would have arrived at the same result. Thus the double refraction by a single molecule becomes proportional to the square of the number of links, as was also found by Hermans. It is to be expected that in a more accurate calculation applied to the pearl necklace with completely free rotation, the result will have to be corrected by a factor which does not differ much from unity. With the partially free rotation of actual molecules the analogous correction factor will be larger than 1; for C−C bonds a preliminary estimate yielded a value between 2 and 3.

6. REMARKS ON THE APPROXIMATIONS INVOLVED

I. Influence of the Pressure Forces

In formula (1) the force which results from the non-uniform pressure in the flow of liquid has been neglected. If a_{x_i} represents the x component of the acceleration **a** at the center of the ith particle and if m_i' is the mass of liquid replaced by the particle, the x component of the force concerned is $m_i'a_{x_i}$. Since in a stationary flow we have

$$a_x=\frac{1}{2}\frac{\partial}{\partial x}(\nabla\Psi)^2,\quad (y),\quad (z)$$

the influence of the pressure would result in an additional term

$$-\tfrac{1}{2}\sum_i m_i'(\nabla\Psi_i)^2$$

in U. If Ψ is considered small of the first order, our approximation amounts to omitting a term of the second order. With the potential $\Psi=-\frac{1}{2}\kappa xy$ used by us, the ratio between the pressure force ma and the frictional force $\zeta v''$ is of the order $m'\kappa/\zeta$, which for a sphere of radius 10^{-7} in water ($\eta=0.01$) is about $10^{-13}\kappa$, i.e., negligible.

II. Influence of Rotation

So far we have not accounted for the rotation of the liquid. If the flow of the liquid consists

exclusively of a uniform rotation, the average behavior of our system can still be described on the basis of an assembly in temperature equilibrium if we insert the distribution

$$W \prod dpdq = \exp\left[-(T-(\mathbf{\Omega I}))/\theta\right] \prod dpdq. \quad (33)$$

Here $\mathbf{\Omega}$ is the angular velocity of the liquid and I the angular momentum of the system. On account of the fact that in the absence of forces I would be an additive integral of motion, such a distribution would be stationary in an ideal gas whose particles are systems of the type considered here. Maxwell already pointed out, that with free particles this distribution corresponds to a uniform rotation of a gas with angular velocity Ω. Similarly, in the present case, where each particle possesses in addition internal degrees of freedom, the distribution mentioned includes a superposed uniform rotation of each of the mass-points constituting the systems. This is at once evident from the identity

$$T-(\mathbf{\Omega I}) = \sum \tfrac{1}{2} m_i(\dot{x}_i^2+\dot{y}_i^2+\dot{z}_i^2) - \sum m_i(\mathbf{\Omega}[\mathbf{r}_i\dot{\mathbf{r}}_i])$$
$$= \sum_i \{\tfrac{1}{2} m_i(\dot{\mathbf{r}}_i - [\mathbf{\Omega r}_i])^2 - \tfrac{1}{2} m_i([\mathbf{\Omega r}_i])^2\},$$

since it shows that the distribution (33) is equivalent to the distribution

$$W = e^{-(T'+U')/\theta},$$

if T' is considered as the kinetic energy referred to the coordinate system rotating with angular velocity Ω, while

$$U' = -\tfrac{1}{2} \sum_i m_i([\mathbf{\Omega r}_i])^2$$

represents the potential of a centrifugal force acting on all the particles. The influence of the pressure forces can be accounted for by the potential

$$U'' = \tfrac{1}{2} \sum_i m_i'([\mathbf{\Omega r}_i])^2.$$

If the system consists of spheres with the same specific weight as that of the liquid, $m_i = m_i'$, and U' and U'' exactly cancel.

If now the system is placed in a liquid which itself rotates with angular velocity Ω, the systematic and the random forces exerted by the liquid will be the same in the rotating coordinate system as in a liquid at rest: the distribution (33) will, therefore, be left undisturbed.

If the flow is stationary but of an arbitrary nature and not irrotational, the equilibrium distribution can no longer be described by one of the simple assemblies known in the kinetic theory of gases. Using a method known from the theory of the Brownian movement,[4] it is then still possible to construct an equation of diffusion which describes the change with time of an arbitrary distribution in phase space. We would then have to determine the stationary solution of this equation. In the special case of the flow (16), representing the superposition of a pure rotation and an irrotational flow, both of which are proportional to κ, the mathematical problem becomes more simple. Yet it would not be permissible to assume that the stationary distribution is now described by a simple combination of (33) and (4), i.e., by

$$W = \exp\left[-(T+\tfrac{1}{2}\kappa I_z - \tfrac{1}{2}\kappa\zeta \sum xy)/\theta\right].$$

This is seen, for instance, from the fact that with increasing κ the system will gradually be oriented parallel to the direction of the flow, whereas according to this formula there can only be question of a preference orientation at 45°. Each of the two terms following T in the exponent applies only in the absence of the other one. However, if their influence on the distribution is small, errors will only occur if one would be interested in effects of the order κ^2. Effects of the order κ will be described by the distribution

$$W = e^{-T/\theta}\{1 - \tfrac{1}{2}\kappa I_z/\theta + \tfrac{1}{2}\kappa\zeta \sum xy/\theta\}.$$

As the term with I_z cannot have any influence on the double refraction (since it corresponds to a uniform rotation of the liquid) we are led to conclude that it was actually permissible to neglect the rotation in the preceding section. The rotation can also be neglected in the viscosity. The terms which must be added to the sum $\sum X''y$ in Section 4 in order to account for the rotation in the determination of δP_{xy}, exactly cancel in as far as quantities $\sim\kappa$ are concerned. This follows at once from the fact, that $\delta P_{xy}=0$ in pure rotation, but it can, of course, also be verified by direct calculation (the term with $-\tfrac{1}{2}\kappa I_z/\theta$ in the last mentioned formula will then also play a part).

A simple estimate shows that even with molecules of a length 10^{-4} cm, it will not be simple to realize κ values of such a magnitude

[4] H. A. Kramers, Physica **7**, 287 (1940).

that κ^2 effects would be perceptible in dilute solutions.

7. RAMIFIED MOLECULES

In virtue of the derivations of the formulas (23) and (31) for viscosity and birefringence, these formulas also hold good for branched molecules; we will only have to insert other expressions for $g_{\mu\nu}$. These $g_{\mu\nu}$'s occur, for instance, in the expression

$$T=\frac{mL^2}{2N}\sum_{\mu\nu} g_{\mu\nu}(\dot{\mu}\dot{\nu}), \quad (\dot{\mu}\dot{\nu})=(\dot{\alpha}_\mu\dot{\alpha}_\nu+\dot{\beta}_\mu\dot{\beta}_\nu+\dot{\gamma}_\mu\dot{\gamma}_\nu),$$

representing the kinetic energy of the molecule if the movement of the center of gravity is omitted. The value of $g_{\mu\nu}$ can now be determined in the following manner.

Cut the molecule at the μth link and at the νth link; it will then fall apart in three pieces, to wit two end pieces which contain, respectively, half the μth and half the νth link, and a middle piece. The number of particles in these three parts is called N_1, N_2, and N_3, respectively; their sum is N. With $\mu=\nu$ we get $N_3=0$.

If $\mu\neq\nu$, the expression

$$T_{\mu\nu}=\frac{mL^2}{2N}\{g_{\mu\mu}(\dot{\mu}\dot{\mu})+2g_{\mu\nu}(\dot{\mu}\dot{\nu})+g_{\nu\nu}(\dot{\nu}\dot{\nu})\},$$

will be equal to the kinetic energy of a macromolecule, in which only the links μ and ν possess non-zero angular velocities $\dot{\omega}_\mu$ and $\dot{\omega}_\nu$ while all other links perform translations only, in such a way that the center of gravity remains fixed in space. $T_{\mu\nu}$ therefore also represents the kinetic energy of a system of three particles with masses mN_1, mN_2, and mN_3, of which both 1 and 3 and 3 and 2 are connected by a rod of length L. Since the g's are numerical coefficients, it will suffice to consider the case where the particles momentarily are lying on a straight line. Introducing the momentary velocities v_1, v_2, and v_3:

$$N_1v_1+N_2v_2+N_3v_3=0,$$

$$v_3-v_1=L|\dot{\omega}_\mu|, \quad v_2-v_3=L|\dot{\omega}_\nu|,$$

we get

$$T_{\mu\nu}=\tfrac{1}{2}m(N_1v_1^2+N_2v_2^2+N_3v_3^2)$$

$$=\frac{mL^2}{2N}\{N_1(N_3+N_2)(\dot{\mu}\dot{\mu})+2N_1N_2(\dot{\mu}\dot{\nu})+(N_1+N_3)N_2(\dot{\nu}\dot{\nu})\}. \quad (34)$$

This shows that the value of $g_{\mu\nu}$ is equal to the product of the numbers of particles in the end pieces which are formed when cutting the μth and the νth link:

$$g_{\mu\nu}=N_1N_2. \quad (35)$$

Specializing $\mu=\nu$, or also directly from (34), we obtain

$$g_{\mu\mu}=N_1N_2 \quad (36)$$

where N_1 and N_2 are the numbers of mass-points in the two pieces in which the molecule falls apart when cutting the μth link.

We will now restrict ourselves to the viscosity. In order to compute the friction from (23), we may assume that with completely free rotation of two adjacent links the average value $\langle(\mu\nu)\rangle_{Av}$ for two different links ($\mu\neq\nu$) is almost always zero, as it was in the unbranched pearl necklace. For the effect of a single molecule on the friction this gives

$$\delta\eta=\frac{\zeta L^2}{6N}\sum_\mu g_{\mu\mu}=\frac{\zeta L^2}{6}\langle N_1N_2\rangle_{Av}, \quad (37)$$

where the angular brackets with subscript $_{Av}$ now indicate the average value over all possibilities of cutting.

For an unbranched molecule this average value becomes

$$\langle N_1N_2\rangle_{Av}=\frac{1}{N}\sum_1^{N-1} N_1(N-N_1)$$

$$\leqq N^2\int_0^1 x(1-x)dx=N^2/6$$

in conformity with the formula (24). For a ramified molecule $\langle N_1N_2\rangle_{Av}$ will always be smaller. For instance, if the molecule consists of s branches of N/s links each, all starting from a single point:

$$\langle N_1N_2\rangle_{Av}=\{1/(2s)-1/(3s^2)\}N^2.$$

For $s=1$ and for $s=2$ this is equal to $N^2/6$, as it should be, but for $s>2$ it is always smaller than $N^2/6$.

8. VISCOSITY CONTRIBUTION OF A MACROMOLECULE CLOSED TO A RING

Let a linear molecule consisting of N particles be closed to a ring by joining the Nth mass point to the 1st particle by means of an Nth link of

length L. The kinetic energy will still be given by

$$T=\frac{mL^2}{2N}\sum_{\mu,\nu=1}^{N-1} g_{\mu\nu}(\dot{\mu}\dot{\nu}), \tag{38}$$

but as a result of the new kinematic bond the possible values of T will be independent of the link which is assumed to have closed the ring. The coefficients $g_{\mu\nu}$ may, therefore, be replaced by the average values of all $g_{\mu\nu}$'s for which the μth and the νth link are separated by the same number of links in the ring:

$$\bar{g}_{\mu\nu}=\frac{1}{N}\sum_{0}^{N-1}\rho\, g_{\mu+\rho,\,\nu+\rho} \cong\frac{1}{6N}\{|\mu-\nu|^3+(N-|\mu-\nu|)^3\}.$$

The link between N and 1 will be equivalent to the others; the numbers μ and ν will vary from 1 to N. In the sum the numbers $\mu+\rho$ (and $\nu+\rho$) must be considered as identical with $\mu+\rho-N$ (and $\nu+\rho-N$) in all cases where $\mu+\rho$ (or $\nu+\rho$) would be larger than N. The third member in the equation is obtained by realizing that the sum must be extended over all possible positions of the closing link, so that it consists of two sums of the type $\sum\mu(N-\mu)\cong N^3/6$ (compare Eq. (24)). If the distance between μ and ν is described by an angle $2\pi\tau=2\pi|\mu-\nu|/N$, which would represent the angular distance between these links if the ring were a circle, one can also write

$$\bar{g}_{\mu\nu}\cong\tfrac{1}{6}N^2(1-3\tau+3\tau^2),\quad 0\leqslant\tau\leqslant 1. \tag{39}$$

The identity of

$$\bar{T}=\frac{mL^2}{2N}\sum\bar{g}_{\mu\nu}(\dot{\mu}\dot{\nu}) \tag{40}$$

with (38) results, of course, from the relations

$$\sum_{\nu=1}^{N}(\dot{\mu}\dot{\nu})=0$$

which in their turn are a result of the ring-condition

$$\sum_{1}^{N}\omega_\nu=0. \tag{41}$$

From (41) it also follows that $\sum_{\mu,\nu}(\dot{\mu}\dot{\nu})=0$, and we may therefore subtract a constant from $\bar{g}_{\mu\nu}$. In other words, instead of (39) one might also write

$$\bar{g}_{\mu\nu}=-\tfrac{1}{2}N^2\tau(1-\tau). \tag{42}$$

The influence of a ring-shaped molecule on the friction will be given by

$$\delta\eta=\frac{\zeta L^2}{6N}\sum_{\mu,\nu}^{N-1} g_{\mu\nu}\langle(\mu\nu)\rangle_{Av}=\frac{\zeta L^2}{6N}\sum_{\mu,\nu}^{N}\bar{g}_{\mu\nu}\langle(\mu\nu)\rangle_{Av}. \tag{43}$$

To calculate the average values $\langle(\mu\nu)\rangle_{Av}$, one would have to know the distribution of the ω's. This distribution is determined in principle by the square root of the determinant A of the quadratic expression $T(\dot{q}_1\cdots\dot{q}_s)$ after transformation into suitable generalized coordinates. It is easy to see that even our former $A^{\frac{1}{2}}$, in which $\vartheta_1\varphi_1,\cdots\vartheta_{N-1}\varphi_{N-1}$ served as generalized coordinates, will represent the distribution concerned, if we restrict ourselves to those values of ϑ and φ for which the distance between the Nth and the 1st particle is L. In fact, it would have been a sufficient approximation if the kinematic relation which expresses this condition is omitted and replaced by the introduction of a potential energy $U'=\frac{1}{2}K(r_{N1}^2-L^2)^2$. Here r_{N1} represents the distance between the 1st and the Nth particle, while K is a constant of sufficient magnitude. The distribution of the ω's would then be described accurately by $A^{\frac{1}{2}}\exp(-U'/\theta)$, and this amounts exactly to the prescription given.

However, without going into detailed calculations, the sum in (43) can be determined for a pearl necklace with completely free rotation if we take into account that the correlation between two different links μ and ν which leads to a non-zero $\langle(\mu\nu)\rangle_{Av}$-value, will almost always be the same, independent of whether μ and ν are now lying close together or not. It thus follows from the ring-condition (41) that

$$0=\textstyle\sum_\nu\langle(\mu\nu)\rangle_{Av}=\langle(\mu\mu)\rangle_{Av}+\sum_{\mu\neq\nu}\langle(\mu\nu)\rangle_{Av} =1+(N-1)\langle(\mu\nu)\rangle_{Av\,\mu\neq\nu}, \tag{44}$$

$$\langle(\mu\nu)\rangle_{Av\,\mu\neq\nu}\cong-\frac{1}{N}.$$

Consequently, if we use the expression (42) for $\bar{g}_{\mu\nu}$:

$$\textstyle\sum_{\mu\nu}\bar{g}_{\mu\nu}\langle(\mu\nu)\rangle_{Av}=\sum_\mu\bar{g}_{\mu\mu}-\frac{1}{N}\sum_{\mu\neq\nu}\bar{g}_{\mu\nu} =0+\frac{1}{N}\cdot N\int_0^1\tfrac{1}{2}N^2\tau(1-\tau)dN\tau =\tfrac{1}{2}N^3(\tfrac{1}{2}-\tfrac{1}{3})=\tfrac{1}{12}N^3. \tag{45}$$

Since the analogous sum was $N^3/6$ for the free linear pearl necklace, it appears that *the ring formation has reduced the influence on the friction to ½ of the original amount.*

For a linear pearl necklace with fixed angle α between two successive links $\sum_\nu \langle(\mu\nu)\rangle_{Av}$ was equal to $\mathrm{ctg}^2 \frac{1}{2}\alpha$, and the sum needed only to be taken over a small number of neighboring links (unless α would be too close to zero). It is clear that in the case of rings, the formula (44) must then be replaced by

$$\langle(\mu\nu)\rangle_{Av} \; {}_{\mu\neq\nu} \backsimeq -\frac{1}{N} \mathrm{ctg}^2 \tfrac{1}{2}\alpha,$$

and that the sum (45) must also be multiplied by a factor $\mathrm{ctg}^2 \frac{1}{2}\alpha$. Thus, here again, as was to be expected, it still holds good that ring closing reduces the effect to ½ of the original figure.

There will now be no further difficulty in the problem of arbitrarily ramified molecules containing one or more separate rings. As soon, however, as the different rings are no longer separate, i.e., if they have one or more chain segments in common, the $\langle(\mu\nu)\rangle_{Av}$'s can no longer be determined in this simple manner.

Editor's Note:

This article is a translation by J. J. Hermans and H. A. Kramers of an original appearing in Physica in January, 1944. Because of wartime restrictions imposed by the Germans, the original appeared in Dutch. The innovation of publishing a translation was thought to be justified by the inaccessibility of the original to many readers because of the language barrier. The editors and publishers of Physica gave their kind permission for the publication of this translation.

THE JOURNAL OF CHEMICAL PHYSICS VOLUME 14, NUMBER 7 JULY, 1946

Conductometric Investigation of Electrolytic Solutions in Hydrocarbons

ANDREW GEMANT
The Detroit Edison Company, Detroit, Michigan

(Received April 22, 1946)

Conductometric investigations were made of electrolytic solutions in xylene and of a hydrocarbon oil both of which have conductivities of from 10^{-12} to 10^{-11} mho/cm at room temperature. The electrolytes introduced were composed of an organic basic and an organic acidic material, the former being an amine. A three-component system (amine, aliphatic acid, and a phenol) was generally required in order to obtain high conductivities at relatively low concentrations of electrolytes. It is shown that the effect of the phenol is only partly caused by the increase of dielectric constant; the chief process is probably a specific one. On the theory that the mechanism consists in the formation of an addition-compound that subsequently dissociates into ions, the experimental data were subjected to an analysis. It appears that generally five or more single molecules combine to form a compound and that the concentration of the compound is a small percentage of the total solute present. The results have a bearing on the problem of deterioration of insulating oils. The high conductivities of the latter, even in the presence of certain colloidal constituents, are ultimately caused by electrolytic ions of the type investigated.

1. INTRODUCTION

IN certain previous publications[1–3] the author has introduced e.m.f. measurements in the study of insulating liquids for the purpose of obtaining additional information on the nature of electrolytic ions in such systems. Up to that time, the measurement of the electrical conductivity was essentially the only tool used for this particular purpose and it seemed that the addition of the e.m.f. method, which is most useful in the study of aqueous and alcoholic solutions, would be of value in this field, too. Results obtained in this series of researches to date seem to justify this enterprise.

The author used the glass electrode for the measurement of hydrogen ion concentrations in hydrocarbon solvents and hydrocarbon oils. E.m.f. data obtained from oils to which a strong acid (organic sulfonic acid) was added could be interpreted quantitatively on the basis of a reversible electrode action of the glass. When,

[1] Andrew Gemant, J. Chem. Phys. **10**, 723 (1942).
[2] Andrew Gemant, J. Chem. Phys. **12**, 79 (1944).
[3] Andrew Gemant, J. Chem. Phys. **13**, 146 (1945).

however, the technique was used for oils that were oxidized in the laboratory, or deteriorated in service, the hydrogen ion concentration appeared much too low to account for the measured electrical conductivity. The conclusion was drawn, therefore, that the cation in such oils was not the hydrogen ion. It should be pointed out that this conclusion was based on direct proof obtained from specific e.m.f. data. This result is in keeping with those obtained by J. D. Piper and co-workers[4]; these authors showed that solutions of purified acids in paraffin oil do not produce the high conductivity present in oxidized oils.

Since the cations in oxidized or deteriorated oils, which exhibit increased conductivity, are not hydrogen ions, the further conclusion was drawn that they must in all probability be organic in nature, just as are the anions. What their exact chemical nature is could probably be found from e.m.f. measurements, if appropriate electrodes were available. In attempting to do further work in this direction, the next step in the research seemed to be the establishment and conductometric investigation of solutions in hydrocarbon oils of electrolytes of which both ions are organic. Obviously, organic amines are best suited for such a purpose, although there are other compounds (certain triphenylcarbinol derivatives, for instance) that under certain circumstances, particularly in combination with halogens, show cation-like behavior. The conclusion that the cations in hydrocarbon solvents are amines is supported in the literature. Fuoss and Kraus[5] investigated the conductivities of tetraisoamylammonium nitrate in mixtures of dioxane and water. J. B. Dickey[6] has obtained a series of patents on treating yarns with certain compounds (diethylcyclohexylamine salts of phosphinated ketones and the like) in order that static electricity be avoided during subsequent weaving. Since the yarns during weaving are in oil, it is likely that the organic salts are dissolved in the oil and form semi-conducting solutions. J. D. Piper and collaborators[4] also have examined, among a great variety of added materials, the effect of salts of organic amines upon the electrical conductivity of paraffin oil; they obtained high conductivities at 80°C.

2. SOLUTIONS IN XYLENE

Although the majority of data in this paper refer to a hydrocarbon oil, several sets of measurements were carried out with xylene and benzene as solvents. As will be shown in the section dealing with hydrocarbon oil, appreciable conductivities at relatively low concentrations of the electrolytes are obtainable only in a three-component system, consisting of an amine, an aliphatic acid, and a phenolic compound. In solvents such as xylene or benzene, however, probably because of their higher dielectric constant, two-component systems (amine and aliphatic acid or amine and phenolic) are sufficient to cause reasonably high conductivities, although even in these solvents the three compounds together are far more effective. In this section solutions in xylene of α-naphthylamine and phenol are dealt with in detail. All chemicals used in this research were high grade commercial products, and were used without additional purification.

The tests consisted in preparing a series of solutions of various normalities with regard to the solutes added, and measuring the conductivities at room temperature in a cell designed by J. C. Balsbaugh.[7] A variable-frequency power factor bridge was used, and the range of frequencies extended from 50 to 20,000 c.p.s. As explained later in this paper in the part dealing with solutions in oil, no variation of the conductivity with frequency was observed during the many checks at several frequencies. In addition to the conductivity, the dielectric constant, too, was determined for each solution of the series.

The obtained conductivities were corrected for the conductivities observed when either of the two components was added separately. This was necessary because the ion formation from electrolytes consisting of organic cations *and* anions was the only point of interest in this connection. Thus, the conductivities caused by either component alone were deducted from the total. If the

[4] J. D. Piper, A. G. Fleiger, C. C. Smith, and N. A. Kerstein, Ind. Eng. Chem. **32**, 1510 (1940); **34**, 1505 (1942).
[5] R. M. Fuoss and C. Kraus, J. Am. Chem. Soc. **55**, 2387 (1933).
[6] J. B. Dickey, U. S. Pat. 2,256,112; 2,286,791, and 2,286,794, 1941 and 1942.
[7] J. C. Balsbaugh and A. G. Assaf, Ind. Eng. Chem. **13**, 515 (1941).

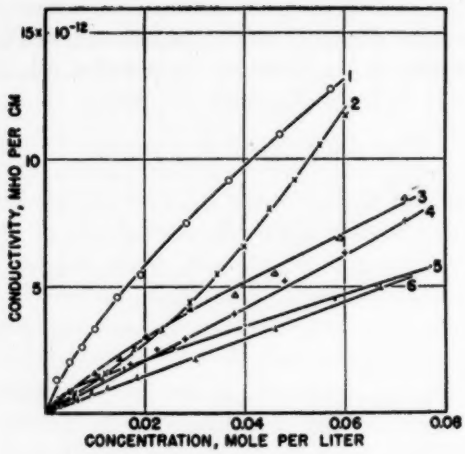

FIG. 1. Conductivity at room temperature *vs.* concentration of solutions in xylene. The conductivities in this as in all other figures are corrected for initial conductivities of the starting solutions, as explained in the text.

Curve 1 = Concentration of α-naphthylamine: varying; that of phenol: 0.23 normal.
Curve 2 = Concentration of α-naphthylamine: 0.23 normal; that of phenol: varying.
Curve 3 = Concentration of α-naphthylamine: varying; that of phenol: 0.16 normal.
Curve 4 = Concentration of α-naphthylamine: 0.16 normal; that of phenol: varying.
Curve 5 = Concentration of α-naphthylamine: varying; that of phenol: 0.08 normal.
Curve 6 = Concentration of α-naphthylamine: 0.08 normal; that of phenol: varying.

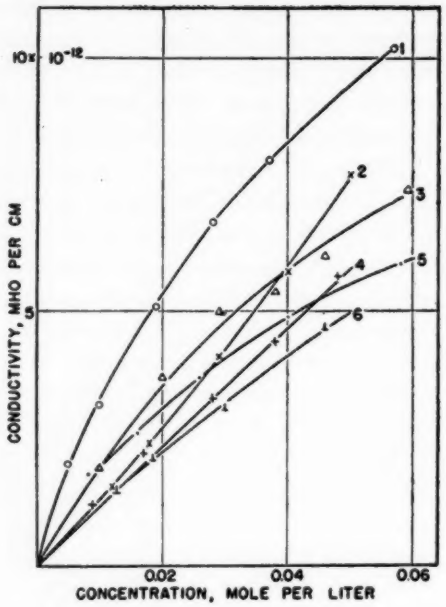

FIG. 2. Conductivity *vs.* concentration of solutions in xylene; conductivity data reduced to a dielectric constant of 2.45.

Curves 1 to 6: the same as in Fig. 1.

hypothesis that ion formation from such types of electrolytes plays an important role in liquid dielectrics is correct, then the corrections applied should be relatively small parts of the total. This expectation was very strikingly fulfilled in the case of oil as solvent, as will be shown later. For xylene the deducted amounts were larger, ranging from about 20 to 35 percent of the total.

In each series the concentration of one component was kept constant while that of the other was increased by steps. In three sets the concentration of α-naphthylamine was kept at, respectively, 0.08, 0.16, and 0.23 normal; in three other sets the concentration of phenol was kept at the same percentages. The results obtained from these six series is shown in Fig. 1 in which the conductivity in mho/cm is plotted against the normality of the component that was varied by steps. The conductivities are all corrected as described above; they are of the order of 10^{-12} to 10^{-11} mho/cm. It was not deemed necessary to present the uncorrected conductivities, as observed, for all series of measurements presented in this paper; as an illustration, however, the uncorrected data will be given for three particular series of solutions dealt with in Section 3*a*.

One of the reasons for the increase in conductivity with increasing concentration is the increase of the dielectric constant. In order to find out in what manner the conductivity depends on the concentration of dissociable material, the effect of the varying dielectric constant must be eliminated. Although the variation of the latter was rather small in this series (from 2.39 to 2.48), such a procedure was considered necessary. It was carried out in the following manner.

One of the six series (with 0.08*n* α-naphthylamine) was repeated with 3.5 percent by volume chloroform added to the solutions. It was assumed that the essential role of the chloroform was to raise the dielectric constant without acting specifically upon the various solutes. By this means the dielectric constant was increased throughout by an increment close to 0.06. The conductivities at corresponding concentrations of phenol were found to differ by a factor close to 1.60. In the narrow range of dielectric constants involved it is safe to take a simple exponential variation between the conductivity and the dielectric constant. In other sections of this paper

a different procedure was employed, in which no use of the special assumption of an exponential variation was made. In order to eliminate the role of the dielectric constant, all conductivities were reduced to an arbitrarily selected value of dielectric constant. The value 2.45, lying in the middle of the range, was selected. The conductivity σ at a dielectric constant D is then reduced to $\sigma_{2.45}$, its value at a dielectric constant 2.45, by the relation:

$$\sigma_{2.45}=\sigma 1.60^{(2.45-D)/0.06}. \quad (1)$$

The corrected conductivity data are presented in Fig. 2; the curves, as can be seen, are somewhat different from those in Fig. 1. The variation of σ shown in Fig. 2 is caused solely by the increase in concentration of the two solutes.

A possible mechanism of ion generation as observed in these systems is the formation of an addition compound with subsequent ionic dissociation (this subject is further discussed at the end of this paper). While it is not maintained that the experimental data furnish compelling proof for this explanation, it is thought to be at least a useful guiding hypothesis for the interpretation of the data. It is possible that a continuation of these studies will indicate the desirability of a different approach to the problem; one of the various other possibilities is, for instance, the theory of multiple ion formation, as suggested by Fuoss and Kraus.[5]

Let us then denote the basic constituent by B, the acidic one by A, and assume that n molecules of B and m of A form a compound B_nA_m:

$$nB+mA\rightleftarrows B_nA_m.$$

If concentrations in mole/liter are denoted by c with respective indices, we have

$$K_a c_B{}^n c_A{}^m = c_{B\ A_m}, \quad (2)$$

TABLE I. Conductivities of solutions in hydrocarbon oil.

Concentration in mole/liter			Conductivity
Tributylamine	Oleic acid	o-Cresol	in mho/cm
0.05	0.05	—	1.7×10^{-14}
0.05	—	0.05	2.9
—	0.05	0.05	2.1
0.05	0.05	0.05	90
0.205	—	0.20	36
0.205	0.038	0.20	1700

where K_a = association constant. If B^+ denotes a positive and A^- a negative ion, formed by dissociation of the addition compound (this is the simplest, although by no means the only possible kind of dissociation), the reaction is

$$B_nA_m\rightleftarrows B^+ + A^-$$

and, with K_d = dissociation constant:

$$K_d c_{B_nA_m} = c_{B^+}c_{A^-}. \quad (3)$$

Since

$$c_{B^+}=c_{A^-}=c_i, \quad (4)$$

where c_i = ionic concentration:

$$K_aK_d c_B{}^n c_A{}^m = c_i{}^2. \quad (5)$$

Since the conductivity σ is given by

$$\sigma = 10^{-3}\Lambda_0 c_i, \quad (6)$$

with Λ_0 = equivalent conductivity, Eq. (5) yields

$$\sigma = k c_B{}^{n/2} c_A{}^{m/2}, \quad (7)$$

with

$$k = 10^{-3}\Lambda_0 (K_aK_d)^{\frac{1}{2}}. \quad (8)$$

In applying Eq. (7) and (8) to the present case, an inspection of Fig. 2 reveals that curves 1, 3, and 5 (variable amine content) follow approximately a square root function, while curves 2, 4,

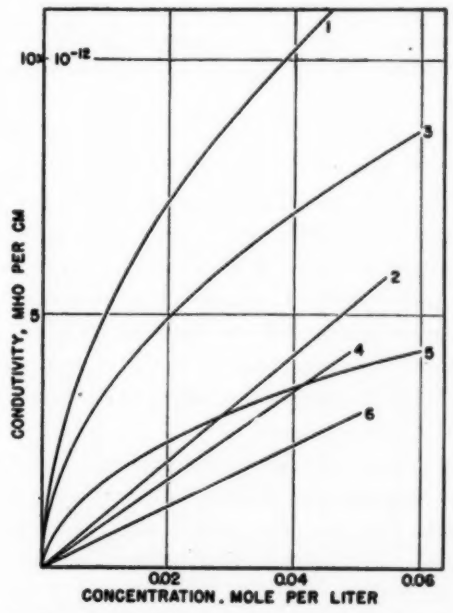

FIG. 3. Conductivity *vs.* concentration of solutions in xylene; calculated from Eq. (7).

Curves 1 to 6: the same as in Figs. 1 and 2.

TABLE II. Dielectric constants and conductivities (uncorrected) for three series of solutions in hydrocarbon oil.

Starting solution: 0.05n oleic acid 0.05n o-cresol			Starting solution: 0.05n tributylamine 0.05n o-cresol			Starting solution: 0.05n tributylamine 0.05n oleic acid		
Normality of tributylamine	Dielectric constant	Conductivity in 10^{-14} mho/cm	Normality of oleic acid	Dielectric constant	Conductivity in 10^{-14} mho/cm	Normality of o-cresol	Dielectric constant	Conductivity in 10^{-14} mho/cm
0.0000	2.210	2.1	0.0000	2.232	2.9	0.0000	2.234	1.75
0.0096	2.245	14	0.0092	2.266	22.5	0.011	2.253	7.1
0.019	2.281	39	0.018	2.289	37	0.022	2.275	17
0.028	2.301	58	0.027	2.303	51	0.032	2.290	32.5
0.036	2.310	71	0.035	2.312	62	0.042	2.310	60
0.044	2.317	80	0.047	2.323	77	0.053	2.325	93
0.052	2.319	91	0.058	2.331	89	0.062	2.341	135
0.060	2.324	100	0.069	2.337	101	0.072	2.355	187
0.067	2.326	106						

and 6 (variable phenol content) are approximately linear. It appears, then, that the main addition compound consists of one molecule of amine ($n=1$) and two molecules of phenol ($m=2$). The obvious disagreement of some of the curves (clearly of curve 2) with this simple behavior indicates that probably several addition compounds are formed, but that the one just mentioned prevails.

The conductivities at concentrations corresponding to the set of curves in Fig. 2 were calculated from Eq. (7) with $n=1$ and $m=2$. The value of k was adjusted so as to obtain an order of magnitude of 10^{-11} for σ at $c=0.06$. The value used was 2.2×10^{-10}. The plot of these calculated data is shown in Fig. 3 which is reasonably similar to Fig. 2.

In further verification of the mechanism here depicted, the measurements of Lucasse[8] may be quoted. The melting points of mixtures of p-toluidine and acetic acid have a maximum of 49°C at 66 percent of acetic acid, corresponding to a compound: 1 amine, 2 acid molecules—exactly the same ratio as the conductivity curves in Fig. 2 indicate. Thus Eq. (7) reproduces the measured data with one arbitrary constant k in a satisfactory manner.

The value of this constant, as required to satisfy the experimental data, may be used for an estimate of K_a, the association constant. In Eq. (8) the order of magnitude of Λ_0 is 60 (mobility of organic ions in a solvent of viscosity of 1 centipoise is around 30) and that of K_d is 10^{-18}; this order of magnitude was obtained[2] for a number of strong electrolytes (acids) in xylene and dioxane. With these figures a value of 10 is obtained for K_a from Eq. (8). This order of magnitude is significant: It shows that the compound formation is not complete (which is the case if K_a is much larger than 1), nor is the amount of compound formed only a very small fraction of the components (which is the case if K_a is much smaller than 1). From Eq. (2) the concentration of the compound can be computed, using $K_a=10$; if, for instance, both components are present in a normality of 0.05, the concentration of the compound is 0.001 which is about 2 percent of the amine.

3. SOLUTIONS IN HYDROCARBON OIL

The hydrocarbon oil used was a typical transformer oil of a viscosity of 0.14 poise at 25°C, a dielectric constant 2.18, and an electrical conductivity 1×10^{-14} mho/cm at 25°C. Three different systems of solutes were investigated which will be treated separately in the following.

(a). Tributylamine—Oleic Acid—o-Cresol Solutions

In testing hydrocarbon oils, it was observed that addition of an acidic and a basic component did not as a rule produce a noticeably increased conductivity at room temperature. The author was first inclined to believe that, concerning hydrocarbon oils, his conclusions with regard to the importance of organic cations were incorrect. Neither aliphatic acids, nor phenolic compounds —both weak acids in aqueous solutions—pro-

[8] W. W. Lucasse, R. P. Koob, and J. G. Miller, J. Phys. Chem. **48**, 85 (1944).

duced an effect, when added separately to solutions of the amine. When, however, acids of both types were added simultaneously to an oil containing an amine, the effect became pronounced. Table I shows that none of the three possible combinations in pairs of the three materials added produced a conductivity noticeably higher than that of the oil alone, while the three materials together had a rather pronounced effect. The last two lines show that even if the amine and cresol were present in excessively high concentrations, producing a conductivity of medium level, addition of relatively small amounts of acid increased the conductivity about fifty times. The correction to be applied to values of σ, in order to obtain the conductivity resulting from the combination alone, is only 2 to 3 percent.

Three series of measurements were carried out, each starting with a combination of two of the three solutes in concentrations of 0.05 mole/liter each. To these solutions the third solute was added in increasing concentrations. The dielectric constants and the total conductivities, as measured, for these three series are shown in Table II.

The dielectric constant D of the starting solutions was about 2.23, increasing with increasing concentration to about 2.34. This increase, while rather small, is significant because of the generally low level of D. The process of reducing the σ-values to one selected value of D was rather important. It was done by repeating all three series with an oil containing 10 percent by volume of chloroform. By this means the above quoted range of dielectric constants was raised to a level of about 2.40 to 2.50. By examining corresponding pairs of data (with and without $CHCl_3$), having conductivities σ and σ' and dielectric constants D and D', various values of σ/σ' were correlated with values of $(D-D')$. Or, since a

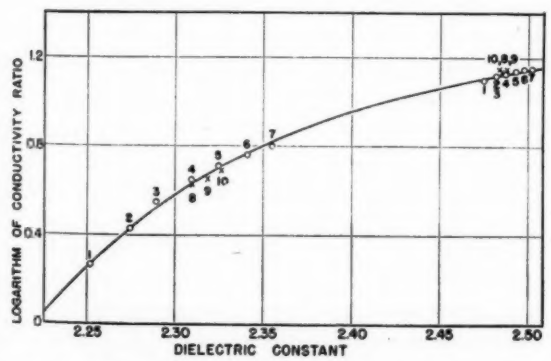

FIG. 4. Logarithm of conductivity ratio of tributylamine —oleic acid—*o*-cresol solutions in hydrocarbon oil *vs.* difference in dielectric constants.

Corresponding figures on curve refer to identical solutions except 10 percent by volume of chloroform added to increase the dielectric constant. × refers to curve 1 of Fig. 5. ○ refers to curve 3 of Fig. 5.

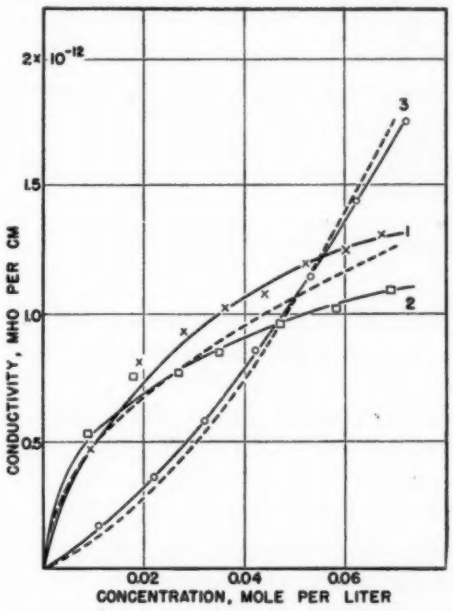

FIG. 5. Conductivity *vs.* concentration of solutions in hydrocarbon oil.

Curve 1: Tributylamine varying; oleic acid 0.05*n*; *o*-cresol 0.05*n*.
Curve 2: Tributylamine 0.05*n*; oleic acid varying; *o*-cresol 0.05*n*.
Curve 3: Tributylamine 0.05*n*; oleic acid 0.05*n*; *o*-cresol varying.
(Conductivity data reduced to a dielectric constant of 2.35.)
× □ ○ and solid lines: experimental data.
Dotted lines: calculated from Eq. (10).

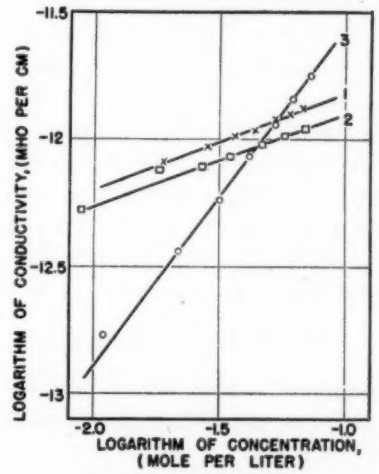

FIG. 6. The same as the solid lines of Fig. 5, plotted on a bilogarithmic scale.

Slope of curve 1 = 0.38.
Slope of curve 2 = 0.38.
Slope of curve 3 = 1.35.

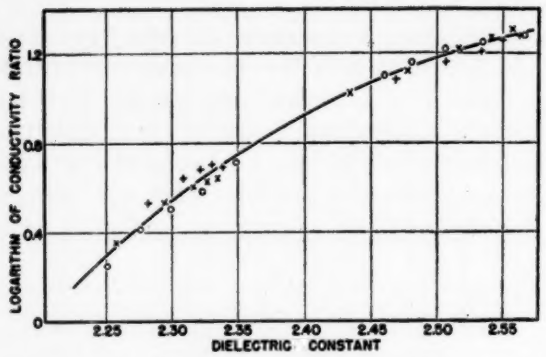

FIG. 7. Logarithm of conductivity ratio of tributylamine-myristic acid—α-naphthol solutions in oil *vs.* difference in dielectric constants.

× refers to curve 1 of Fig. 8.
+ refers to curve 2 of Fig. 8.
○ refers to curve 3 of Fig. 8.

plot of log (σ/σ') *vs.* D was attempted, values of $(\log\sigma - \log\sigma')$ were correlated with values of $(D-D')$.

These correlated data were then plotted in the manner shown in Fig. 4: differences in ordinates were plotted against differences in abscissas, pairs of data being shown by identical figures on the curve. As can be seen, the absolute value of the conductivity does not enter into the plot, and the curve is assumed to hold independently of the latter. With the aid of this curve all data were reduced to $D=2.35$, an average value for the range covered. Curve 1 of Fig. 5 refers to varying amine concentration, curves 2 and 3 to varying acid and *o*-cresol concentrations, respectively. The conductivities increase to about 2×10^{-12} mho/cm, an order of magnitude often found in deteriorated oils. The values are lower than for corresponding concentrations in xylene partly because of the higher viscosity of the solvent.

The same guiding hypothesis that was used in the previous case might be used here, too. Apart from the n molecules of base B, and m molecules of acid A, l molecules of a phenolic compound P will combine into a compound $B_nA_mP_l$:

$$nB+mA+lP\rightleftarrows B_nA_mP_l$$

that subsequently supplies a positive and a negative ion. Instead of Eq. (5) we then have:

$$K_aK_dc_B{}^nc_A{}^mc_P{}^l=c_i{}^2, \qquad (9)$$

and instead of Eq. (7):

$$\sigma=kc_B{}^{n/2}c_A{}^{m/2}c_P{}^{l/2}. \qquad (10)$$

Inspecting Fig. 5, curves 1 and 2 are found to follow approximately a square root function, while curve 3 is a $1\frac{1}{2}$ power function. The same curves plotted bilogarithmically in Fig. 6 reveal straight lines with slopes of 0.38, 0.38, and 1.35, respectively. The dotted lines in Fig. 5 were calculated from Eq. (10) according to these powers and made to cross at $c=0.05$ as they should if Eq. (10) were strictly correct. Since curves 1 and 2 do not coincide, Eq. (10) can be only approximately valid.

With $n=1$, $m=1$, and $l=3$, it appears that one molecule of amine, one molecule of acid, and three molecules of phenol combine into one: thus, a fairly large molecule results. The possible structure of such an addition compound will be discussed in the last section (discussion) of this paper.

The constant k corresponding to the calculated dotted lines in Fig. 5 has a value of 1.9×10^{-9}. This permits K_a to be estimated from Eq. (8). In the oil of viscosity 0.14 poise, it can be estimated[3] that Λ_0 is around 4 and K_d is of the order of magnitude of 2×10^{-16}. This gives $K_a=1\times10^3$. Hence, with all three components present in a concentration of 0.05 mole/liter each, the concentration of the compound is 4×10^{-4}, about 1 percent of the amine present.

(b). Tributylamine—Myristic Acid—α-Naphthol Solutions

As mentioned in Section 2, the chemicals used in this research were not subjected to laboratory purification. This implies that a repetition of these tests with purified materials would yield numerically somewhat different results. In particular, the objection could be raised against the data presented under (*a*) that oleic acid and *o*-cresol always contain admixtures and that the effect was, at least in part, caused by them. The low conductivity found in any pair of the three

TABLE III. Conductivities of solutions in a hydrocarbon oil.

Concentration in mole/liter			Conductivity in mho/cm
Tributylamine	Myristic acid	α-Naphthol	
0.05	0.05	—	1.4×10^{-14}
0.05	—	0.05	7.9
—	0.05	0.05	5.5
0.05	0.05	0.05	400

materials, however, can be brought against such objection.

To clarify this point further, a combination was chosen in which oleic acid was replaced by myristic acid and *o*-cresol by α-naphthol, both crystalline materials. The program for this part of the work was the same as that for the previous part. Three sets of solutions were investigated; each set contained two of the materials each 0.05 normal and the third material in increasing amounts. The "zero values" are shown in Table III. The conductivity of the solution containing all three components is 4×10^{-12}, more than four times that of the previous combination. This finding is reassuring in that impurities have probably only a secondary role in the effect observed.

The effect of the dielectric constant was evaluated in the same manner as before; the result of this "plot of differences" is shown in Fig. 7. Both this plot and Fig. 4 show that the effect of the dielectric constant increases with decreasing value of the latter, in keeping with the theory of Bjerrum.[9]

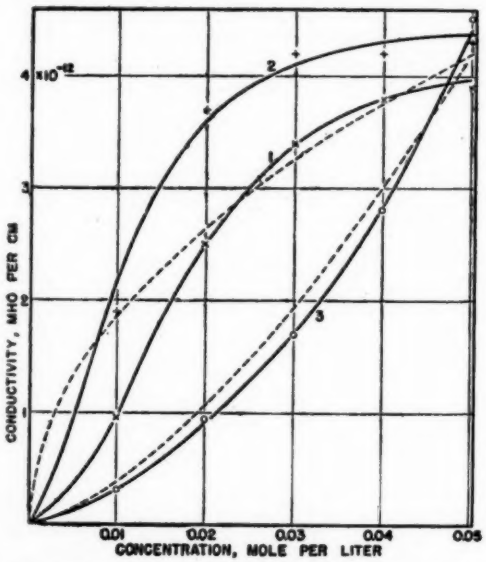

FIG. 8. Conductivity *vs.* concentration of solutions in hydrocarbon oil.

Curve 1: Tributylamine varying; myristic acid: 0.05*n*; α-naphthol: 0.05*n*.
Curve 2: Tributylamine 0.05*n*; myristic acid: varying; α-naphthol: 0.05*n*.
Curve 3: Tributylamine 0.05*n*; myristic acid: 0.05*n*; α-naphthol: varying.
(Conductivity data reduced to a dielectric constant of 2.35.)
X + O and solid lines: experimental data.
Dotted lines: calculated from Eq. (10).

[9] D. A. MacInnes, *The Principles of Electrochemistry* (Reinhold Publishing Corporation, New York, 1939), p. 372.

The conductivities, reduced to $D=2.35$, are shown in Fig. 8. As the dotted curves ($\frac{1}{2}$ and $1\frac{1}{2}$ power) show, the former is not in agreement with the experimental data below 0.01 normality. It appears that the type of the reaction changes with increasing concentration of the components. The experimental data are, however, not considered sufficiently complete to permit further interpretation of this upward trend of the curves at the origin. Using the location of the dotted lines, an evaluation analogous to the previous one gives $k=7.5\times10^{-9}$; $K_a=2\times10^{4}$, and the concentration of the compound for all three components present in 0.05 molar concentration is 6×10^{-3}, i.e., twelve percent of the amine present. The large conductivity effect obtainable with this combination is caused, according to the mechanism assumed, by an increased tendency for addition compound formation. The compound molecule containing three molecules of α-naphthol must have appreciable size.

(c). Triethanolamine—Oleic Acid Solutions

In addition to the series discussed, some tests were carried out with an amine containing

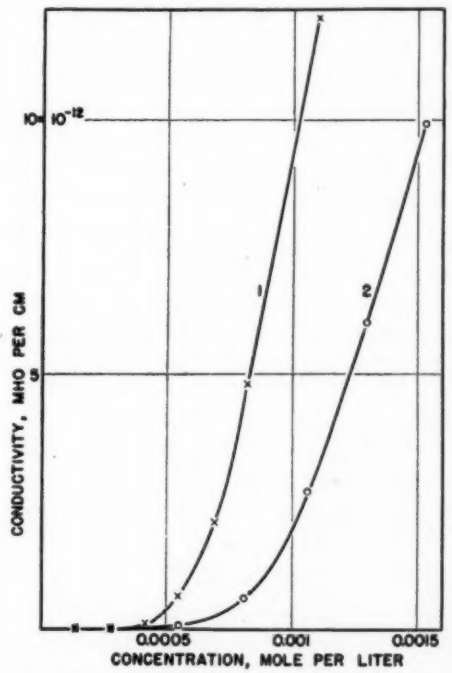

FIG. 9. Conductivity *vs.* concentration of solutions in hydrocarbon oil.

Curve 1: Triethanolamine: varying; oleic acid: 0.06*n*
Curve 2: Triethanolamine: varying; oleic acid: 0.03*n*.

hydroxyl groups: triethanolamine. Because of the low solubility of this compound only low concentrations were investigated, giving clear solutions —at least to the naked eye. The concentration limit at which inhomogeneity appeared was rather sharp, and measurements were carried out only well below that limit.

The dielectric constant was remarkably constant in these measurements (from 2.20 to 2.22), so that no correction in this respect was necessary. The results from two series are presented in Fig. 9. Curve 1 refers to an oleic acid content of 0.06 normal; curve 2, to one 0.03 normal. The concentrations of the amine are shown on the abscissa; the range covered was below 0.0015 normal. Solutions up to an amine concentration of about 0.01 normal were clear.

Because of the low solubility of this amine (in fact, it is insoluble in oil alone and dissolves only in the presence of the acid) the existence of a second phase, contributing by a Maxwell-Wagner effect to the high conductivity, might be suspected. In this case σ should be a function of frequency, and in particular, if measured with d.c. voltages, distinctly less. While a check of σ using several frequencies was occasionally carried out in all the series reported, a few data relating to this particular combination are given in Table IV. Even the second of the listed solutions, having the high conductivity of 10^{-10} at room temperature, shows no variation in the range between a frequency of 20,000 and d.c. voltages; this solution, by the way, remains clear to the naked eye even after prolonged standing. Accordingly, a Maxwell-Wagner effect on interphases can be ruled out.

The data obtained in this combination are not deemed sufficiently complete for the drawing of quantitative conclusions. In attempting to apply the mechanism suggested (compound formation with subsequent dissociation), the steepness of the curves suggests that a relatively large number of molecules are involved in the compound formation. An estimate of about eight molecules of amine and four molecules of acid is in keeping with the trend of the curves; the relatively large size of the compound is in agreement with the observed low solubility of the amine.

TABLE IV. Conductivities at various frequencies of solutions in hydrocarbon oil.

Concentration in mole/liter Triethanolamine	Oleic acid	Frequency, c.p.s.	Conductivity in mho/cm
0.00082	0.06	10,000	4.8×10^{-12}
0.00082	0.06	1,000	4.6
0.00082	0.06	100	4.4
0.00082	0.06	50	4.6
0.0068	0.06	20,000	96×10^{-12}
0.0068	0.06	10,000	96
0.0068	0.06	1,000	96
0.0068	0.06	d.c.	100

4. DISCUSSION OF THE RESULTS

While, for the sake of a systematic presentation, part of the discussion, particularly a quantitative interpretation of the data, has been included in the corresponding sections dealing with experimental results, two subjects deserve special consideration. One of these is the mechanism of conductivity in the three-compound systems in oil. The other subject is the bearing of the presented results on the problem of deterioration of insulating oils.

(a). Mechanism of Conductivity in the Three-Component Systems in Oil

If the conductivity is produced in a two-component, base-acid system, there can be little doubt that the mechanism is compound formation with subsequent ionic dissociation. Consequently the equations presented in Section 2 of this paper are probably safely founded. The extension of this mechanism to the three component base-acid-phenolic system, however, is not quite as obvious. One might first think of another possibility, namely, that the phenol simply plays the role of an addition to the solvent, increasing the dielectric constant of the latter. Hence, its action would be merely electrostatic. This possibility cannot be strictly disproved, but tests carried out with chloroform to show the effect of the dielectric constant upon the conductivity rule against it. Table V gives a few figures that are instructive in this respect. Solutions containing the phenolic component have a σ over 10^{-12}; those without the phenolic have, in spite of a considerable amount of $CHCl_3$, a σ below 10^{-12}. The first solution has a σ larger than the second, although its dielectric constant is lower than that of the second; the same is true if

TABLE V. Conductivities of solutions in hydrocarbon oil.

Concentration, mole/liter							
Tributyl-amine	Oleic acid	Myristic acid	*o*-cresol	α-naphthol	Chloroform	Dielectric constant	Conductivity mho/cm
0.05	0.05	—	0.072	—	—	2.35	1.9×10^{-12}
0.05	0.05	—	—	—	1.25	2.46	0.47
0.05	0.05	—	0.072	—	1.25	2.50	4.7
0.05	—	0.05	—	0.05	—	2.35	4.4
0.05	—	0.05	—	—	1.25	2.46	0.45
0.05	—	0.05	—	0.05	1.25	2.56	17

the fourth and fifth solutions are compared. It can be concluded that, although the purely electrostatic effect of the components is not negligible, the phenols have an effect on σ markedly greater than the electrostatic one.

Assuming, therefore, a compound formation between the three components, a question arises regarding the chemical structure of the compound. The amount of information contained in this paper is clearly not sufficient to answer this question in a definite manner. However, some indication as to the correct answer can be found in using the concept of resonance.[10]

The unshared pair of electrons of the amino nitrogen attracts a proton; this is the reason for the formation of an addition compound between an amine and an acid. The same holds for an addition between an amine and a phenol or a naphthol. If, now, an addition between an acid and a phenol should take place that leaves both hydroxyls free (hence, *not* an ester formation), then such a compound would be considerably stabilized through resonance in the presence of an amine, even if such a compound would be unstable in the absence of an amine. As an illustration of such resonating structures, formulas I and II are given; the position of the electron pair of the nitrogen is different in the two cases. If more than one molecule of the phenol or naphthol is attached to the acid, the stability of the compound is further increased. The experimental data presented indicate this to be the case. The addition of the phenol to the acid is probably due to secondary valencies; this structure obviously needs further elucidation. It should be pointed out that there are theoretical considerations that might be raised against the likelihood of such resonating structures.

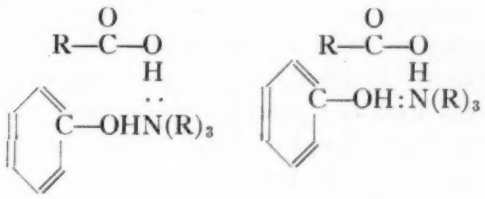

I II

Once a compound of the type suggested is formed—and, if it is formed, its concentration should be reasonably large, as shown in the previous sections—its dissociation to a small extent into ions is understandable. Even if the aliphatic acid itself in the oil is extremely weak, the presence of the phenol groups considerably strengthens its acidity.[10] The reason for this effect is, partly at least, the $^{-}CO^{+}$ dipole-moment of the phenol. More than one phenol group in the compound would further enhance this effect. The result of the dissociation is then the positive $HN^{+}(R)_3$ ion with the rest of the compound as the negative ion.

(b). Bearing of the Results Presented on the Problem of Deterioration of Oils

In investigating ionic solutions in oils, the question arises, to what extent are the ionic components responsible for the high conductivities of deteriorated oils. It is certain that such oils quite often reveal the presence of colloidal materials that appear to be related to their high conductivity. This standpoint is particularly emphasized by J. D. Piper and his co-workers.[11]

In the following it is shown that, even if colloidal particles add to the conductivity of oils,

[10] G. W. Wheland, *The Theory of Resonance* (John Wiley and Sons, Inc., New York, 1944), p. 167 *et seq.*

[11] Joseph Sticher and J. D. Piper, Ind. Eng. Chem. **33**, 1567 (1941).

the ultimate carriers of the electricity are in all probability molecularly dispersed ions. Three cases are now considered.

(1) If the inhomogeneity takes the form of a microscopic second phase dispersed in the oil, a Maxwell-Wagner effect might contribute to the conductivity. This, as the theory of the effect reveals, is ultimately caused by the bulk conductivity of the two phases, hence, by electrolytic ions.

(2) If the inhomogeneity is a colloidally dispersed second phase, a so-called lyophobic colloid, the particles might, owing to their charge, exhibit cataphoresis, thus contributing to the total conductivity.[12] Judging from aqueous solutions, the charges upon such particles are caused by preferential adsorption of one kind of the electrolytic ions present in the bulk of the liquid.

(3) If the inhomogeneity is a lyophilic colloid, in the majority of cases a so-called macromolecular solution, then an electrolytic dissociation of such macromolecules contributes to the conductivity. Examples are proteins, soaps, and the particles in Oden's sulphur sol. In these cases the concepts of the collodial particle and of the macromolecular electrolytic ion merge into one.

It is not maintained that the solutions investigated are identical with deteriorated oils. The exact nature of the ionic components can certainly vary within considerable limits.

Concerning the presence of acids and aromatic alcohols, these are probably formed during the oxidation of the oil. Concerning the basic component, the average total nitrogen content of oils appears to be about 0.03 percent, i.e., 0.02 molar. Assuming this nitrogen to be largely basic in character, this concentration is exactly in the range that was found to produce conductivities of the order of magnitude 10^{-12} to 10^{-11} mho/cm (the same as in deteriorated oils). In particular, if traces of hydroxyamines are formed during oxidation, the effectiveness of the nitrogen is considerably increased, as has been shown. It is generally agreed that the nitrogen in oils is present in the form of cyclic compounds, and it is of interest to note in this connection that substitution of the cyclic piperidine for tributylamine produced conductivities comparable to those presented in Section 3. Nevertheless, the presence of other types of organic cations, such as oxonium ions and triarylcarbinols, has also to be considered, although they are much weaker bases than the amines.

A more accurate answer as to the chemical nature of organic ions present in oxidized oils could be given, if specifically acting electrodes for e.m.f. measurements could be developed. The author is at present engaged in a research to find out whether this is possible.

[12] Andrew Gemant, J. Phys. Chem. **43**, 743 (1939).

Accommodation Coefficients for Heat Conduction Between Gas and Bright Platinum, for Nine Gases Between 80°K (or Their Boiling Points) and 380°K

EDWARD R. GRILLY, WILLIAM J. TAYLOR,*,[1] AND HERRICK L. JOHNSTON
Department of Chemistry of The Ohio State University, Columbus, Ohio

(Received May 10, 1946)

Accommodation coefficients toward bright platinum for air, oxygen, nitric oxide, carbon monoxide, carbon dioxide, nitrous oxide, methane, hydrogen, and helium are computed from the $(1/K_a)$ *versus* $(1/P)$ slopes of the thermal conductivity measurements of Taylor and Johnston and of Johnston and Grilly. The results—which cover the temperature range 80°K to 380°K—are tabulated for the several gases, and are collected in a graph where comparison with results obtained by other investigators are also included. Our results with hydrogen rise toward a coefficient of unity with lowering temperature, in confirmation of measurements by others, but those for other gases drop steeply at temperatures between room temperature and that of liquid air. Our data are in generally good agreement with the recent accurate work of Amdur, Jones, and Pearlman, at room temperature. The accommodation coefficients which are derived from the reciprocal K *versus* reciprocal P plots differ slightly from Knudsen accommodation coefficients, and are referred to as "Maxwell-Knudsen" coefficients. Equations are derived which give the relationship between the reciprocal slopes, the temperature jump constants g', and the M-K accommodation coefficients.

ALTHOUGH the literature contains comparatively little data on the accommodation coefficients of gases below room temperature, it is generally assumed that these tend to approach unity as T approaches zero. In connection with measurements of the thermal conductivities of gases, recently completed in this laboratory[2,3] for the temperature range of 80° to 380°K, by the hot wire method, it was possible to evaluate accommodation coefficients on the cell wire of bright platinum.

RELATION BETWEEN ACCOMMODATION COEFFICIENT AND RECIPROCAL PLOT

The calculation of accommodation coefficients, from the thermal conductivity data, is based on the experimental slopes of the reciprocal plots of "apparent" conductivity *versus* pressure, for various pressures used in the cell. The "apparent" conductivity, K_a, of the gas is obtained, as outlined in the initial paper[2] of this series, by applying to the experimental (uncorrected) conductivity, K_u, all the necessary corrections except that for the "temperature-jump" effect. The latter is the effect of the temperature discontinuity which exists at a gas-solid interface when heat flows across the interface.[4] The temperature in the body of a gas will vary in a way determined by the boundary conditions of the system. Thus the temperature varies linearly with distance for heat flow between parallel plates, and linearly with the logarithm of the radial distance for heat flow between concentric cylinders (as in a hot wire cell). However the particular way in which the gas molecules incident upon the surface are reflected from it (or re-emitted after adsorption), and, further, the way in which the reflected and incident molecules interact through collisions, affects the condition of the gas within a few mean-free-path lengths of the surface. As a result the temperature in the gas near the surface will deviate from the functional relation which obtains in the body of the gas, and the extrapolation of the latter relation to the surface will yield a temperature different than the temperature of the surface. This temperature discontinuity will be denoted by δT.[5]

Experiment has established, and the theory, in so far as it has been developed, supports the fact that δT is proportional to the temperature gradient in the gas at the surface (as extrapolated from the body of the gas), and is inversely pro-

* Present address: American Petroleum Institute Research Project 44, National Bureau of Standards, Washington, D. C.

[1] Fellow of the Charles A. Coffin Foundation 1939–40; E. I. du Pont Fellow 1940–41.

[2] W. J. Taylor and H. L. Johnston, J. Chem. Phys. **14**, 219 (1946).

[3] H. L. Jolnston and E. R. Grilly, J. Chem. Phys. **14**, 233 (1946).

[4] E. H. Kennard, *Kinetic Theory of Gases* (McGraw-Hill Book Company, Inc., New York, 1938), Sections 176–177.

[5] The actual temperature of the gas at the surface will also differ from the temperature of the surface, although by an amount less than δT.

portional to the pressure of the gas (or directly proportional to the mean-free-path length). Thus

$$\delta T = g\frac{\partial T}{\partial r} = (g'/p)\frac{\partial T}{\partial r}, \quad (1)$$

where g' is independent of the pressure, p. The constant g has been called the temperature jump distance.[4] It is suggested that g' be called the temperature jump coefficient.

In the hot wire cell a temperature discontinuity is found at the surface of the cell wire, and to a lesser extent at the surface of the cell wall. The discontinuity which enters into the derivation of the equations for the present cell is δT, as defined here. As a result of these discontinuities, the apparent conductivity of the gas is a function of the pressure of the gas (as well as of other constants of the gas and of the apparatus). It has been shown previously[2] that a plot of the reciprocal of the apparent conductivity, K_a, *versus* the reciprocal of the pressure, yields a straight line, and that the intercept at $(1/p)=0$ is the reciprocal of the true conductivity, K, or

$$1/K_a = 1/K + A/P. \quad (2)$$

The slope A is related to the coefficient g' of Eq. (1) by the expression[2]

$$A = \frac{d(1/K_a)}{d(1/p)} = \frac{1}{\ln (r_2/r_1)} \times [(g_1'/K_1r_1)+(g_2'/K_2r_2)], \quad (3)$$

where the subscripts 1 and 2 refer to the surfaces, or temperatures, of the cell wire and the cell wall, respectively. The term (g_2'/K_2r_2) in Eq. (3) makes only a small contribution, since $(g_2'/K_2) \cong (g_1'/K_1)$, and $(1/r_2)=0.032(1/r_1)$. It is therefore permissible to set (g_2'/K_2) equal to (g_1'/K_1), whereupon Eq. (3) may be solved for g_1',

$$g_1' = \ln (r_2/r_1)\cdot[(1/r_1)+(1/r_2)]^{-1}\cdot K_1A. \quad (4)$$

If in Eqs. (1) to (4), r is expressed in centimeters, and p in centimeters of mercury, then g' has the units centimeters times centimeters of mercury. On introducing the dimensions of the present cell, Eq. (4) becomes,

$$g_1' = 0.0426\cdot K_1A. \quad (4a)$$

The constant g_1' is dependent upon the nature of the gas and of the surface, but is independent of the dimensions of the apparatus[6] or of the pressure of the gas. It should be emphasized that the validity of Eq. (1) is confirmed by the fact that the observed data are precisely in accord with Eq. (2), and that the values of g_1' calculated from Eq. (4) are not dependent upon any detailed theory of the interaction of the molecules of the gas with the surface. The usefulness of g' lies in the fact that it may be used with Eq. (1) to calculate δT for the same gas and surface in any other situation in which they occur. In such a case the derivative in Eq. (1) is merely the derivative normal to the surface, whether the surface is curved or flat.

The accommodation coefficient of the gas molecules on the surface has been calculated from the value of g' and a theoretical relation connecting these two constants.

Knudsen's accommodation coefficient, for heat conduction across a gas-solid interface, is defined as the ratio[4]

$$a = (E_i - E_r)/(E_i - E_r'), \quad (5)$$

when E_i is the energy carried (per unit time) by the stream of molecules incident upon the surface, E_r is the energy carried by the molecules reflected (or re-emitted) from the surface, and E_r' is the energy that would be carried by the reflected molecules if they were issuing as a stream out of a body of gas at equilibrium at the temperature of the surface.[7] This accommodation coefficient is therefore the ratio of the net energy actually flowing across the surface to the value the latter would have if the incident stream of molecules were unchanged but the reflected stream were replaced by a stream in "thermal equilibrium" with the solid. A theoretical relation between g' and Knudsen's accommodation coefficient has not as yet been obtained and probably no simple relation between them exists, because of the complex nature of the actual stream of incident molecules. However, it is possible to relate g' to a slightly different

[6] It is assumed that, as in the case in the present measurements, the length of the mean free path in the gas is small relative to the diameter of the cell wire.

[7] The "pressure" of this gas is to have a value such that the issuing stream contains the same number of molecules as the actual incident and reflected streams.

constant, defined as

$$a' = (E_i - E_r)/(E_i' - E_r'). \quad (6)$$

E_i, E_r, and E_r' have been defined following Eq. (5),[8] and E_i' is the energy the incident stream of molecules would carry if the temperature gradient in the body of the gas continued uniformly to the surface (in which case the temperature discontinuity at the surface would be δT of Eq. (1)). It is suggested that a' be called the Maxwell-Knudsen accommodation coefficient, since the definition is based upon the work of both men.[4] The expression relating g' and a' is[4]

$$g' = (2\pi RMT)^{\frac{1}{2}}\left(\frac{K}{2C_v+R}\right)\left(\frac{2-a'}{a'}\right), \quad (7)$$

where R is the molar gas constant, M is the molecular weight of the gas, and K and C_v are the thermal conductivity and heat capacity (at constant volume) of the gas at the temperature T(°K) of the surface. On introducing the value of R and appropriate conversion factors, and solving for a', Eq. (7) becomes:

$$a' = \left[(1/2) + \frac{0.583}{(MT)^{\frac{1}{2}}}\frac{C_v+0.994}{K}g'\right]^{-1}, \quad (8)$$

where the units are: C_v, calories per degree per mole; K, calories per centimeter per degree per second; and g', centimeters times centimeters of mercury.

The only approximation of any significance in the derivation of Eq. (7) is the assumption that the heat capacity for internal energy (excluding translation) of a stream of molecules issuing from a body of gas at equilibrium is the same (per mole) as for the entire gas. This assumption is not likely to be seriously in error unless there is a strong correlation between the average internal energies of the molecules and their translational velocities. Account is taken of the fact that the heat capacity for translational energy is $2R$ for the issuing stream as compared with $3R/2$ for the entire gas.

TABLE I. Accommodation coefficients of air on bright platinum.

T, °K	$d(1/K)/d(1/P)$	g'	a'	T, °K	$d(1/K)/d(1/P)$	g'	a'
94	378	33	0.62	224	405	83	0.79
104	145	14	1.11	248	434	97	0.78
139	254	33	0.90	270	448	107	0.78
155	299	44	0.85	280	491	121	0.75
167	505	79	0.62	318	547	149	0.73
171	383	62	0.75	344	576	167	0.72
198	313	58	0.88	382	574	181	0.74

[8] However in the present case the stream for E_r' is defined to contain the same number of molecules as the stream for E_i' (rather than for E_i, as in footnote 7).

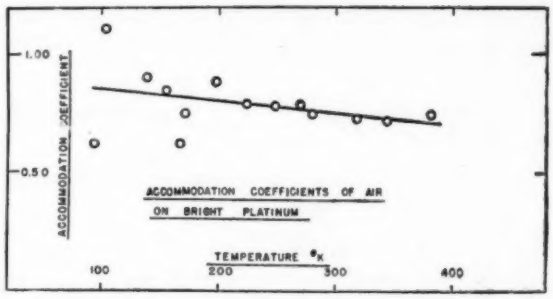

FIG. 1. Accommodation coefficient of air on bright platinum.

It seems desirable to recognize that g' yields the accommodation coefficient a', rather than a. Measurements at lower pressures, such that free-molecule conduction exists, are generally considered to yield the Knudsen coefficient, a. However, it should be pointed out that approximations have been necessary in the theoretical treatment of free-molecule conduction.[9] A comparison of values of a and a' would indicate the difference between the values of E_i and E_i' in Eq. (6).

The accommodation coefficients for air, obtained by Taylor and Johnston[2] are given in Table I, and are graphed in Fig. 1. Those for the eight gases investigated by Grilly and Johnston[3] are given in Tables II–IX, inclusive, and are graphed in Fig. 2. Units employed in the several tables are as follows: T, wire temperature in degrees Kelvin; P, centimeters of mercury; K, (apparent), calories per centimeter per second per degree $\times 10^5$; g', centimeters $\times$ centimeters of mercury $\times 10^5$.

The pressures, at which apparent K's for air were obtained by Taylor and Johnston are given in Table IV of their paper, and are not quoted here. Certain of Taylor and Johnston's results—namely those for wire temperatures of 104° and 139°K—are based on plots of three points that were not quite linear. The remaining points below 175° were based on runs at only two pressures. This probably accounts for the spread

[9] E. H. Kennard, reference 4 (Sections 178–179).

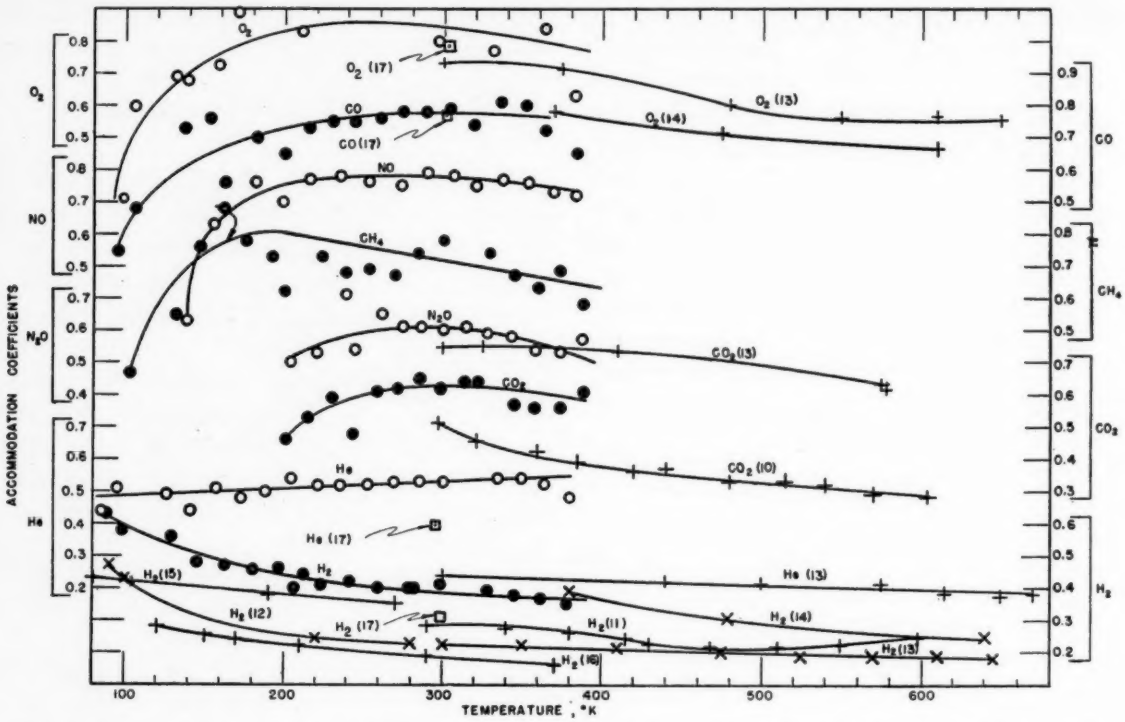

FIG. 2. Accommodation coefficient of several gases on bright platinum. Experimental points, ○ ● This research, + □ Other investigators (references indicated).

TABLE II. Accommodation coefficients of oxygen on bright platinum.

T, °K	P_1	P_2	P_3	K_1	K_2	K_3	$\frac{d(1/K)}{d(1/P)}$	g'	a'
99	1.125	3.35	9.36	2.000	2.029	2.033	1020	93	0.31
106	1.870	4.05	8.99	2.103	2.108	2.111	440	44	0.60
132	1.625	4.21	9.20	2.768	2.767	2.771	403	50	0.69
139	1.711	4.63	8.12	2.838	2.846	2.852	420	56	0.68
159	1.537	4.39	6.65	3.298	3.312	3.318	400	61	0.73
172	1.541	5.05	9.27	3.648	3.668	3.667	280	47	0 89
212	1.125	4.16	11.09	4.422	4.469	4.481	374	73	0.83
297	1.294	3.90	11.09	6.044	6.138	6.165	472	127	0.80
331	2.000	5.00	8.99	6.709	6.779	6.801	520	155	0.77
364	1.406	4.73	8.64	7.356	7.483	7.513	475	156	0.84
383	1.556	4.08	8.61	7.676	7.868	7.920	750	258	0.63

TABLE III. Accommodation coefficients of nitric oxide on bright platinum.

T, °K	P_1	P_2	P_3	K_1	K_2	K_3	$\frac{d(1/K)}{d(1/P)}$	g'	a'
139	1.851	5.72	10.72	2.763	2.781	2.795	940	121	0.33
156	1.646	4.28	10.86	3.139	3.153	3.161	440	63	0.63
182	1.387	6.46	10.01	3.689	3.717	3.720	364	61	0.76
199	1.312	5.27	9.97	4.020	4.064	4.070	450	80	0.70
216	2.530	5.89	10.65	4.381	4.398	4.404	396	78	0.77
235	1.531	6.75	10.48	4.733	4.780	4.785	410	87	0.78
253	1.511	5.07	10.53	5.064	5.114	5.129	444	101	0.76
273	1.697	5.20	10.40	5.461	5.515	5.530	466	113	0.75
290	1.871	4.73	10.44	5.776	5.827	5.842	446	114	0.79
306	1.975	5.41	10.50	6.079	6.135	6.151	472	126	0.78
320	1.756	5.87	10.51	6.325	6.405	6.423	512	143	0.75
337	1.711	4.86	10.53	6.621	6.704	6.730	500	147	0.77
353	1.756	4.70	10.44	6.912	7.001	7.037	544	165	0.76
369	1.712	4.36	10.56	7.188	7.292	7.341	592	188	0.73
383	1.761	4.78	10.58	7.437	7.557	7.597	596	197	0.72

of their data below 175°K. For purposes of extrapolation—i.e., to obtain thermal conductivities—the slight non-linearity is less serious than in the determination of accommodation coefficients, where slopes themselves are used.

Comparisons with results obtained by other investigators[10–17] are included in Fig. 2. The measurements in references 13 to 17 were made at low pressures, where free molecule conduction exists, and presumably yield values of Knudsen's accommodation coefficient a, while those in references 10 to 12 were made at higher pressures ($p>1$ cm), and should yield essentially the

[10] C. T. Archer, Proc. Roy. Soc. (London) **A165**, 474 (1938).
[11] H. S. Gregory (Spencer-Gregory), Proc. Roy. Soc. (London) **A149**, 35 (1935).
[12] H. Spencer-Gregory and E. H. Dock, Phil. Mag. **25**, 129 (1938).
[13] L. B. Thomas and F. Olmer, J. Am. Chem. Soc. **65**, 1036 (1943).
[14] W. B. Mann, Proc. Roy. Soc. (London) **A146**, 776 (1934).
[15] M. Knudsen, Ann. d. Physik **34**, 593 (1911).
[16] H. H. Rowley and K. F. Bonhoeffer, Zeits. f. physik. Chemie **B21**, 84 (1933). Recalculated by Thomas and Olmer, reference 13.
[17] I. Amdur, M. C. Jones, and H. Pearlman, J. Chem. Phys. **12**, 159 (1944).

accommodation coefficient a'.[18] Both types of measurements refer to a platinum surface saturated with gas, with the exception of some of the measurements of Mann[14] which were made on a gas free surface.[19]

TABLE IV. Accommodation coefficients of hydrogen on bright platinum.

T, °K	P_1	P_2	P_3	K_1	K_2	K_3	$\frac{d(1/K)}{d(1/P)}$	g'	a'
88	1.608	4.57	10.60	13.74	13.84	13.87	130	80	0.63
98	1.518	4.65	10.90	15.18	15.33	15.38	152	112	0.58
129	2.045	5.38	11.76	19.57	19.78	19.83	164	140	0.56
145	1.886	5.29	12.23	21.94	22.27	22.41	214	208	0.48
162	1.857	5.26	10.76	24.19	24.66	24.77	220	236	0.47
180	1.850	4.67	11.12	26.27	26.80	27.02	236	280	0.46
197	1.507	4.01	11.04	28.10	28.84	29.20	232	298	0.46
206	2.005	5.02	10.48	24.53	30.28	30.61	296	396	0.40
212	1.373	4.80	10.80	29.84	31.08	31.37	254	347	0.44
223	2.085	4.83	10.49	31.78	32.57	32.94	288	416	0.41
241	1.811	5.45	10.60	33.81	35.07	35.40	290	459	0.42
259	1.866	5.03	10.68	35.65	37.00	37.48	302	490	0.40
279	1.846	5.30	10.73	37.43	39.02	39.52	316	541	0.40
282	1.339	4.26	10.45	36.57	38.75	39.55	316	545	0.40
298	1.607	4.48	12.42	38.39	40.36	41.14	304	539	0.41
328	1.309	4.78	12.01	39.81	43.05	43.95	348	665	0.39
345	1.518	4.77	9.35	41.35	44.34	45.11	362	715	0.38
361	1.464	4.53	10.38	42.17	45.69	46.70	390	795	0.37
378	1.493	5.07	10.75	43.11	47.19	48.31	430	905	0.35

TABLE V. Accommodation coefficients of carbon dioxide on bright platinum.

T, °K	P_1	P_2	P_3	K_1	K_2	K_3	$\frac{d(1/K)}{d(1/P)}$	g'	a'
201	1.882	4.37	8.39	2.054	2.065	2.069	875	85	0.46
215	1.722	4.24	8.44	2.264	2.273	2.280	710	76	0.53
230	1.722	4.95	9.86	2.504	2.516	2.522	620	72	0.59
243	1.771	4.17	9.89	2.716	2.739	2.747	900	108	0.48
258	1.781	5.17	9.31	2.973	2.990	2.996	590	80	0.61
271	1.646	4.66	9.33	3.208	3.229	3.238	590	87	0.62
285	1.647	4.05	8.08	3.464	3.487	3.496	570	90	0.65
298	1.567	4.08	8.09	3.703	3.730	3.743	580	97	0.62
313	1.567	4.08	6.93	3.974	4.007	4.021	610	110	0.64
321	1.184	3.30	6.95	4.116	4.169	4.186	580	109	0.64
344	1.743	4.31	10.37	4.571	4.616	4.637	670	139	0.57
357	1.743	4.71	10.04	4.838	4.891	4.912	700	154	0.56
373	1.702	4.63	10.05	5.165	5.229	5.257	710	166	0.56
388	1.707	4.21	9.66	5.497	5.567	5.594	620	153	0.61

TABLE VI. Accommodation coefficients of nitrous oxide on bright platinum.

T, °K	P_1	P_2	P_3	K_1	K_2	K_3	$\frac{d(1/K)}{d(1/P)}$	g'	a'
204	2.115	4.19	10.41	2.157	2.163	2.171	825	83	0.50
220	1.772	4.77	10.27	2.416	2.428	2.434	680	76	0.53
238	1.906	4.57	8.66	2.743	2.749	2.756	460	55	0.71
244	1.862	4.79	9.83	2.840	2.857	2.864	685	89	0.54
261	1.777	4.92	10.06	3.143	3.160	3.167	530	77	0.65
274	1.847	4.52	10.59	3.386	3.406	3.415	590	91	0.61
286	1.702	4.86	10.91	3.624	3.649	3.661	570	93	0.61
301	1.448	4.31	10.90	3.897	3.931	3.949	580	102	0.60
314	1.748	4.78	10.89	4.160	4.193	4.207	590	112	0.61
327	1.611	6.04	12.30	4.430	4.483	4.498	640	128	0.59
342	1.591	5.15	12.25	4.733	4.791	4.814	660	142	0.58
357	2.367	5.12	11.20	5.070	5.109	5.132	720	165	0.54
373	2.049	5.30	11.13	5.399	5.455	5.484	740	181	0.53
387	2.203	5.67	10.96	5.731	5.790	5.814	660	170	0.57

[18] However, the accommodation coefficient calculated in references 10 to 12 is not identical with a' because the theory used by these workers differs from that presented here. In this connection, see the comment of Kennard (reference 4, pages 323–324), on the formula used by Dickins, reference 20 (Proc. Roy. Soc. (London) **A143**, 517 (1934)). Gregory (reference 11) presumably used the same formula as Dickins, while Archer (reference 10) and Spencer-Gregory and Dock (reference 12) used a different theory developed by one of them.

TABLE VII. Accommodation coefficients of carbon monoxide on bright platinum.

T, °K	P_1	P_2	P_3	K_1	K_2	K_3	$\frac{d(1/K)}{d(1/P)}$	g'	a'
95	1.832	5.56	10.00	1.790	1.795	1.801	790	67	0.35
106	2.140	4.91	10.20	2.029	2.035	2.037	550	52	0.48
138	1.628	5.27	9.58	2.702	2.711	2.714	350	53	0.73
154	1.901	5.40	10.10	3.037	3.049	3.051	350	47	0.76
163	1.782	5.55	10.00	3.230	3.246	3.256	560	81	0.56
183	2.333	5.48	11.08	3.658	3.670	3.676	410	66	0.70
200	1.771	4.94	11.11	3.967	3.988	4.006	510	90	0.65
215	1.786	4.89	11.01	4.264	4.291	4.301	440	85	0.73
230	1.632	4.56	11.01	4.548	4.582	4.595	440	89	0.75
244	1.637	4.60	10.74	4.814	4.852	4.866	430	95	0.75
260	1.776	4.40	10.76	5.097	5.148	5.151	440	99	0.76
274	1.766	4.53	10.68	5.341	5.381	5.400	445	105	0.78
289	1.363	4.40	9.99	5.579	5.650	5.670	450	111	0.78
304	1.796	4.38	10.03	5.865	5.912	5.936	450	117	0.79
319	1.800	4.57	9.68	6.223	6.171	6.194	520	140	0.74
336	2.512	6.33	10.35	6.426	6.466	6.485	460	130	0.81
352	2.099	5.43	10.38	6.689	6.756	6.770	470	140	0.80
364	2.467	5.26	10.96	6.912	6.970	6.996	550	168	0.72
384	3.153	8.65	11.20	7.268	7.334	7.346	650	207	0.65

TABLE VIII. Accommodation coefficients of methane on bright platinum.

T, °K	P_1	P_2	P_3	K_1	K_2	K_3	$\frac{d(1/K)}{d(1/P)}$	g'	a'
103	1.901	4.36	7.38	2.438	2.445	2.448	450	50	0.37
132	1.518	4.87	10.86	3.174	3.186	3.192	330	47	0.55
147	1.781	4.88	11.05	3.593	3.597	3.604	220	35	0.76
162	1.682	4.23	10.37	3.979	3.995	3.994	180	32	0.88
176	2.025	4.66	10.01	4.394	4.393	4.400	230	45	0.78
192	2.066	3.98	9.78	4.775	4.787	4.798	270	57	0.73
200	2.245	4.96	9.95	5.203	5.227	5.237	360	80	0.62
223	1.876	4.41	10.81	5.640	5.661	5.679	275	73	0.73
238	2.095	5.06	11.42	6.061	6.092	6.106	320	87	0.68
253	2.190	5.95	11.28	6.492	6.527	6.541	320	92	0.69
269	2.160	5.06	11.27	6.948	6.986	7.010	340	105	0.67
284	1.607	4.34	11.21	7.406	7.471	7.495	300	98	0.74
300	1.955	5.17	10.86	7.930	7.975	8.006	280	97	0.78
329	1.911	4.95	10.85	8.853	8.934	8.961	310	127	0.74
344	1.886	4.64	10.70	9.374	9.468	9.512	360	149	0.67
359	2.300	5.53	10.75	9.974	10.069	10.112	390	172	0.63
373	2.015	5.30	10.80	10.535	10.667	10.695	350	161	0.68
388	2.100	5.07	10.94	11.112	11.264	11.331	440	217	0.58

TABLE IX. Accommodation coefficients of helium on bright platinum.

T, °K	P_1	P_2	P_3	K_1	K_2	K_3	$\frac{d(1/K)}{d(1/P)}$	g'	a'
85	1.885	4.46	10.37	15.31	15.55	15.65	325	220	0.44
95	2.054	4.88	10.32	16.65	16.92	16.94	280	200	0.51
126	2.219	5.46	11.09	19.36	19.71	19.78	300	256	0.49
141	2.188	5.42	11.24	20.62	21.12	21.27	410	382	0.44
157	2.139	5.32	11.40	22.26	22.76	22.95	360	359	0.51
173	2.068	5.11	11.08	23.61	24.24	24.52	400	427	0.48
188	2.078	5.06	11.26	24.82	25.51	25.85	410	463	0.50
204	2.139	5.27	11.18	26.19	26.96	27.25	400	475	0.54
221	2.228	5.49	11.33	27.63	28.47	28.81	415	521	0.52
235	2.178	5.30	11.59	28.71	29.67	30.08	430	563	0.52
252	2.019	4.98	11.38	29.79	30.98	31.48	445	609	0.52
269	2.113	5.07	11.31	30.99	32.20	32.75	450	644	0.53
285	2.073	5.13	11.25	32.03	33.43	34.01	460	683	0.53
300	2.188	5.38	11.15	33.13	34.58	35.19	480	736	0.53
334	1.567	3.58	9.00	34.03	36.17	37.28	480	785	0.54
349	1.457	3.73	9.04	34.64	37.33	38.32	485	816	0.54
364	1.655	4.31	10.64	35.36	38.08	39.19	540	927	0.52
380	1.775	4.60	10.66	36.04	38.85	40.03	590	1035	0.48

[19] However, the work of Amdur, Jones, and Pearlman (reference 17) indicates that in some earlier work, including

In the figure the ordinate scale for each gas has been shifted for better distribution of the points, but qualitatively all the gases are in order of the magnitudes of their accommodation coefficients.

DISCUSSION OF RESULTS

Our own values of a' agree reasonably well with the values of a obtained by Amdur, Jones, and Pearlman,[17] which are probably the most reliable values of a (on a gas-saturated platinum surface) in the literature. This comparison is perhaps the best evidence now available that these two accommodation coefficients do not differ very greatly.

As shown by Fig. 2, the literature is generally lacking in measurements of accommodation coefficients below room temperature—hydrogen (and some data with helium, on glass) being the only gas for which data are published. The accommodation coefficients for hydrogen rise with descending temperature—as confirmed in our own work with this gas. It is generally assumed that the accommodation coefficients of all gases—on all surfaces—tend toward unity as the temperature is lowered. This is because the surface becomes covered with an adsorbed layer of the gas which is thought to be conducive to more efficient energy interchange. However, our own results with gases other than hydrogen consistently indicate sharp decreases in accommodation coefficients at temperatures somewhat below that of the room. This effect is, in fact, most marked for those gases that are most strongly adsorbed. We plan, sometime, to measure the accommodation coefficient of hydrogen in the neighborhood of its boiling point to discover whether hydrogen also will behave like the other gases in its region of high adsorption.

Some differences among results by different investigators is probably to be expected since we are dealing with a surface effect and surface conditions are probably not exactly comparable.

The observed accommodation coefficient is dependent on the average efficiency of transfer to the surface of the several kinds of molecular energy (translational, rotational, and vibrational) which may be excited in the gas. Some experiments of Knudsen[20] indicate that the accommodation coefficients for translational and rotational energies in hydrogen are essentially the same.

However, it is probable that in general the efficiency of energy transfer is somewhat different for internal degrees of freedom (particularly for vibration) than it is for translation. This has been considered by Shafer, Rating, and Eucken,[21] who assign much lower coefficients to vibrational and rotational than to translational energy. For example, for carbon dioxide at 3°C they assign an accommodation coefficient of unity for translation and rotation but of only 0.13 for vibration.

A relatively low accommodation coefficient for vibrational energy may partially explain the decrease of the accommodation coefficient for the total energy which is generally observed at higher temperatures. However, it cannot explain the decrease at low temperatures observed for several gases in this research.

We see no obvious explanation of the shapes of the curves at low temperatures, and regard it as desirable to investigate the effect further with other gases, and with hydrogen and helium at liquid hydrogen temperatures.

that of Thomas and Olmer (reference 13), the pressure of the gas may have been too low to attain complete saturation of the surface. Accommodation coefficients measured in the region of partial saturation would be expected to be a function of the pressure of the gas.

[20] W. Knudsen, Ann. d. Physik **6**, 129 (1930).

[21] K. Shafer, W. Rating, and A. Eucken, Ann. d. Physik **42**, 176 (1942).

THE JOURNAL OF CHEMICAL PHYSICS VOLUME 14, NUMBER 7 JULY, 1946

Statistical Mechanics of Multimolecular Adsorption

II. Localized and Mobile Adsorption and Absorption

TERRELL L. HILL
Department of Chemistry, University of Rochester, Rochester, New York
(Received April 2, 1946)

It is shown that the transition from localized to mobile adsorption (in the first adsorbed layer) takes place at rather low temperatures for potential barriers of around 1000 cal./mole or less, so that localized physical adsorption should be a very rare phenomenon at the temperatures usually employed in adsorption experiments. Since the BET (and Langmuir) isotherm actually assumes localized adsorption, a new approximate isotherm equation is derived here on the basis of a mobile first layer obeying a two-dimensional van der Waals' equation. This isotherm is in semiquantitative agreement with the two-dimensional phase changes observed by Jura and co-workers, and by earlier workers, at very low pressures. The localized-mobile transition in the absorption of hydrogen by metals is mentioned briefly. The relationships between (1) the two-dimensional equation of state of a monolayer, (2) the adsorption isotherm of the monolayer, and (3) the ordinary three-dimensional equation of state of the gas being adsorbed are discussed in some detail.

I. INTRODUCTION

IN most cases at ordinary temperatures, a molecule which is held to the surface of a solid by van der Waals forces is able to migrate rather freely over the surface.[1a] In order to do this the molecule must, in general, be able to pass over potential barriers (of the order of 400 cal./mole[1a] in physical adsorption) which arise because of the periodic structure of the surface of the solid and the resulting periodic variation (in two dimensions) of the energy of adsorption. However, at sufficiently low temperatures, such a molecule will be restricted to a localized[1b] site at a potential minimum, with vibrations about the equilibrium point replacing translational motion in two dimensions. At intermediate temperatures, the situation is rather more complicated.

We have been referring above to molecules in the first adsorbed layer. Whether these molecules are localized or mobile, the behavior of molecules (if any) in second and higher adsorbed layers is generally assumed to resemble the behavior of molecules in the liquid state, and hence these latter molecules are not localized. However, at temperatures below the melting point of the adsorbed phase, this would naturally not be the case.

As is well known, mobile monolayers exhibit a phase change which is analogous to ordinary condensation. This phase change is usually studied experimentally on the surface of a liquid, but there have been a few studies of two-dimensional condensation on the surface of a solid.[2] Presumably these experiments involving solid surfaces have always dealt with mobile rather than localized monolayers. The theoretical problem involved in studying the condensation of a mobile surface layer is essentially the same as for the usual type of condensation. A completely rigorous treatment has not been accomplished because of mathematical complications, but certain semi-empirical methods are quite useful.

It is clear from theoretical considerations[3] that "condensation" of a localized monolayer is also possible. The theory of the phase change in this case is a good deal simpler (though still requiring

[1a] For a recent discussion of this point, see S. Brunauer, *The Adsorption of Gases and Vapors* (Princeton University Press, Princeton, 1943), pp. 448–454.

[1b] The term "localized" will be used here to refer to molecules whose motions in the two surface dimensions can be described as primarily vibrational, with only relatively infrequent shifts from one potential minimum to another. These shifts can of course occur in any case by the process of evaporation and condensation. By "mobile" molecules will be meant molecules whose motions in the two surface dimensions are essentially those of a two-dimensional gas or liquid, with no effective constraint due to the *periodic variation* of the energy of adsorption over the surface. The energy of adsorption itself of course constrains the motion to two dimensions.

[2] See reference 1a, pp. 437–440. Also, see reference 10.

[3] R. H. Fowler and E. A. Guggenheim, *Statistical Thermodynamics* (University Press, Cambridge, England, 1939), pp. 429–443.

approximations) than for a mobile monolayer, essentially because of the restriction to discrete sites which makes it somewhat easier to enumerate possible states and energies of the system. A statistical treatment leads to Langmuir's isotherm if interactions between adsorbed molecules are neglected, and to a sudden phase change, at temperatures below a critical temperature, if interactions are not neglected. As far as the writer is aware, the condensation of a localized monolayer has never been studied experimentally.

The general problem is thus rather complicated. Not only are different phases possible for an adsorbed layer (for example, gas, liquid expanded, liquid condensed, solid), but one must also consider (1) the low temperature localized-mobile transition, (2) the possibility of multimolecular adsorption at higher pressures, and, in this case, (3) the properties of second and higher layers.

In Section II we shall consider the transition from localized to mobile adsorption when the adsorbed phase is quite dilute. A few remarks will also be made about the absorption of hydrogen by metals, since this is a closely related problem in some respects. In Section III we derive an approximate adsorption isotherm for multimolecular adsorption when the first layer is mobile. Relations between the two-dimensional equation of state and the adsorption isotherm and between the two- and three-dimensional equations of state are discussed in Sections IV and V, respectively.

II. THE LOCALIZED-MOBILE TRANSITION

Adsorption

We consider in this paper only the simplest case. Several possible generalizations will be obvious. We assume that: (1) The potential energy function restricting free migration of an adsorbed molecule over the surface is of the form[4a]

$$U=\tfrac{1}{2}V\left(1-\cos\frac{2\pi x}{d}\right)+\tfrac{1}{2}V\left(1-\cos\frac{2\pi y}{d}\right),$$
$$=\tfrac{1}{2}V\left(2-\cos\frac{2\pi x}{d}-\cos\frac{2\pi y}{d}\right), \qquad (1)$$

where the maximum potential barrier is $V_0=2V$, and d is the distance between potential minima along both x and y axes (the surface lattice is thus assumed to be simple cubic); and (2) the number of molecules, N, adsorbed in the area $\mathfrak{A}=l^2$ is sufficiently small so that (a) interactions between adsorbed molecules may be neglected (the mobile case may then be treated as a perfect gas and the two-dimensional gas pressure will be less than the two-dimensional vapor pressure of the condensed phase—solid or liquid—so condensation will not take place when mobility is acquired, as will ordinarily be the case), and (b) the number of sites available to each of the N adsorbed molecules in the localized case is essentially $n^2=l^2/d^2$. That is, the probability of any two molecules being in the same site is assumed negligible, and it is not necessary to invoke a special "exclusion principle" restricting the number of molecules per site to one. Although the following discussion will be based on the above simplifications, the general conclusions arrived at should not be affected by further refinements.

It is easy to see that under assumption (2), above, a partition function for the system of the form

$$Q=\frac{1}{N!}f^N, \qquad (2)$$

where f is the partition function for a single molecule over the entire area $\mathfrak{A}$, is correct not only for the mobile case but also for the localized case. In the latter case we would ordinarily write

$$Q=\frac{n^2!}{N!(n^2-N)!}f_v{}^N, \qquad (3)$$

where f_v is the partition function for a single molecule in a single site. Since we are assuming $n^2\gg N$, Eq. (3) becomes

$$Q=\frac{(n^2)^N}{N!}f_v{}^N=\frac{1}{N!}(n^2f_v)^N, \qquad (4)$$

which is the same as Eq. (2) with $f=n^2f_v$, thus taking into account correctly the degeneracy (n^2) in the localized case.

[4a] If the dimensions of the molecule are large compared to d, the situation is more complicated. But there will still be a periodic potential function. Other things being equal, the potential barrier should be smaller the larger the molecule.

We proceed now to formulate f for the two degrees of freedom of interest here. In order to do this, a study must first be made of the possible energy levels of the system, the system being a single molecule of mass m in the area $\mathfrak{A}=l^2$ with the potential energy given by Eq. (1). The two-dimensional quantum-mechanical problem here is essentially equivalent to the one-dimensional problem encountered in studying restricted rotation in molecules such as ethane. This makes it possible to use some of the results and tables obtained by Pitzer and Gwinn,[4b] after a suitable correlation of parameters. Also, it appears that a rather accurate method of approximation suggested by Pitzer and Gwinn should be quite adequate and very convenient for adsorption studies, so we shall consider it in some detail as applied to the present problem rather than discuss further the more exact results obtained by these authors. The approximation consists of using the following partition function:

$$f=f_{\text{classical}}\times\frac{f_{\text{harmonic osc-quantal}}}{f_{\text{harmonic osc-classical}}}. \tag{8}$$

The classical partition function here is

$$f_{\text{class}}=\frac{1}{h^2}\int_{-\infty}^{\infty}\int_{0}^{l}\times\exp(-H/kT)dxdydp_xdp_y, \tag{9}$$

where

$$H=\frac{p_x^2}{2m}+\frac{p_y^2}{2m}+\tfrac{1}{2}V\left(2-\cos\frac{2\pi x}{d}-\cos\frac{2\pi y}{d}\right). \tag{10}$$

On performing the integrations over the momenta, we have

$$f_{\text{class}}=\frac{2\pi mkT}{h^2}\exp(-V/kT)\times\left[\int_0^l\exp\left(\frac{1}{2}\frac{V}{kT}\cos\frac{2\pi x}{d}\right)dx\right]^2, \tag{11}$$

$$=\frac{2\pi mkT}{h^2}l^2\exp(-V/kT)I_0^2\left(\frac{V}{2kT}\right), \tag{12}$$

[4b] K. S. Pitzer, J. Chem. Phys. **5**, 469 (1937); K. S. Pitzer and W. D. Gwinn, J. Chem. Phys. **10**, 428 (1942).

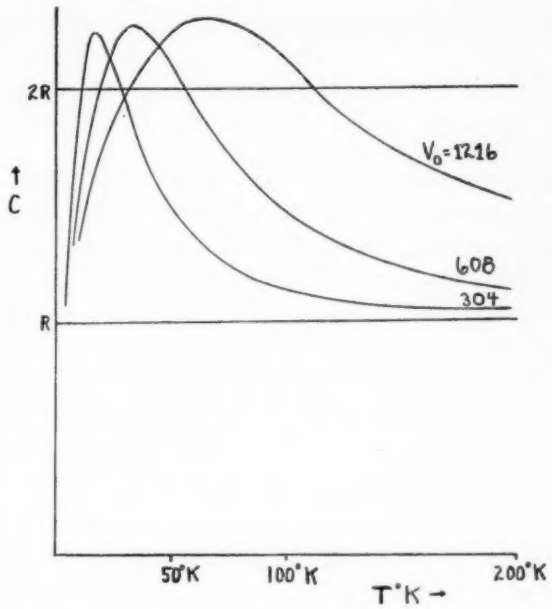

FIG. 1. Heat capacity of adsorbed argon.

where $I_0(u)$ is a modified Bessel function of the first kind. Also,

$$f_{\text{har osc-quant}}=n^2/[1-\exp(-h\nu/kT)]^2, \tag{13}$$

$$f_{\text{har osc-class}}=n^2(kT/h\nu)^2, \tag{14}$$

with

$$\nu=(V/2md^2)^{\frac{1}{2}}. \tag{15}$$

Substituting Eqs. (12)–(14) into Eq. (8) gives

$$f=\frac{2\pi n^2ue^{-2u}I_0^2(u)}{(1-e^{-Ku})^2}, \tag{16}$$

$$u=V/2kT,\quad K=(2h^2/md^2V)^{\frac{1}{2}}. \tag{17}$$

The two limiting expressions are, as expected:

$$u\text{ large}:\quad f=n^2/(1-e^{-Ku})^2, \tag{18}$$

$$u\text{ small}:\quad f=\frac{2\pi mkT}{h^2}l^2. \tag{19}$$

Equation (18) follows from

$$\lim_{u\to\infty}I_0(u)=\frac{e^u}{(2\pi u)^{\frac{1}{2}}}, \tag{20}$$

and we have used $n^2d^2=l^2$ to obtain Eq. (19).

Finally, the complete partition function for the

two degrees of freedom is

$$Q=\frac{1}{N!}f^N. \tag{21}$$

The contribution of these degrees of freedom to the thermodynamic functions may be obtained in the usual way. For example, for the heat capacity, one finds

$$C=Nk\left\{-1+2u\left[u-\frac{I_1(u)}{I_0(u)}-u\frac{I_1^2(u)}{I_0^2(u)}\right]+\frac{2K^2u^2e^{-Ku}}{(1-e^{-Ku})^2}\right\}. \tag{22}$$

As an illustration we have plotted C against T, in Fig. 1, for different values of $V_0=2V$, for argon adsorbed on potassium chloride. The true value of V_0 is probably about 400 cal./mole.[5] Actually, to save labor, Table IV of Pitzer's[4b] paper was used instead of Eq. (22). The connection between our notation and his is found by putting

$$I\text{ (moment of inertia)}=mr^2=ml^2/4\pi^2,$$

since $l=2\pi r$. This becomes clear if one considers the problem of a particle constrained to move in a circular path. The motion can be thought of either as rotation or translation (even if a perfectly reflecting barrier is introduced, blocking the path). One finds that K is related to the variable n^2/IV used by Pitzer by

$$10^{-36}n^2/IV=31.25K^2, \tag{23}$$

where V is in cal./mole.

The theoretical form of the heat capacity curve, as given in Fig. 1, has apparently not been observed experimentally. In fact the only work of this type seems to be that of Simon and Swain[18] in which the heat capacity of adsorbed argon on charcoal was measured. This experimental heat capacity curve resembles that of a one-dimensional harmonic oscillator. There have been several conflicting interpretations of this result. In any case, this example is unsatisfactory from our point of view because of the high porosity of the adsorbent and the large amount of argon adsorbed, leading to complications not taken into account in the present theory.

The transition from vibration to translation is continuous and takes place over an appreciable temperature range. However, one may indicate the general temperature region in which the transition occurs by noting that the heat capacity for the two degrees of freedom passes through a maximum at about $T=V_0/10R$, this temperature being fairly insensitive to K (values of K of interest here will correspond in general to $10^{-36}n^2/IV<8$). It is therefore clear, since V_0 is generally of the order of 500 cal./mole or less, that the transition is in progress at quite low temperatures and that true localized physical adsorption should be a very rare phenomenon indeed at temperatures ordinarily used in adsorption work, although intermediate cases should be somewhat more common (e.g., around 90°K). Certainly the mobile case is the rule and not the exception. Thus the above analysis tends to confirm the similar view expressed by Brunauer[1a] concerning the mobility of physically adsorbed molecules. In chemical adsorption the situation is, of course, radically different because of much higher potential barriers (see the discussion of absorption below).

At the low pressures being considered here the adsorption isotherm is linear, the amount adsorbed being proportional to the pressure. The constant of proportionality is in turn proportional to the partition function f, Eq. (16). It is through the partition function f that the amount of adsorption at low pressures and temperatures will depend on the localized-mobile transition.

Absorption

As is made clear by Fowler and Guggenheim,[6] the absorption of hydrogen by certain metals bears some resemblance to the adsorption of molecules on the surface of a solid. Both localized and mobile absorption are to be expected and both are found experimentally. We should merely like to point out here that there is an analogous localized-mobile transition problem in absorption, but in three dimensions instead of two. Since localized absorption is very common, the

[5] W. J. C. Orr, Trans. Faraday Soc. **35**, 1247 (1939). The curves given are not exact, of course, since the theoretical potential function used is more symmetrical than the actual (potassium chloride) one.

[6] See reference 3, pp. 554–563.

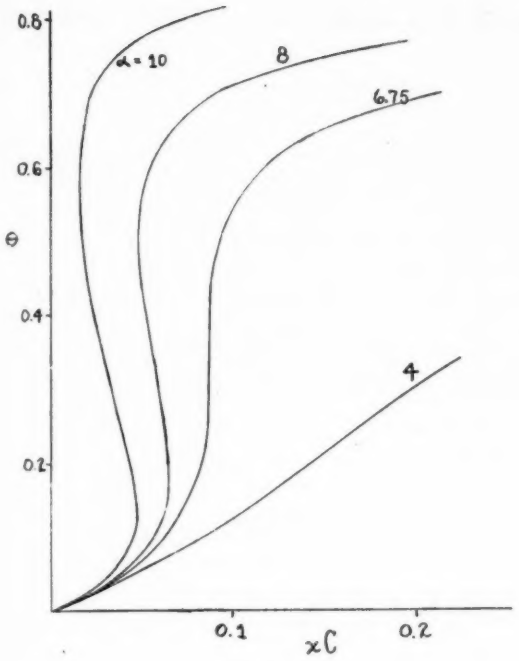

FIG. 2.

potential barriers must be much greater in this case. This is caused, at least in some cases, by chemical absorption—the formation of metal hydrides, MH_n, at the absorption sites (metal atoms).

III. MULTIMOLECULAR ADSORPTION ON A MOBILE FIRST LAYER

The Brunauer-Emmett-Teller[7] theory of multimolecular adsorption is a generalization of Langmuir's theory of unimolecular adsorption. As is pointed out in the statistical versions,[8,9] these theories are based on the assumption of localized sites. Since localized physical adsorption is really rather uncommon, it would seem worthwhile to derive a multimolecular adsorption isotherm on the assumption of a mobile first layer. We shall confine ourselves in this paper to a treatment which is only slightly more general than the corresponding statistical treatment[9] for a localized first layer, which leads to the BET equation. The BET model neglects interactions between molecules in the same layer. We shall also neglect these interactions, except in the first layer where they will be taken into account in an approximate manner (by the use of Eq. (24)).

We assume for simplicity that the X molecules in the first layer obey van der Waals' equation in two dimensions. It should be recognized at the outset that the choice (there seems to be no satisfactory alternative at the present time) of such a crude equation of state will give the resulting theory only semi-quantitative significance. However, the theory should still be useful in contributing to an understanding of the problem. We also neglect the existence of more than one liquid phase in using this equation of state. Thus we shall write

$$(\varphi+a'X^2/\mathfrak{A}^2)(\mathfrak{A}-Xb')=XkT, \qquad (24)$$

where φ is the two-dimensional pressure, $\mathfrak{A}$ is the area, and a' and b' are constants. The associated partition function (for these two degrees of freedom) which leads to this equation of state is

$$\frac{1}{X!}\left[\frac{2\pi mkT}{h^2}(\mathfrak{A}-Xb')\exp(a'X/\mathfrak{A}kT)\right]^X. \qquad (25)$$

We therefore write for the separate partition functions of the X molecules in the first adsorbed layer and the $N-X$ molecules in higher layers, respectively,

$$Q_S=\frac{1}{X!}\left[jj_n\exp(\epsilon_1/kT)\times\frac{2\pi mkT}{h^2}(\mathfrak{A}-Xb')\exp(a'X/\mathfrak{A}kT)\right]^X, \qquad (26)$$

$$Q_L=\frac{(N-1)!}{(N-X)!(X-1)!}[j_L\exp(\epsilon_L/kT)]^{N-X}, \qquad (27)$$

in which j is the internal partition function, j_n the partition function for vibrations normal to the surface, $-\epsilon_1$ the potential energy of a molecule in the first layer due to interaction between the molecule and the surface, and j_L and $-\epsilon_L$ the partition function and potential energy of molecules in higher layers (assumed to be liquid-like). Equation (27) is the same as Eq. (4) in the first paper of reference 9, while Eq. (26) is the analog of Eq. (3) in that paper. We are thus assuming that molecules in the first layer behave like a two-dimensional van der Waals' gas and that addi-

[7] See reference 1a, Chapter VI.
[8] R. H. Fowler, Proc. Camb. Phil. Soc. **31**, 260 (1935).
[9] T. L. Hill, J. Chem. Phys. **14**, 263 (1946); A. B. D. Cassie, Trans. Faraday Soc. **41**, 450 (1945).

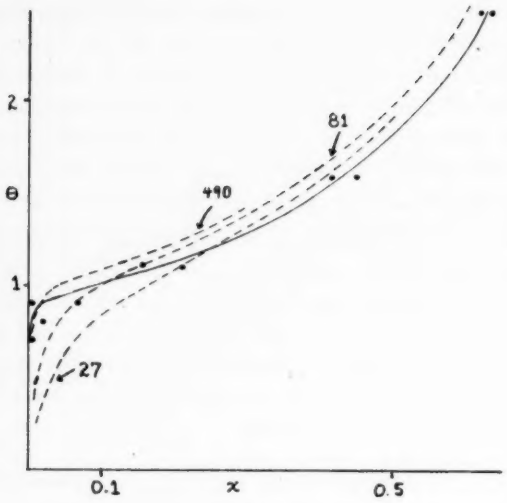

FIG. 3.

tional molecules may build up higher layers on top of the X sites presented by the first layer.

The equilibrium value of X is found from

$$\frac{\partial \log Q_S Q_L}{\partial X}=0. \tag{28}$$

We neglect unity compared to N and X in Eq. (27) and find, from Eq. (28),

$$\frac{(N-X)(\mathfrak{A}-Xb')}{X^2}\exp\left(-\frac{Xb'}{\mathfrak{A}-Xb'}+\frac{2a'X}{\mathfrak{A}kT}\right)=\frac{j_L\exp\left[(\epsilon_L-\epsilon_1)/kT\right]}{jj_n 2\pi mkT/h^2}. \tag{29}$$

The chemical potential of the adsorbed phase is

$$\frac{\mu_A}{kT}=-\frac{\partial \log Q_S Q_L}{\partial N}=\log\frac{N-X}{N}-\log j_L-\frac{\epsilon_L}{kT}. \tag{30}$$

For the gas phase,

$$\frac{\mu_G}{kT}=\frac{\mu_0(T)}{kT}+\log p, \tag{31}$$

where p is the gas pressure and $\mu_0(T)$ need not be specified further for our purposes. At equilibrium, $\mu_A=\mu_G$:

$$\log\frac{N-X}{N}-\log j_L-\frac{\epsilon_L}{kT}=\frac{\mu_0(T)}{kT}+\log p. \tag{32}$$

For the pure liquid

$$-\log j_L-\frac{\epsilon_L}{kT}=\frac{\mu_0(T)}{kT}+\log p_0, \tag{33}$$

where p_0 is the vapor pressure of the liquid at T. Subtracting Eq. (33) from Eq. (32) gives

$$(N-X)/N=p/p_0=x \tag{34}$$

or

$$X=N(1-x). \tag{35}$$

If we now substitute Eq. (35) into Eq. (29) to eliminate X, there results

$$C=\frac{\theta(1-x)^2}{x(1-\theta+\theta x)}\times\exp\left[\frac{\theta(1-x)}{1-\theta+\theta x}-\alpha\theta(1-x)\right], \tag{36}$$

$$C=\frac{b'jj_n}{j_L}\frac{2\pi mkT}{h^2}\exp\left[(\epsilon_1-\epsilon_L)/kT\right], \tag{37}$$

$$\theta=Nb'/\mathfrak{A},\quad \alpha=2a'/b'kT.$$

The quantity θ corresponds to v/v_m in the BET theory. It is not possible to solve Eq. (36) for θ or x explicitly. In order to calculate an isotherm, for given values of C and α, one must find by trial the value of x which satisfies Eq. (36) for each value of θ chosen.

There are several special cases of interest:

(1) At low pressures ($x\ll 1$), Eq. (36) simplifies to

$$x=\frac{1}{C}\frac{\theta}{1-\theta}\exp\left(\frac{\theta}{1-\theta}-\alpha\theta\right). \tag{38}$$

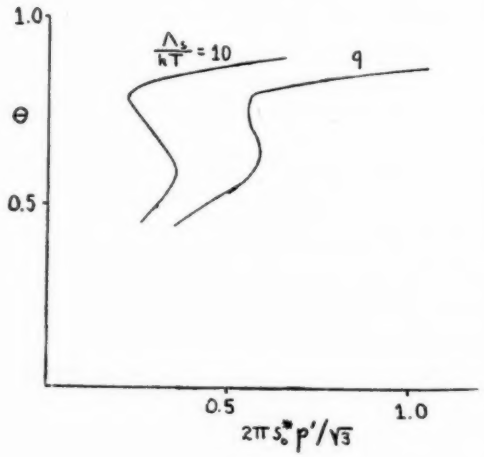

FIG. 4.

It should be emphasized that this equation can also be derived directly from Eq. (26) alone, if only unimolecular adsorption is allowed. That is, it follows from Eq. (24) and does not depend on any of the assumptions concerning the behavior of layers other than the first. In most cases of interest, Eq. (38) is an excellent approximation to Eq. (36) up to values of θ of about 0.7 or 0.8. Then second and higher layers begin to build up and θ becomes increasingly larger than Eq. (38) would predict. We have plotted, in Fig. 2, θ against Cx for several values of α, using Eq. (38). The critical value of α is $\alpha_c=27/4$, or $T_c=8a'/27b'k$. This is, of course, also the critical temperature of the equation of state, Eq. (24). The other critical values are $\theta_c=\frac{1}{3}$ and $x_c=0.0869/C$. These results are of interest in connection with the recent communication of Jura, Loeser, Basford, and Harkins[10] reporting a first-order phase change for n-heptane on the surface of silver at 15°C and $p=0.019$ mm ($x=0.00070$). Clearly, the present theoretical treatment is in semiquantitative agreement with their results (see also reference 2). As we have arbitrarily chosen van der Waals' equation as the equation of state, one should not expect more than this. Since C will generally be of the order of 100 or more, x_c is in the neighborhood of 10^{-3}–10^{-4}. Hence this phase change is to be expected at quite low pressures ordinarily, as is emphasized by Jura and co-workers on the basis of their experimental work.

(2) If we set $a'=0$ and $b'=0$, the first layer is a perfect gas. Equation (36) then reduces to

$$N=\frac{\mathfrak{A}C}{b'}\frac{x}{(1-x)^2}, \tag{39}$$

a result obtained by Cassie[11] by an incorrect argument.[9]

(3) If the exponential factor in Eq. (36) is ignored, one obtains, on solving for θ,

$$\theta=Cx/(1-x)(1-x+Cx), \tag{40}$$

which is the BET equation.

Returning now to the general isotherm, Eq. (36), we have plotted in Fig. 3 as an illustration the isotherm for $C=490$ and $\alpha=8$. The dotted curves are ordinary BET curves for comparison, with $c=490$, 81, and 27. The solid points above the $\alpha=8$ curve are for $\alpha=12$ and those below are for $\alpha=4$. It will be observed that Eq. (36) is not very sensitive to α (except at low pressures). It is also not very sensitive to C, when $x>0.1$. For example, in this region the points for $\alpha=4$ and $C=490$ are also approximately the points for $\alpha=8$ and C equal to about 10. However, the sensitivity to C at low pressures is considerable, as is indicated in Fig. 2.

Perhaps the most noticeable difference between the mobile isotherm, Eq. (36), and the BET isotherm is that the former associates much lower pressures with values of θ less than, say, 0.8. In general this is in the direction of a correction of a well-known fault of the BET equation, but unfortunately Eq. (36) seems to over correct considerably. It should be remarked that this property (low pressures) of Eq. (36) is caused primarily by the fact that we are taking into account interactions between molecules in the first layer and not to the fact that the molecules are mobile. As will be seen in a later paper of this series, if one takes these interactions into account in a localized first layer a condensation can take place[3] at pressures which are also very low. But in this localized condensation θ jumps from almost zero to almost unity, and $\theta_c=\frac{1}{2}$.

While the equations of this section should not be expected to provide a really satisfactory agreement with experiment, it is of some interest to know to what extent they are actually applicable and useful. In a paper to be published at a later date, Dr. George Jura will discuss this question, using experimental data obtained at the University of Chicago.

Finally, the question arises as to whether a more satisfactory equation of state might be used. A possibility that suggests itself is the equation of Devonshire.[12] Actually, the general form (Fig. 4) of the adsorption isotherm thus obtained at low pressures (corresponding to Eq. (38)) is not nearly as satisfactory as Eq. (38) itself, obtained from van der Waals' equation, judging from the experimental curves of Jura and

[10] G. Jura, *et al.*, J. Chem. Phys. **13**, 535 (1945). See also reference 20.

[11] A. B. D. Cassie, Trans. Faraday Soc. **41**, 450 (1945).

[12] A. F. Devonshire, Proc. Roy. Soc. **163A**, 132 (1937).

co-workers (which are the only ones available up to the present time). For example, θ_c (Devonshire) $=0.71$, which appears to be much too high. The adsorption isotherm is derived in Appendix I.

IV. RELATIONS BETWEEN THE TWO-DIMENSIONAL EQUATION OF STATE AND THE ADSORPTION ISOTHERM

The equation of state of an adsorbed phase can be related thermodynamically to the adsorption isotherm through the Gibbs equations (Appendix II). However, thermodynamics can tell us only very little about the equation of state and adsorption isotherm separately. The following equations represent the best that can be done (the notation is summarized in Appendix II):

$$p(\Gamma, T)=\exp\left\{\left[\left(\frac{\partial A}{\partial N}\right)_{\mathfrak{A},T}-\mu^0(T)\right]\Big/kT\right\}, \quad (41)$$

$$\varphi(\Gamma, T)=-(\partial A/\partial\mathfrak{A})_{N,T}. \quad (42)$$

Thermodynamics does not provide $A(\mathfrak{A}, N, T)$ or $\mu^0(T)$. In order to proceed we must turn to statistical mechanics.

We shall confine the discussion to mobile monolayers as this is the case in which φ is of most interest. A corresponding treatment can be given for other systems, using the appropriate partition function. We have,

$$A=-kT\log Q, \quad (43)$$

where Q is the partition function. The problem thus becomes one of finding Q. In analogy with Eq. (26), we employ here

$$Q=\frac{1}{N!}\left[jj_n\exp(\epsilon_1/kT)\frac{2\pi mkT}{h^2}\right]^N Q_r$$

$$=\frac{1}{N!}Q_1{}^N Q_r, \quad (44)$$

where Q_r is the usual configuration integral

$$Q_r=\int\cdots\int e^{-W/kT}dx_1dy_1\cdots dx_Ndy_N, \quad (45)$$

and $W(x_1,\cdots y_N)$ is the potential energy of interaction between the N adsorbed molecules.

In Eq. (44), Q_1 is independent of $\mathfrak{A}$ so that

$$\varphi=-\frac{\partial A}{\partial\mathfrak{A}}=kT\frac{\partial\log Q}{\partial\mathfrak{A}}, \quad (46)$$

$$=kT\frac{\partial\log Q_r}{\partial\mathfrak{A}}. \quad (47)$$

We now express p in terms of Q_r. In Eq. (41),

$$\frac{\partial A}{\partial N}=-kT\frac{\partial\log Q}{\partial N}, \quad (48)$$

$$=kT\left(\log N-\log Q_1-\frac{\partial\log Q_r}{\partial N}\right) \quad (49)$$

(assuming that Q_1 is independent of N) and, as is well known,[3]

$$\frac{\mu^0(T)}{kT}=-\log\left[\frac{(2\pi mkT)^{\frac{1}{2}}kTj_G}{h^3}\right], \quad (50)$$

where j_G is the internal partition function of a molecule in the gas phase. Substituting Eqs. (49) and (50) in Eq. (41), there results

$$p'=p\left\{\frac{j}{j_G}\cdot\frac{hj_n\exp(\epsilon_1/kT)}{(2\pi mkT)^{\frac{1}{2}}kT}\right\}$$

$$=N\exp\left(-\frac{\partial\log Q_r}{\partial N}\right), \quad (51)$$

which defines p'. When the internal degrees of freedom of adsorbed molecules are not appreciably influenced by interactions with the surface, $j=j_G$. It is often convenient to rewrite Eq. (51) in the form (compare Eqs. (36) and (37)):

$$p'=\frac{p}{p_0}\left\{\frac{jj_n}{j_L}\frac{2\pi mkT}{h^2}\exp\left[(\epsilon_1-\epsilon_L)/kT\right]\right\}$$

$$=N\exp\left(-\frac{\partial\log Q_r}{\partial N}\right), \quad (52)$$

in which we have made use of Eq. (33).

Equations (47) and (51) give φ and p in terms of Q_r. Q_r depends on N and $\mathfrak{A}$ and on the intermolecular forces between the N adsorbed molecules. If the nature of these forces is known, it is possible in principle to derive Q_r from Eq. (45).

However, because of mathematical difficulties, approximations[13] must be resorted to in practice.

When the surface does not effectively influence the intermolecular forces between adsorbed molecules, the right-hand members of Eqs. (47) and (51) are independent of the properties of the surface and depend only on Γ, T, and the properties of the gas being adsorbed. If the adsorption of a given gas is studied on several different surfaces, all of which satisfy the above condition, it is clear that $\varphi(\Gamma, T)$ and $p'(\Gamma, T)$ should be the same for all the surfaces. That is, for surfaces of this type, the two-dimensional equation of state of a given gas is independent of the surface, and the adsorption isotherm $\Gamma(p, T)$ depends on the surface only to the extent that in plotting Γ against p, p must be multiplied by an appropriate constant (which depends on the surface) for each surface in order to make the different adsorption isotherms coincide. This might be the basis of an approximate method of determining the surface area of a solid from the known surface area of another solid[14] (or of determining the relative surface areas of several solids). For, if both surfaces are in the class being discussed, any unusual features of the adsorption isotherms (e.g., phase changes) will occur at the same value of $\Gamma = N/\mathfrak{A}$. Hence if $N_1/\mathfrak{A}_1 = N_2/\mathfrak{A}_2$ and if N_1, N_2 and $\mathfrak{A}_1$ are known, $\mathfrak{A}_2$ may be calculated.

The question naturally arises as to what combinations of adsorbents and adsorbates are likely to exhibit the phenomenon, discussed above, of the independence of $\varphi(\Gamma, T)$ and $\Gamma(p', T)$ on the adsorbent. There will obviously be a wide range of examples, depending primarily on the polar properties of adsorbent and adsorbate.[15] The most unfavorable case, from the present point of view, would be the adsorption of a substance with a strong permanent dipole moment on a plane of an ionic crystal having all ions of the same type (e.g., the 100 plane in caesium iodide). The permanent dipoles of the adsorbed molecules will all be oriented approximately in the same direction thus introducing a repulsive orientation effect between them. There will be an additional and similar effect because of a further dipole induced by the ions of the crystal. The attractive dispersion forces and the short range repulsive forces between adsorbed molecules should be relatively unaffected by the surface. But the over-all effect of the adsorbent on the forces between the adsorbed molecules would be considerable in this case. On the other hand, the most favorable combination would be the adsorption of a gas without permanent moments (dipole, quadrupole, etc.) on a non-polar surface (e.g., argon on graphite, charcoal, metals, mercury). In such a case the dispersion and repulsive forces between the adsorbed molecules should be essentially the same as in the gas phase. Without an experimental or a detailed theoretical study of the question, it is rather difficult to say very much about intermediate cases. However, it is clear that the most important criterion for the independence of $\varphi(\Gamma, T)$ and $\Gamma(p', T)$ on the adsorbent is that the adsorbent be non-polar (non-ionic, no oriented dipoles). This is perhaps more crucial than the presence or absence of permanent moments in the adsorbed molecules.

The above argument implies that the most suitable gases would be those that are small and spherically symmetrical. There is another reason for this. Regardless of whether or not the surface is polar, a large or non-spherical molecule will tend to be oriented on the surface in such a way as to give a large "contact" between the surface and the adsorbed molecule (e.g., heptane molecules would lie flat on the surface rather than assume all possible orientations with the same probabilities as in the gas phase). This will clearly lead to a different intermolecular potential function for adsorbed molecules as compared to molecules in the gas phase. Also, the extent to which a molecule is flattened by a surface will be a function of the nature of the surface (even if the surfaces considered are non-polar). Hence, not only will the intermolecular potential function be different (in this case), for adsorbed molecules and molecules in the gas phase but the potential function will also be different for adsorbed molecules on different surfaces, because of varying degrees of flattening.

A further complication is that the most desirable molecules, such as argon, may not be

---

[13] See pp. 423–426 of reference 3. For a van der Waals gas

$$Q_\tau = (\mathfrak{A} - Nb')^N \exp(a'N^2/\mathfrak{A}kT).$$

For a perfect gas, $Q_\tau = \mathfrak{A}^N$.

[14] See also D. H. Bangham, Proc. Roy. Soc. **A147**, 175 (1934).

[15] See Chapters VII and VIII of reference 1a.

TABLE I. Two-dimensional critical constants for *n*-heptane.

	Experimental			Theoretical	
	Silver	Ferric oxide	Graphite	Lennard-Jones and Devonshire	Van der Waals
T_{2c}	$14.9°C < T_{2c} < 25°C$	29°C	31°C	13°C	−3°C
$\frac{\mathfrak{A}_c}{N}$	$310A^2 < \frac{\mathfrak{A}_c}{N} < 2200A^2$	$900A^2$	$400A^2$	$82A^2$	$110A^2$
φ_c	$\varphi_c > 0.18$ erg/cm²	0.45 erg/cm²	1.05 erg/cm²	1.9 erg/cm²	0.87 erg/cm²

completely mobile at temperatures sufficiently low to study two-dimensional condensation.

In view of the above restrictions there is naturally some question as to just how many, if any, actual systems will satisfy the various requirements (to some reasonable degree of accuracy). This question must be settled by experiment. At the present time, experimental data do not exist for a suitable test of this point. Practically all of the work in this field (phase changes on solids) has been done at the University of Chicago by Harkins, Jura, and co-workers, but the systems studied so far are not suitable, for the reasons discussed above, to test the arguments of this or the following section.

V. RELATIONS BETWEEN THE TWO- AND THREE-DIMENSIONAL EQUATIONS OF STATE

In this section also we shall only consider mobile monomolecular adsorption. There has been some interest in the past in the relation between the two- and three-dimensional critical temperatures but there has not been as much discussion of the more general problem of the relations between the two- and three-dimensional equations of state. The two equations are obviously closely connected. In the ideal case (discussed at the end of Section IV), the law of force between molecules is essentially the same, but the two equations of state differ in that: (1) in the adsorbed phase, the configuration integral Q_τ (Eq. (45)) is over $x_1, \cdots y_N$ as compared to $x_1, \cdots z_N$; and (2) in the adsorbed phase,

$$\varphi = kT\frac{\partial \log Q_\tau}{\partial \mathfrak{A}}, \tag{53}$$

as compared to

$$P = kT\frac{\partial \log Q_\tau}{\partial V}. \tag{54}$$

Experimental evidence on the ratio of the two-dimensional critical temperature to the three-dimensional critical temperature, T_{2c}/T_{3c}, is not at all plentiful. There is a certain amount of indirect evidence[16] which is contradictory. The best (until recently) direct evidence[12,17,18] indicates that two-dimensional condensation does not occur at temperatures well below T_{3c}, but the ratio T_{2c}/T_{3c} was not actually measured.

On the theoretical side, using the method (for spherical molecules) which Lennard-Jones and Devonshire[19] applied successfully to three-dimensional condensation, Devonshire[12] found that, according to the theory, $T_{2c}/T_{3c} = 0.53$. As pointed out by Devonshire, this value agrees qualitatively with the experimental work mentioned above[17,18] (as far as that work goes). Of considerably more interest is the fact that, in the condensation of *n*-heptane on silver recently reported by Jura and co-workers,[10] the critical temperature was found to lie between 14.9°C and 25°C. As will be clear from the discussion at the end of the preceding section, heptane is not a very satisfactory molecule for this type of comparison; but it is still interesting that, using the known value of $T_{3c} = 266.8°C$, the temperatures 14.9°C and 25°C lead to a value of T_{2c}/T_{3c} between 0.53 and 0.55, in excellent agreement (somewhat fortuitous, no doubt) with Devonshires prediction.[20]

[16] See pp. 440–444 of reference 1a.

[17] H. Cassel and K. Neugeberger, J. Phys. Chem. **40**, 523 (1936).

[18] F. Simon and R. L. Swain, Zeits. f. physik. Chemie **B28**, 189 (1935).

[19] J. E. Lennard-Jones and A. F. Devonshire, Proc. Roy. Soc. **163A**, 53 (1937).

[20] After the present manuscript was submitted, a paper appeared by Jura, Loeser, Basford, and Harkins (J. Chem. Phys. **14**, 117 (1946)) in which this agreement is also discussed. In a private communication, Dr. Jura has kindly supplied me with the critical constants for heptane on ferric oxide and on graphite. These values are given in Table I. They are somewhat more exact than the values published in the above reference. The T_{2c}/T_{3c} ratio for

Although the theory of Lennard-Jones and Devonshire[19] is quite successful in predicting critical temperatures of gases, it is not very successful in predicting critical volumes and pressures. Hence, it is perhaps not surprising to find that the theoretical critical two-dimensional pressure φ_c and area $\mathfrak{A}_c$, calculated (see below) from the theory and the experimental three dimensional values for n-heptane, do not seem to agree very well with the two-dimensional experimental values. This may be seen in Table I[20] and in the curves given by Jura and co-workers.[10,20] We also include in Table I, for purposes of comparison, the corresponding theoretical values (also based on the three-dimensional experimental values) obtained if one uses the appropriate two- and three-dimensional van der Waals' equations (see below). In the critical region one should not, of course, take van der Waals' equation very seriously, but these results are still of some interest. Although neither Devonshire's theory nor van der Waals' equation should lead to very good values of the critical area, it is probably true that the large discrepancy between the theories and experiment is owing at least in part to some special cause. That is, as mentioned by Jura and co-workers,[20] the experimental critical areas are really much higher than one would expect.

The van der Waals values in Table I were obtained by carrying through the two-dimensional statistical treatment of the hard sphere model with an attractive energy proportional to r^{-6} for $r>r_0$. The approximations made were the same as in the corresponding three-dimensional treatment given by Mayer and Mayer.[21] This leads to the evaluation of the two-dimensional van der Waals constants. If the two- and three-dimensional equations of state are

$$\left(\varphi+\frac{a'N^2}{\mathfrak{A}^2}\right)(\mathfrak{A}-Nb')=NkT, \tag{55}$$

$$\left(P+\frac{aN^2}{V^2}\right)(V-Nb)=NkT, \tag{56}$$

one finds

$$b'=2\left[\pi\left(\frac{r_0}{2}\right)^2\right]=2\alpha_0=\frac{\pi}{2}\left(\frac{3b}{2\pi}\right)^{\frac{2}{3}}, \tag{57}$$

$$a'=\frac{\pi u_0 r_0^2}{4}=\frac{\pi a}{4b}\left(\frac{3b}{2\pi}\right)^{\frac{2}{3}}, \tag{58}$$

where α_0 is the projected area of a hard sphere of radius $r_0/2$ and $-u_0$ is taken as the potential energy of interaction between two molecules practically in contact ($r\rightarrow r_0$). Using the expressions for the critical constants in terms of the van der Waals constants, one obtains the following relations between the two- and three-dimensional critical constants:

$$T_{2c}=0.50T_{3c}, \tag{59}$$

$$\frac{\mathfrak{A}_c}{N}=\frac{3\pi}{2}\left(\frac{V_c}{N}\cdot\frac{1}{2\pi}\right)^{\frac{2}{3}}=1.38\left(\frac{V_c}{N}\right)^{\frac{2}{3}}, \tag{60}$$

$$\varphi_c=\frac{P_c\left(\frac{V_c}{N}\cdot\frac{1}{3}\right)^{\frac{2}{3}}}{\pi\left(\frac{3}{2\pi}\right)^{\frac{2}{3}}}=0.361P_c\left(\frac{V_c}{N}\right)^{\frac{2}{3}}. \tag{61}$$

It will be noted in particular that $T_{2c}/T_{3c}=0.50$, according to this model.

The corresponding equations for the theory of Lennard-Jones and Devonshire are approximately:

$$T_{2c}=0.53T_{3c}, \tag{62}$$

$$\mathfrak{A}_c/N=1.03(V_c/N)^{\frac{2}{3}}, \tag{63}$$

$$\varphi_c=0.79P_c(V_c/N)^{\frac{2}{3}}. \tag{64}$$

These are based on the following approximate values estimated from the data and curves given by Lennard-Jones and Devonshire (in their notation except for T_{2c} and T_{3c}):

$$\left.\begin{aligned} p_c v_0/NkT_{3c}&=0.36, & p_{sc}s_0/NkT_{2c}&=0.71;\\ \Lambda/kT_{3c}&=9, & \Lambda_s/kT_{2c}&=8.6;\\ v_c/v_0&=1.8, & s_c/s_0&=1.4. \end{aligned}\right\} \tag{65}$$

---

both ferric oxide and graphite is 0.56. The critical areas and pressures for heptane on the three surfaces are not in agreement. This is certainly not surprising (see the discussion at the end of Section IV). One gets the impression that T_{2c} is not nearly so sensitive to varying conditions as $\mathfrak{A}_c$ and φ_c.

[21] J. E. Mayer and M. G. Mayer, *Statistical Mechanics* (John Wiley and Sons, Inc., New York, 1940), pp. 262–269. As Mayer and Mayer point out, the correct results are obtained here by a convenient but slightly incorrect argument (cancellation of errors).

It should be of considerable interest to find experimental values of the numerical constants[22] appearing in Eqs. (62)–(64) and in Eqs. (59)–(61). The question is, will these experimental constants, in suitable cases, be independent of the adsorbent and adsorbate? If, as there is some reason to expect, constant "constants" are indeed found, say, for small spherical non-polar adsorbates on non-porous non-polar adsorbents, the values of these constants should be useful in providing an additional check on theories of the liquid state and condensation. That is, if both two- and three-dimensional versions of a theory are worked out, as was done by Lennard-Jones and Devonshire, the theoretical constants of Eqs. (62)–(64) may be calculated and compared with experiment.

It is planned to carry out in this laboratory some experimental work in connection with the theoretical problems discussed in Sections III, IV, and V.

The author is indebted to Professor K. S. Pitzer, Dr. George Jura, and Dr. P. H. Emmett for their helpful comments.

APPENDIX I

We use the notation of Devonshire in this Appendix. For Devonshire's model the configuration integral Q_τ is

$$Q_\tau=\left\{\pi a^2 Ng\exp\left[\frac{\Lambda_s}{kT}(1.06\theta^3-0.5\theta^6)\right]\right\}^N, \tag{69}$$

with

$$\theta=s_0/s, \tag{70}$$

$$g=\int_0^1 \exp\left[\frac{\Lambda_s}{kT}\{-\theta^6 l_s(y)+2\theta^3 m_s(y)\}\right]dy. \tag{71}$$

The θ defined above has approximately the same physical significance as the θ in Section III. Using $a^2=2s/\sqrt{3}N$, Eq. (69) becomes

$$Q_\tau=\left\{\frac{2\pi sg}{\sqrt{3}}\exp\left[\frac{\Lambda_s}{kT}(1.06\theta^3-0.5\theta^6)\right]\right\}^N. \tag{72}$$

This gives Q_τ as a function of s and N. After obtaining $\frac{\partial \log Q_\tau}{\partial N}$, as required by Eq. (51), there results finally

$$p'=\frac{\sqrt{3}}{2\pi s_0{}^*}\cdot\frac{\theta}{g}\cdot\exp\left[-\frac{\Lambda_s}{kT}\left\{\theta^3\left(4.24+6\frac{g_m}{g}\right)-\theta^6\left(3.5+6\frac{g_l}{g}\right)\right\}\right] \tag{73}$$

or, in a form which is more convenient for calculations,

$$p'=\frac{\sqrt{3}}{2\pi s_0{}^*}\cdot\frac{\theta}{g}\cdot\exp\left[\frac{p_s s}{NkT}-1-\frac{\Lambda_s}{kT}(1.06\theta^3-0.5\theta^6)\right]. \tag{74}$$

The tables given by Devonshire for $\Lambda_s/kT=9$ and 10 were used to calculate $2\pi s_0{}^* p'/\sqrt{3}$, as plotted in Fig. 4.

The critical values of Λ_s/kT and s/s_0 are estimated by Devonshire to be approximately 8.6 and 1.4, respectively. Hence, $\theta_c=1/1.4=0.71$.

APPENDIX II

In studying an adsorbed insoluble surface phase of a single substance which is in equilibrium with the same substance in gaseous form, there are certain thermodynamic variables which are most useful: the surface area $\mathfrak{A}$, the equilibrium number of adsorbed molecules N (in the area $\mathfrak{A}$), the absolute temperature T, the pressure p of the gas phase in equilibrium with the adsorbed phase, the two-dimensional (spreading) pressure φ of the adsorbed phase, and the Helmholtz free energy A of the adsorbed phase. $\mathfrak{A}$, N, and T may most conveniently be thought of as independent variables and p, φ, and A as dependent variables. Also, $\mathfrak{A}$, N, and $A(\mathfrak{A}, N, T)$ are extensive properties while T, $p(\mathfrak{A}, N, T)$, and $\varphi(\mathfrak{A}, N, T)$ are intensive properties. Hence p and φ may be written $p(\Gamma, T)$ and $\varphi(\Gamma, T)$ and the same is true of $A/\mathfrak{A}$, where $\Gamma=N/\mathfrak{A}$, the surface concentration.

We wish to consider the relations between the adsorption isotherm, which is obtained experimentally in the form $p(\Gamma, T)$ or $\Gamma(p, T)$, and the equation of state $\varphi(\Gamma, T)$. We assume for convenience that the gas phase is a perfect gas so that μ_G, the chemical potential of this phase, may be written

$$\mu_G=\mu^0(T)+kT\log p. \tag{75}$$

In an exact treatment, we would replace p by the fugacity. The chemical potential μ_A of the adsorbed phase is, by definition,

$$\mu_A=(\partial A/\partial N)_{\mathfrak{A},T}. \tag{76}$$

At equilibrium,

$$\mu_A=\mu_G, \tag{77}$$

$$(\partial A/\partial N)_{\mathfrak{A},T}=\mu^0(T)+kT\log p. \tag{78}$$

This equation relates A and p. The corresponding relation between A and φ is contained in the thermodynamic definition of φ:

$$\varphi=-(\partial A/\partial\mathfrak{A})_{N,T}. \tag{79}$$

The next step is to eliminate A from Eqs. (78) and (79).

---

[22] The fact that constants are expected which are independent of the gas (if the intermolecular potential function is of the same form for different gases, and is identical for a given gas in two and three dimensions) follows from the law of corresponding states, especially as discussed by Fowler and Guggenheim (reference 3, pp. 342–345). Partly in their notation we have

$$\begin{aligned} kT_{3c}&=\text{const.}\times\Lambda^*,\\ V_c/N&=\text{const.}\times r^{*3},\\ P_c&=\text{const.}\times\Lambda^*/r^{*3}; \end{aligned} \tag{66}$$

and also

$$\begin{aligned} kT_{2c}&=\text{const.}\times\Lambda^*,\\ \mathfrak{A}_c/N&=\text{const.}\times r^{*2},\\ \varphi_c&=\text{const.}\times\Lambda^*/r^{*2}. \end{aligned} \tag{67}$$

Combining these equations,

$$\begin{aligned} T_{2c}/T_{3c}&=\text{const.},\\ \mathfrak{A}_c/N&=\text{const.}\times(V_c/N)^{\frac{1}{3}},\\ \varphi_c&=\text{const.}\times P_c(V_c/N)^{\frac{1}{3}}. \end{aligned} \tag{68}$$

Integrating Eq. (78) for fixed values of $\mathfrak{A}$ and T,

$$A(\mathfrak{A}, N, T)=\int_0^N [\mu^0(T)+kT\log p]dN, \tag{80}$$

since $A(\mathfrak{A}, 0, T)=0$. Therefore, using Eqs. (79) and (80), and keeping T constant in the following,

$$-\varphi=\int_0^N \frac{\partial}{\partial\mathfrak{A}}[\mu^0(T)+kT\log p]dN, \tag{81}$$

$$=kT\int_0^N \left(\frac{\partial \log p}{\partial\mathfrak{A}}\right)_N dN. \tag{82}$$

Now, since $p=p(\Gamma)$,

$$\left(\frac{\partial \log p}{\partial\mathfrak{A}}\right)_N=\left(\frac{\partial\Gamma}{\partial\mathfrak{A}}\right)_N\frac{d\log p}{d\Gamma}=-\frac{\Gamma}{\mathfrak{A}}\frac{d\log p}{d\Gamma}. \tag{83}$$

Equation (82) becomes

$$\varphi=kT\int_0^\Gamma \Gamma\frac{d\log p}{d\Gamma}d\Gamma \tag{84}$$

or

$$\varphi=kT\int_0^p \Gamma d\log p. \tag{85}$$

In differential form, Eq. (85) is

$$d\varphi=\Gamma kTd\log p. \tag{86}$$

Equations (85) and (86) are the familiar Gibbs equations as applied to this type of adsorption. The derivation given here proves helpful in relating the thermodynamic and statistical aspects of the problem. It will be noted from the derivation that Eqs. (85) and (86) are thermodynamically exact, except for the assumption that the gas phase behaves like a perfect gas. These equations are also general, applying to monomolecular, multimolecular, mobile, and localized adsorption on a solid or liquid. Of course φ is not of much physical interest except for the case of mobile monomolecular adsorption.

The usual procedure in obtaining the equation of state from the experimentally determined adsorption isotherm $\Gamma(p)$ is to evaluate $\varphi(p)$ from Eq. (85), and then, by combining $\Gamma(p)$ and $\varphi(p)$, find $\varphi(\Gamma)$ at the given temperature.

THE JOURNAL OF CHEMICAL PHYSICS VOLUME 14, NUMBER 7 JULY, 1946

Time-Dependence of Boundary Tensions of Solutions

I. The Role of Diffusion in Time-Effects

A. F. H. WARD AND L. TORDAI
Faculty of Technology, University of Manchester, Manchester, England

(Received April 19, 1946)

The variation of surface tension of solutions with time has in some cases, where the change is over within a few seconds or less, been explained on the basis of diffusion. This paper attempts a rigorous mathematical analysis of the role that diffusion might play in such time-effects. The limitations of diffusion theories which have been proposed previously are discussed. A general theory of diffusion to the surface is derived, which allows for back-diffusion and which makes no special assumptions of a physical nature. It is possible to use Fick's equation to calculate the total amount of solute which diffuses from a semi-infinite bulk solution into the surface if the concentration immediately under the surface is known at various times throughout the process. It is shown how the latter information may be deduced from the variation of surface tension with time together with final equilibrium values of surface tension. The methods of this theory are applied to analyze recent data on time-effects of short duration. It is concluded that even in cases where the variation of the surface tension is over in less than a second the rate-determining process is not diffusion. Even for these very rapid changes one is therefore led to assume the existence of an activation barrier which determines the rate of adsorption.

INTRODUCTION

MANY instances have been reported of the surface tension of solutions being a function of time. In some cases this has been ascribed to slow chemical changes in the bulk of the solution.[1] But many observed time-variations cannot be explained in this way. The change in surface tension may occur very slowly, over a period of several days.[2,3] On the other hand, variations of an apparently similar kind may be complete in a few hours or within an hour.[4–6] In some cases the time-effect may last only for a

[1] A. Lottermoser and B. Baumgürtel, Trans. Faraday Soc. **31**, 200 (1935).

[2] N. K. Adam and H. L. Shute, Trans. Faraday Soc. **31**, 205 (1935).

[3] N. K. Adam and H. L. Shute, Trans. Faraday Soc. **34**, 758 (1938).

[4] K. S. G. Doss, Kolloid Zeits. **84**, 138 (1938).

[5] K. S. G. Doss, Kolloid Zeits. **86**, 205 (1939).

[6] H. V. Tartar, V. Sivertz, and R. E. Reitmeier, J. Am. Chem. Soc. **62**, 2375 (1940).

few seconds to a few minutes.[7] Finally, time-variations of surface tension have been observed which are complete within a fraction of a second.[8–11] Quite recently, the authors have shown that interfacial tensions may also be time-dependent.[12] The same theory may not explain all these effects; in fact many different explanations have been proposed. A review of these explanations is not contemplated here, but merely an examination of the role that diffusion to the surface may play.

The suggestion that diffusion of the solute to the surface was the cause of the alteration of surface tension with time was first made by Milner,[13] who did not, however, treat the theory quantitatively. Equations to describe the phenomenon in terms of diffusion have been deduced by Bond and Puls,[8] Doss,[5] Ross,[14] and Langmuir and Schaefer.[15] Their treatments involve various approximations and simplifying assumptions. Although no generally exact quantitative treatment of diffusion to the surface has been put forward, it seems clear that many of the observed cases of alteration of boundary tension with time are very much too slow to be explained by diffusion. In general terms, there is some kind of activation barrier, which hinders the establishment of the adsorbed film.[4,12] For those cases where the alteration of surface tension with time is very rapid, diffusion theories so far put forward are insufficiently exact to determine critically whether the variation with time can be entirely attributed to diffusion. The object of the present paper is to develop a general theory of diffusion to the surface which will allow a definite decision to be made in any case as to whether diffusion is a complete explanation of the time-variation or whether some additional effect must be sought.

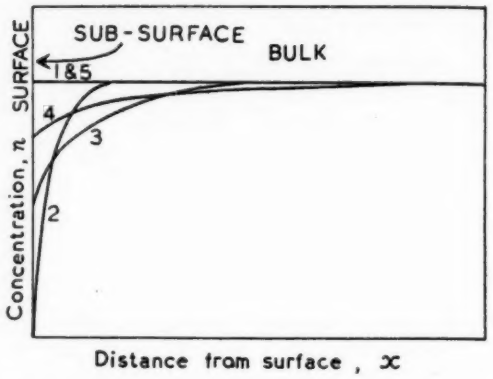

FIG. 1. Successive stages in concentration gradient from surface into the bulk solution during diffusion to the surface. (1) initial; (2), (3), and (4) intermediate; and (5) final stages.

NATURE OF DIFFUSION PROCESS

Before the diffusion theory is developed, it is convenient to give a physical description of the process. We may suppose that initially there is a solution of uniform concentration and at a certain instant a plane surface (solution/air) is created. At this moment the concentration of solute in the surface is the same as the bulk concentration. If the solute is a substance which is positively adsorbed, its molecules are in a position of lower potential energy in the surface than in the bulk. Although individual molecules move in all directions, the resultant flow of solute molecules is in a direction from the bulk to the surface. The region of the bulk solution, with a thickness of a few molecular diameters only, immediately next to the surface, is referred to here as the "sub-surface." At the initial stage in the formation of the adsorbed layer, solute molecules will diffuse from the bulk to the sub-surface more slowly than they pass from the sub-surface to the surface, on the assumption that equilibrium is established instantaneously between the latter two regions. This is so, because initially the surface is practically empty and every molecule arriving at the surface is likely to arrive at an empty "site" and become adsorbed. For all practical purposes the sub-surface concentration may be regarded as falling from its initial value to zero immediately.

Eventually, as the surface becomes fuller, there is an increased probability that a solute molecule in the sub-surface will arrive at a portion of

[7] J. W. McBain and D. A. Wilson, J. Am. Chem. Soc. **58**, 379 (1936).
[8] W. N. Bond and H. O. Puls, Phil. Mag. [7] **24**, 864 (1937).
[9] C. C. Addison, J. Chem. Soc., p. 252 (1944).
[10] C. C. Addison, J. Chem. Soc., p. 477 (1944).
[11] C. C. Addison, J. Chem. Soc., p. 98 (1945).
[12] A. F. H. Ward and L. Tordai, Nature **154**, 146 (1944).
[13] S. R. Milner, Phil. Mag. [6] **13**, 96 (1907).
[14] S. Ross, J. Am. Chem. Soc. **67**, 990 (1945).
[15] I. Langmuir, and V. J. Schaefer, J. Am. Chem. Soc. **59**, 2400 (1937).

the surface already occupied by the adsorbed solute. Such a molecule will, of course, remain in the sub-surface, which will accumulate solute molecules more rapidly than these are passed on to the surface. As soon as the concentration in the sub-surface is sensibly different from zero we must consider the possibility of back-diffusion from the sub-surface to the bulk. The sub-surface concentration will continue to rise until eventually, at equilibrium, it will have a concentration equal to that in the bulk (on the assumption that the bulk region can be regarded as an infinite reservoir of solute molecules). Successive stages in the concentration gradient are shown in Fig. 1.

If the sub-surface concentration at each instant is known throughout this process, the diffusion of molecules from the bulk to the sub-surface might be treated by application of the ordinary diffusion equations. But in fact the sub-surface concentrations cannot be obtained directly. The experimental measurements are the values of the surface tension at various times. Assumptions have to be made relating the surface tension to the sub-surface concentration. It is partly on account of the approximate nature of these assumptions that previous treatments of this problem have been inadequate.

Doss[4,5] avoided this difficulty in his study of the slow adsorption of benzopurpurin at an air/water surface by measuring directly the surface concentration at various times by compressing the surface film and measuring the area under a definite pressure. However, his theoretical treatment was inaccurate. He neglected back-diffusion from the surface to the bulk. His calculations were based on the Einstein diffusion equation for the mean displacement of a particle, but in the application of this he assumed that the molecules reaching the surface all started from a region where the concentration equalled the bulk concentration. This would only be true at the very beginning and at the end of the diffusion process, and the assumption is equivalent to neglecting the concentration gradient near the sub-surface. This same fundamental inaccuracy is also to be found in the treatment by Ross,[14] who follows Doss's method very closely. Ross compensates for certain deficiencies in the diffusion theory by supposing that the adsorption layer is multimolecular. The hypothesis of thick layers on the surface of solutions containing such simple solutes is, however, not acceptable. It has been shown recently[16] that the assumption of monolayers of the solute on the surface of these solutions satisfies the thermodynamical requirement that the activities of the solute in the bulk and surface phases, respectively, shall be proportional to each other. It would therefore appear unjustifiable to postulate the existence of multimolecular layers to explain this new effect.

A diffusion theory was proposed by Bond and Puls[8] based on Fick's diffusion equation. Since this is a statistical equation based on the behavior of all the molecules, it should allow a general solution to be derived, and if appropriate boundary conditions are employed, it should cover both forward- and back-diffusion. However, Bond and Puls made the limiting assumptions that the adsorption layer could be supposed to be almost unoccupied and that the lowering of surface tension was proportional to the concentration. This restricts their treatment to the initial stages only of the diffusion process. In addition, their final integrated equation

$$(\bar{q}-q)/\bar{q}=\exp\left[-(2/\pi^{\frac{1}{2}})(t/\tau)^{\frac{1}{2}}\right],$$

(their Eq. (9)), which has been quoted and used by other workers, is in fact incorrect, presumably because of an erroneous integration procedure.

SIMPLE DIFFUSION THEORY

A simple theory may be developed first for the early stages in the diffusion when the backward movement of solute from the sub-surface to the bulk may be neglected. The surface is then sufficiently empty to take up solute molecules as fast as they arrive and the sub-surface concentration is practically zero. The problem is analogous to that of the diffusion of heat from an infinite conductor, initially at uniform temperature, into a conductor of infinite conductivity placed in contact.

Let n=concentration in the solution at a distance x from the surface at a time t. From the equations for heat flow in the analogous case[17]

[16] A. F. H. Ward and L. Tordai, Trans. Faraday Soc. (in press).

[17] H. S. Carslaw, *Mathematical Theory of Heat Conduction* (MacMillan and Company, London, 1921), p. 34.

we obtain the equation

$$\frac{\partial n}{\partial x}=\frac{n_0}{(\pi Dt)^{\frac{1}{2}}}\exp\left(-\frac{x^2}{4Dt}\right), \quad (1)$$

where n_0 is the constant bulk concentration and D is the diffusion coefficient defined by Fick's equation

$$\partial n/\partial t=D\partial^2 n/\partial x^2. \quad (2)$$

At the extreme edge of the bulk solution, i.e., the sub-surface, where $x=0$, Eq. (1) is simplified to

$$(\partial n/\partial x)_{x=0}=n_0/(\pi Dt)^{\frac{1}{2}}, \quad (3)$$

and the rate of diffusion across 1 cm^2 of the plane, $x=0$, is given by

$$(\partial M/\partial t)_{x=0}=-Dn_0/(\pi Dt)^{\frac{1}{2}}. \quad (4)$$

Hence, the amount of solute which has diffused across this plane into the surface up to the time, t, i.e., the surface concentration at that time, M, is given by

$$M=\int_0^t\left(\frac{\partial M}{\partial t}\right)_{x=0}\cdot dt=2n_0\left(\frac{Dt}{\pi}\right)^{\frac{1}{2}}. \quad (5)$$

This equation is identical with one used by Langmuir and Schaefer[15] to explain diffusion of ions into monolayers.

GENERAL DIFFUSION THEORY

It is also possible to develop a more general theory which will make allowances for back-diffusion. Such a theory may be derived from Eq. (2) and the treatment is applied to a single phase extending from the bulk (assumed infinite in extent) to the sub-surface, but not including the surface. No assumptions regarding the relation between surface and sub-surface concentrations are introduced at this stage and the solution is therefore quite general.

Consider linear diffusion of solute molecules towards the boundary plane $x=0$ of a semi-infinite liquid solution. The bulk concentration remains effectively constant (n_0) during the process. The concentration in the sub-surface varies with time and may be expressed as $\phi(t)$. To obtain a solution of the problem it is possible to utilize a mathematically analogous theorem in heat conduction, based on Eq. (2) and the use of Green's functions[17] (p. 173). The temperature v at a distance x from the surface of the semi-infinite solid of thermal conductivity κ, initially at temperature v_0 with its surface at temperature $\phi(t)$ at time t is given by

$$v=\frac{v_0}{2(\pi\kappa t)^{\frac{1}{2}}}\int_0^\infty\left\{\exp\left[-\frac{(x-x')^2}{4\kappa t}\right]-\exp\left[-\frac{(x+x')^2}{4\kappa t}\right]\right\}dx+\frac{x}{2(\pi\kappa)^{\frac{1}{2}}}\int_0^t\phi(\tau)\frac{\exp\left[-\frac{x^2}{4\kappa(t-\tau)}\right]}{(t-\tau)^{\frac{3}{2}}}d\tau, \quad (6)$$

where $\tau(\tau<t)$ is the time at which an instantaneous point source of unit strength, at a distance x' from the surface, generates heat. It is important to note that Eq. (6) is made up of two terms. The first term corresponds to a flow of heat from the bulk region (which is initially at temp. v_0) towards the surface (initially at zero temp.). The second term represents a flow of heat in the opposite direction, from the surface at temp. $\phi(t)$ towards the bulk (initially at zero temp.). In the diffusion nomenclature, we are interested in obtaining

$$(\partial n/\partial x)_{x\to 0},$$

where n, the concentration, replaces v; n_0 and D replace v_0 and κ. D is the diffusion coefficient. To simplify the problem we employ two sets of transformations. In the first term we may write

$$x'=x+2(Dt)^{\frac{1}{2}}\xi \quad \text{and} \quad x'=-x+2(Dt)^{\frac{1}{2}}\xi,$$

for the first and second integrals, respectively. In the second term

$$\mu=x/2(D(t-\tau))^{\frac{1}{2}}, \quad \text{that is,} \quad t-\tau=x^2/4D\mu^2.$$

With such a change of variables Eq. (6) reduces to

$$n=\frac{2n_0}{\pi^{\frac{1}{2}}}\int_0^{x/2(Dt)^{\frac{1}{2}}}\exp(-\xi^2)d\xi+\frac{2}{\pi^{\frac{1}{2}}}\int_{x/2(Dt)^{\frac{1}{2}}}^\infty\phi\left(t-\frac{x^2}{4D\mu^2}\right)\exp(-\mu^2)d\mu. \quad (7)$$

It will be convenient to treat the two terms in Eq. (7) separately. It will be assumed that the first term contributes $\partial n_1/\partial x$ and the second $\partial n_2/\partial x$ to give the total $\partial n/\partial x$. Differentiation of the first term with respect to x gives

$$\frac{\partial n_1}{\partial x}=\frac{n_0}{(\pi Dt)^{\frac{1}{2}}}\exp\left(-\frac{x^2}{4Dt}\right). \tag{8}$$

If x tends to zero in Eq. (8), we obtain Eq. (3) and for the amount of solute, M_1, contributed by this direction of flow, an expression is obtained which is identical with Eq. (5).

Turning our attention to the second term in Eq. (7) and writing $a=x/2(Dt)^{\frac{1}{2}}$, we obtain

$$n_2\frac{\pi^{\frac{1}{2}}}{2}=\int_a^\infty \phi\left(t-\frac{a^2}{\mu^2}t\right)\exp(-\mu^2)d\mu. \tag{9}$$

The integrand in Eq. (9) may be expanded by Maclaurin's theorem to give

$$n_2\frac{\pi^{\frac{1}{2}}}{2}=\sum_0^\infty \frac{(-1)^r}{r!}a^{2r}t^r\phi(t)\int_0^\infty \exp(-\mu^2)\mu^{-2r}d\mu,$$

and by repeated integration by parts we obtain the series

$$\begin{aligned}n_2\frac{\pi^{\frac{1}{2}}}{2}&=\phi(t)\int_a^\infty \exp(-\mu^2)d\mu\\&\quad+\sum_1^\infty a\frac{(-1)^r}{r!}t^r\phi^{(r)}(t)\\&\quad\times\left[\frac{1}{(2r-1)}-\frac{2a^2}{(2r-1)(2r-3)}\right.\\&\quad\left.+\frac{2^2a^4}{(2r-1)(2r-3)(2r-5)}-\cdots\right].\end{aligned} \tag{10}$$

Differentiating with respect to a, we have

$$\begin{aligned}\frac{\pi^{\frac{1}{2}}}{2}\frac{\partial n_2}{\partial a}&=-\exp(-a^2)\phi(t)\\&\quad+\sum_1^\infty \frac{(-1)^r}{r!(2r-1)}t^r\phi^{(r)}(t)+O(a^2),\end{aligned} \tag{11}$$

and letting $a\to 0$ as $x\to 0$ the final result is

$$\left(\frac{\partial n_2}{\partial x}\right)_{x=0}=-\frac{1}{(\pi Dt)^{\frac{1}{2}}}\sum_0^\infty \frac{(-1)^r t^r}{(2r-1)r!}\phi^{(r)}(t), \tag{12}$$

the first few terms of this series being

$$-\frac{1}{(\pi Dt)^{\frac{1}{2}}}\left\{\phi(t)+t\phi'(t)-\frac{1}{6}t^2\phi''(t)+\frac{1}{30}t^3\phi'''(t)-\cdots\right\}.$$

It is more convenient to express the series (12) as an integral. It is easily shown that

$$\left(\frac{\partial n_2}{\partial x}\right)_{x=0}=-\frac{1}{2(\pi D)^{\frac{1}{2}}}\int_0^t \frac{\phi(z)}{(t-z)^{\frac{1}{2}}}dz, \tag{13}$$

where z is a variable; for putting $(t-z)=\theta^2$ we obtain an integral which can be expanded by Maclaurin's theorem to give Eq. (12).

The amount of solute, M_2, which flows from the surface in the direction of the bulk, must next be determined. Starting from Fick's equation

$$(\partial M_2/\partial t)_{x=0}=-D(\partial n_2/\partial x)_{x=0},$$

we are led to consider the integral

$$M_2=\frac{1}{2}\left(\frac{D}{\pi}\right)^{\frac{1}{2}}\int_0^t\int_0^t \frac{\phi(z)}{(t-z)^{\frac{1}{2}}}dzdt. \tag{14}$$

It can be shown that Eq. (14) reduces to

$$M_2=-\left(\frac{D}{\pi}\right)^{\frac{1}{2}}\int_0^t \frac{\phi(z)}{(t-z)^{\frac{1}{2}}}dz. \tag{15}$$

To prove the equivalence of Eqs. (14) and (15) use will be made of Cauchy's theorem on n-times repeated integrals. This theorem, together with a process involving differentiation and integration to fractional orders enables us to complete the proof.

If we put

$$F(t)=\frac{1}{\Gamma(n)}\int_0^t (t-z)^{n-1}\phi(z)dz, \tag{16}$$

then

$$\frac{1}{\Gamma(n)}\int_0^t (t-z)^{n-1}\phi(z)dz=\int_0^t \frac{(t-z)^{n-1}}{(n-1)!}\phi(z)dz, \tag{17}$$

and Cauchy's theorem states

$$\int_0^t \frac{(t-z)^{n-1}}{(n-1)!}\phi(z)dz=\mathbf{D}^{-n}\phi(t). \tag{18}$$

The operator, $\mathbf{D}^{-1}$, stands for $\int_0^t \cdots dz$, whereas $\mathbf{D}^1$ has its usual meaning d/dz. For our particular case we have

$$F(t)=\int_0^t \frac{\phi(z)}{(t-z)^{\frac{1}{2}}}dz.$$

From Eqs. (16)–(18) we obtain

$$F(t)=\Gamma(\tfrac{1}{2})\mathbf{D}^{-\frac{1}{2}}\phi(t). \qquad (19)$$

We are interested in finding the derivative, $F'(t)$, and to show that it gives an integral, such as occurs in Eq. (13). We can write

$$F'(t)=\frac{d}{dt}\int_0^t \frac{\phi(z)}{(t-z)^{\frac{1}{2}}}dz$$

$$=\Gamma(\tfrac{1}{2})\mathbf{D}\mathbf{D}^{-\frac{1}{2}}\phi(t)=\Gamma(\tfrac{1}{2})\mathbf{D}^{\frac{1}{2}}\phi(t). \qquad (20)$$

From Eqs. (17), (18), and (20) we have

$$F'(t)=\Gamma(\tfrac{1}{2})\frac{1}{\Gamma(-\frac{1}{2})}\int_0^t (t-z)^{-\frac{1}{2}-1}\phi(z)dz$$

$$=-\tfrac{1}{2}\int_0^t \frac{\phi(z)}{(t-z)^{\frac{3}{2}}}dz, \qquad (21)$$

which is the result required to prove the equivalence of Eqs. (14) and (15).

For the two opposing processes we now have

$$M=2\left(\frac{D}{\pi}\right)^{\frac{1}{2}}\left\{n_0 t^{\frac{1}{2}}-\int_0^{t^{\frac{1}{2}}}\phi(z)d[(t-z)^{\frac{1}{2}}]\right\}, \qquad (22)$$

where the expression for M_2 is written in a slightly different form which has advantages from the point of view of numerical computation.

It is possible to derive the expression for M_2 in a very much simpler but less rigorous way. Consider a semi-infinite liquid solution with zero initial concentration, the surface concentration being kept constant at a value c. After the lapse of time t, the amount which has diffused inward from the surface (taken as the positive direction) is given by

$$M'=2c\left(\frac{Dt}{\pi}\right)^{\frac{1}{2}}. \qquad (23)$$

From this system we can reproduce another with a varying surface concentration $\phi(t)$. It is assumed that the surface concentration is changed in a stepwise manner so that Eq. (23) still applies for a short time, during which the surface concentration is constant and yet the stepwise change is taken to approximate $\phi(t)$, the latter being given by a smooth curve. Such an argument assumes, justifiably, that each portion of the solute which diffuses from the surface during one of the periods with a constant surface concentration, c_n, continues its diffusion independently of any other portions of the solute. This is equivalent to the assumption that the diffusion is an ideal process, that is to say that the diffusion coefficient is independent of concentration.

We have then

Δc_0 on the surface during diffusion from $t=0$ to $t=T$,
Δc_1 on the surface during diffusion from $t=1$ to $t=T$,
.....,
Δc_n on the surface during diffusion from $t=n$ to $t=T$,

where $T=$ time needed to reach equilibrium conditions between bulk and surface. The total diffusion inward from the surface in the interval between $t=0$ and $t=T$ is obtained by summation

$$\sum M'=2\left(\frac{D}{\pi}\right)^{\frac{1}{2}}\sum_0^T \Delta c_t(T-t)^{\frac{1}{2}}. \qquad (24)$$

We can make the approximation as good as we please by decreasing the duration of each step. In the limit, the expression (24) can best be represented by plotting $\phi(t)$ against $(T-t)^{\frac{1}{2}}$ and multiplying the area under the curve by $2(D/\pi)^{\frac{1}{2}}$. This is the integral

$$2\left(\frac{D}{\pi}\right)^{\frac{1}{2}}\int_0^{T^{\frac{1}{2}}}\phi(t)d[(T-t)^{\frac{1}{2}}], \qquad (25)$$

which is identical in form with the corresponding part in Eq. (22) except for the sign. In Eq. (22) M_2 is naturally negative as it represents diffusion away from the surface taken in a negative direction.

CALCULATION OF DIFFUSION COEFFICIENTS

The Eq. (22) enables us in theory to obtain either M or D if one of the two is known. Unfortunately, explicit integration in Eq. (22) is not possible as $\phi(t)$ is not known explicitly. We can, however, employ a physical artifice which makes graphical integration possible and gives M the surface concentration at time t.

If it is assumed that there is no activation barrier between the sub-surface and the surface and that diffusion is the sole reason for the delay in establishing adsorption equilibrium, then the time required for the solute to diffuse from the sub-surface to the surface is very much smaller than the time required for diffusion equilibrium to be established between bulk and sub-surface. At any instant, there is a state of equilibrium between the surface and the sub-surface with respect to the solute.

The observed boundary tension is determined by the concentration of solute in the surface and this is in turn determined by the concentration in the sub-surface, $\phi(t)$. If a certain value of the boundary tension (γ) corresponds to a certain value of $\phi(t)$, say c, at any moment during the diffusion, that particular value of γ would also be obtained under equilibrium conditions when the concentrations in the sub-surface and the bulk were both equal to c. The relationship between γ and $\phi(t)$ can therefore be obtained from observations made under equilibrium conditions when diffusion has ceased. Values of the equilibrium boundary tension are plotted against the corresponding concentrations. In this way, from observed values of γ during the diffusion process, the variation of $\phi(t)$ with time may be found without the necessity of making arbitrary assumptions about the relationship between γ and the surface concentration and between the latter and $\phi(t)$. In this way the integral for M_2 can be evaluated in terms of $D^{\frac{1}{2}}$, for the period of time which is necessary for equilibrium to be established. The values of M (=Gibbs' Γ) at equilibrium may be obtained independently by application of the Gibbs' equation to the observed relationship between the concentration and the equilibrium boundary tension. Since M is known in units of $D^{\frac{1}{2}}$, it is then possible to calculate D.

This method makes it possible to obtain diffusion coefficients from measurements of boundary tensions which vary with time. These will, of course, only be equivalent to the conventional diffusion coefficients if there is nothing in the nature of the physical system to invalidate the assumption of instantaneous equilibrium between the surface and the sub-surface. If this assumption is not true, and there is an activation barrier between the surface and the sub-surface, the value of D calculated from surface tension measurements (which will be referred to as D_s) will be a complex quantity characteristic of both diffusion and the crossing of the barrier. In such a case either of the processes may assume a controlling role. For a calculated value of D_s which is of the same order of magnitude as the conventional D, the normal diffusion process is the slower of the two. In such a case the existence of a small additional barrier at the surface would become a trivial question, as no possible experiment could be devised to investigate the nature of this barrier. For a calculated value of D_s which is smaller than the conventional D it is evidently the barrier at the surface which has the controlling role. If D_s is very small, the diffusion process can be neglected in comparison with the activated adsorption.

Quantitative conclusions cannot, however, be drawn from such very small values of D_s, for it must be borne in mind that in such a case the assumption of instantaneous equilibrium between surface and sub-surface is invalidated and no great significance can be attached to the calculated value of D_s. The theory should therefore give the correct value of the diffusion coefficient (as compared with the conventional value) if the process is purely a diffusion process, but if the calculated value of D_s is smaller than the usual bulk diffusion coefficient, it indicates that diffusion is not the rate-determining process.

A series of short time-effects have been investigated by Addison,[9-11] who measured the surface tensions of freshly formed surfaces of aqueous solutions of fatty alcohols, at intervals of a small fraction of a second. He employed the oscillating jet method and measured changes of surface tension with time, up to about one second, by which time equilibrium had been established after a rapid initial fall. Experimental results were reported for *n*-amyl, iso-amyl, *n*-hexyl, *n*-heptyl, and *n*-octyl alcohols at 20°C, some of them at several concentrations. The theory developed in this paper was applied to Addison's data and values of D_s were obtained by the graphical integration method. Calculated values of D_s are collected in Table I (column 6).

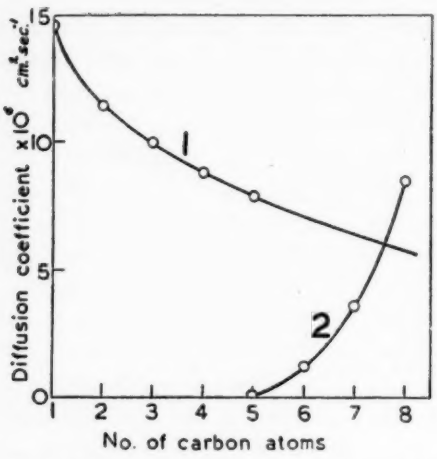

FIG. 2. Variation of calculated and observed diffusion coefficients with chain-length. (1) Observed D. (2) Calculated D_s.

DISCUSSION

Values of Γ have been obtained by the use of the approximate Gibbs' equation (using concentrations) since activity values for solutions of these alcohols were not available. For the lower alcohols at the lowest concentrations this was a sufficiently good approximation. It may be seen from Table I that for the highest concentration of *n*-hexyl alcohol the calculated value of Γ (8.67×10^{-10}) is obviously too high. This is probably caused by the divergence between concentration and activity. Since a high value of Γ yields a high value of D_s, it appears that if accurate activity data were used the values of D_s in column 6 would at any rate be no higher than those given. They may therefore be taken safely as an upper limit.

The conventional diffusion coefficient (D) for iso-amyl alcohol in water has been obtained by Thovert[18] as 6.9×10^{-6} cm^2 sec.$^{-1}$ at 15°C, corresponding to 7.9×10^{-6} at 20°C. The calculated value of D_s in Table I is 56 times smaller than this. Therefore diffusion is not the rate-determining process here, and a further activation barrier must exist. Experimental values of diffusion coefficients are not available for the higher alcohols. But the probable values may be seen in Fig. 2, where the curve of experimental values of D for the lower alcohols (curve 1) is extrapolated. The decrease in D with increase in the size of the molecule would be expected from the Stokes-Einstein formula

$$D=kT/6\pi r\eta.$$

Curve 2 shows the values of D_s calculated from Addison's data for the lowest concentrations in each case. Up to heptyl alcohol the values of D_s are all lower than the correct values of D. But the most convincing argument against the process being merely diffusion is not so much the fact that $D_s<D$ as the general trend of D_s to increase with chain-length. This is the opposite of what would be expected for a diffusion coefficient. The fact that D_s for octyl alcohol is of the right order of magnitude for agreement with D is therefore probably fortuitous. Thus the numerical results indicate that the rate of adsorption in these cases is not determined by diffusion.

Some doubt is thrown on the experimental values for the higher alcohols considered in Table I because of the probability that equilibrium was not attained. If $\phi(t)$ is plotted against the time, the curve should flatten when equilibrium is reached. These values are plotted in Fig. 3, for *n*-amyl alcohol (0.04544 molal) and *n*-octyl alcohol (0.0007962 molal).

It will be observed that the curve for *n*-amyl alcohol flattens out satisfactorily within the time of observation. The curve for *n*-octyl alcohol indicates that equilibrium may not have been attained within 0.11 sec., the time of the final observation.

Available literature seems to indicate that the time required to obtain equilibrium surface tensions increases very rapidly with chain-length for solutions of aliphatic acids. King,[19] using a drop-weight method, found that drop-lives of at

TABLE I.

(1) Solute (alcohols)	(2) Molality	(3) $M_1\times D^{\frac{1}{2}}$ $\times10^6$	(4) $M_2\times D^{\frac{1}{2}}$ $\times10^6$	(5) $\Gamma\times10^{10}$ mole/cm^2	(6) $D_s\times10^6$ cm^2/sec.
n-amyl	0.01136	2.026	1.348	2.93	0.185
n-amyl	0.02272	3.242	2.445	3.98	0.250
n-amyl	0.04544	5.612	3.750	5.92	0.100
iso-amyl	0.01384	2.410	1.620	2.97	0.141
n-hexyl	0.00245	0.895	0.707	2.09	1.28
n-hexyl	0.00735	2.620	2.290	3.77	1.31
n-hexyl	0.01226	4.360	4.070	5.44	3.62
n-hexyl	0.02161	5.975	5.240	8.67	1.39
n-heptyl	0.001724	0.645	0.497	2.83	3.66
n-octyl	0.0007962	0.298	0.127	4.98	8.48

[18] J. Thovert, Ann. d. Physik [9] 2, 369 (1914).

[19] H. H. King, Kansas State Agr. Col., Agr. Exp. Station, Tech. Bull., No. 9 (1922).

least five minutes were required to attain steady values of surface tension with all acids above *n*-butyric acid. For solutions of nonylic acid 30-minute drops had to be used and for decylic acid, the surface tension was still falling after 30 minutes. Addison,[20] working with solutions of decylic acid, found that times of the order of a minute were required to reach a "dynamic equilibrium" and that this was followed by a further slow fall of surface tension. These observations appear to throw more doubt on the existence of a real equilibrium, for solutions of long chain alcohols, after the lapse of a tenth of a second or less. Further experimental information on this point would be valuable.

To explain the apparent increase in "migrational velocity" of the solute molecule with increasing chain-length, Addison has defined this velocity in quantitative terms and assumed that the main factors controlling the rate of adsorption were the free energy change on adsorption and the distance of the solute molecule from the surface. While it is not at all obvious why the velocity of a solute molecule traveling towards the surface should depend on its distance from it, it is even less acceptable to suppose that this velocity should depend on the lowering of the surface tension by the adsorption of the solute molecule. In any physical or chemical change a system may undergo, the velocity of the change depends not on the difference in the free energies between the initial and final states, but on any intermediate activation barriers. The numerical calculations of Addison are further invalidated by his use of the Gibbs' equation for calculating surface excesses at stages prior to the establishment of equilibrium.

The authors have been carrying out experiments on the time-dependence of interfacial tension between water and solutions of long chain compounds in hexane.[12] Full details of this

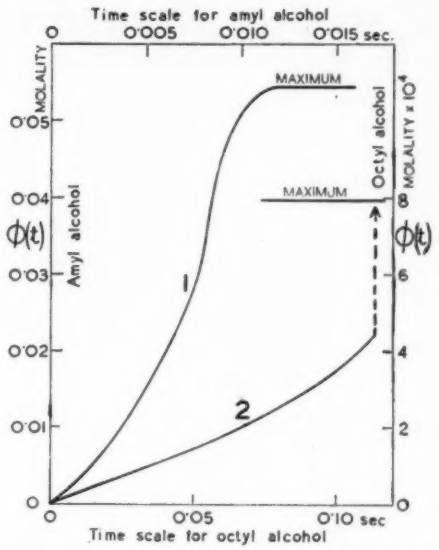

FIG. 3. Change of sub-surface concentration with time. (1) Amyl alcohol. (2) Octyl alcohol.

work will be published shortly, but an example may be given now to support the conclusions reached above. For solutions of palmitic acid in hexane values of $\phi(t)$ were obtained from a complete set of equilibrium interfacial tension data. The surface concentration was obtained by means of an equation of state proposed by Langmuir.[21] For a concentration of 0.04101 molal the calculated value of D_s so obtained was 5.66×10^{-13}, a value about 10^7 times smaller than the expected magnitude of the diffusion coefficient. It is clear that in this system also there is an activation barrier between the sub-surface and the surface.

We are much indebted to Dr. J. Howlett, Mr. W. K. Burton, and Mr. A. Howarth for several helpful discussions. We also wish to thank Imperial Chemical Industries, Ltd. (Dyestuffs Division) for a grant to one of us (L.T.) during part of the time in which this work was carried out.

[20] C. C. Addison, Nature **156**, 600 (1945).

[21] I. Langmuir, J. Chem. Phys. **1**, 756 (1933).

Letters to the Editor

THIS section will accept reports of new work, provided these are terse and contain few figures, and especially few halftone cuts. The Editorial Board will not hold itself responsible for opinions expressed by the correspondents. Contributions to this section should not exceed 600 words in length and must reach the office of the Managing Editor not later than the 15th of the month preceding that of the issue in which the letter is to appear. No proof will be sent to the authors. The usual publication charge ($3.00 per page) will not be made and no reprints will be furnished free.

Jones-Ray Effect, Wettability, and Zeta-Potential

HANS M. CASSEL
Speedry Products, Inc., New York 6, New York
May 28, 1946

EXCEPT for an observation of Heydweiller[1] who noticed that chlorate solutions wetted the glass he used poorly, no consideration seems to have been given to the possibility that the presence of ions in solution may affect the angle of contact. In interpreting the Jones-Ray effect,[2] so far, perfect wettability of the capillary walls has been taken for granted. The explanation suggested by Langmuir[3] appears to be in accord with a great deal of experimental evidence.[4] However, it is difficult to reconcile his hypothesis with the Laplace equilibrium condition at the meniscus/film boundary in the limiting case of absolutely pure liquids where no difference of osmotic pressures can be thought of. An alternative view is here presented, namely that an increase of the wetting angle may be involved in the apparent decrease of surface tensions as found with minute concentrations of strong electrolytes.

The cylindrical capillary layer adjacent to a perfectly wetting meniscus is usually treated as if it were a "duplex film" of liquid in bulk. However, one should be aware of the fact that its vapor pressure is smaller than that of a hollow cylinder of liquid in mass of equal diameter whose vapor pressure equals that of a capillary film of twice the capillary radius. Therefore, the capillary film should be recognized as an "adsorbed phase."[5] Accordingly, one should not conclude that its "surface tension" is equal to that of the liquid, or that its "interfacial tension" at the film/solid boundary is the same as that of the liquid/solid interface. It appears also questionable that the solubilities of electrolytes or non-ionic substances are the same in the capillary film as in the liquid, because the dielectric constants may be different, that of the film probably being smaller.

The following is based upon Gibbs' treatment of "Surfaces of Discontinuity between Solids and Fluids"[6] which implies that the "surfaces of tension" coincide closely with the physical surfaces of the solids, no matter what the thickness of the adsorbed films, provided that the radii of curvature are very large in proportion to the film thickness.

According to Neumann's equation the "apparent surface tension" of the liquid equals the difference of the vapor solid surface tension, σ', and the liquid/solid interfacial tension, σ. Whatever the value of the contact angle, a change in capillary height will result from the adsorption of a third component and the desorption of solvent by which the difference of the tensions is altered:

$$d(\sigma'-\sigma) = -(\Gamma_2'-\Gamma_2)d\mu_2-(\Gamma_3'-\Gamma_3)d\mu_3. \quad (1)$$

Here, the negative quantity of solvent adsorbed at the liquid/solid interface can be neglected in comparison to the excess adsorbed in the film. The excess of the third component in the film comprises the quantity adsorbed at the film/solid interface and the total amount dissolved in the film volume per unit area:

$$(c_3'/c_2')\Gamma_2'. \quad (2)$$

The molar potentials of solvent and solute are (approximately) correlated by the (Duhem) equation:

$$c_2d\mu_2+c_3d\mu_3=0, \quad (3)$$

where c_2 and c_3 are the numbers of moles per unit volume. Equation (1), therefore, assumes the form:

$$d(\sigma'-\sigma)=\left[\Gamma_2'\left(\frac{c_3}{c_2}-\frac{c_3'}{c_2'}\right)-\Gamma_3'+\Gamma_3\right]d\mu_3, \quad (4)$$

which for very small concentrations reduces further to:

$$d(\sigma'-\sigma)=(\Gamma_3-\Gamma_3')d\mu_3. \quad (5)$$

Hence, in the range of minute concentrations, an increase or decrease in capillary height would solely depend on whether the excess of adsorbed solute is greater at the liquid/solid interface or at the film/solid interface.

Regarding the possibility that the dielectric constant of the film is smaller than that of the solvent in mass, the behavior of sugar solutions would appear as quite normal. In case of electrolytes, at first view, the same might be expected. However, Langmuir's[7] theory of the potential distribution between parallel solid surfaces as a function of their distance seems to open an understanding of the reverse case.

There is also experimental evidence in favor of the present interpretation. The diffuse double layer in the vicinity of an insulator of high Z-potential is obviously of the same character as that of a highly polarized metal electrode in contact with an electrolyte solution. Now, the contact angles of gas bubbles attached to metal electrodes have been the subject of extensive studies by Frumkin and his co-workers[8] who have established the fact that the contact angle decreases when the potential increases. Accordingly, it is logical to conclude that the Jones-Ray effect is caused by an increase of the wetting angle resulting from a decrease in the Z-potential at the solution/solid interface.

[1] A. Heydweiller, Ann. d. Physik (4) **33**, 148 (1910).
[2] G. Jones and W. A. Ray, J. Am. Chem. Soc. **59**, 187 (1937).
[3] I. Langmuir, Science **88**, 430 (1938).
[4] L. A. Wood and L. B. Robinson, J. Chem. Phys. **14**, 258 (1946).
[5] H. M. Cassel, J. Chem. Phys. **12**, 115 (1944); J. Phys. Chem. **48**, 195 (1944).
[6] J. W. Gibbs, *Collected Works* I, 328 (1928).
[7] I. Langmuir, J. Chem. Phys. **6**, 891 (1938).
[8] A. Frumkin, *Couche Double, Electrocapillarité, Surtension* (Hermann and Cie., Paris, 1936), p. 17.

Note on the Rigid Multi-Layer Postulate of Eversole and Lahr

G. A. H. ELTON
Physical Chemistry Laboratory, Battersea Polytechnic, London, England
June 6, 1946

EVERSOLE and Lahr[1] have interpreted certain electrokinetic measurements as indicating properties of rigidity in part of the double layer at solid-electrolyte interfaces, a view held by von Buzagh[2] and others. They have used[1] published zeta-potential figures to deduce and thicknesses of from 3A to 63A for the rigid layer in aqueous salt solutions, values which could be accommodated by classical double layer theory, although Bikerman[3] is of the opinion that any rigid layer is caused by the inherent roughness of all solid surfaces. In a later experimental paper,[4] Eversole and Lahr produce evidence which, it is claimed, substantiates the previous calculations and indicates a rigid layer of thickness about 100A for water against quartz.

In the experiments of Eversole and Lahr the "distance of separation," ^{t}air, between a quartz lens and plate placed together in air was determined interferometrically. Water was then condensed between the lens and plate and the new "distance of separation," ^{t}water, determined. Negative values both for ^{t}air and ^{t}water were obtained, but it was assumed that the subtraction of ^{t}air from ^{t}water eliminated the error to which the negative values were due, and gave the thickness of the rigid layer. The validity of this assumption is to be questioned, in view of the very large variations in the individual values of ^{t}air and ^{t}water. The results obtained by Eversole and Lahr (five in number) are given in Table I.

Although the deviation from the mean in each series is as much as 600A, the conclusion drawn is that the total layer thickness, "subject of course to considerable experimental error," is about 200A. Since this involves two interfaces, the layer thickness at one surface is taken as 100A.

If now Students "t-test" for significance of differences between means of small populations, as described by Evans[5] is applied to the above results, there is indicated approximately a 75 percent probability that the difference between the means of the two series in Table I is not significant, because of the wide variation within each series.

Using an interferometric principle similar to that of Eversole and Lahr and a more developed technique, details of which will be published later, the writer has found no evidence for the presence of these layers in water, methyl alcohol or toluene. Some of the results obtained are given in Table II. (In the last column of this table, P indicates the approximate probability of insignificance in the difference of the means, as determined by Students "t-test".)

TABLE I.

Expt.	^{t}air A	^{t}water A	"Layer thickness" (^{t}water − ^{t}air) A
1	−1210	−870	330
2	− 950	−800	160
3	− 90	+140	230
4	−1160	−840	320
5	− 350	−220	130
Mean	− 75_2	− 51_8	23_4

TABLE II.

Liquid	Expt.	^{t}air A	^{t}liquid A	(^{t}liquid − ^{t}air) A	P
Water	1	20	15	− 5	
	2	− 5	5	10	
	3	− 5	0	5	
	4	10	0	−10	
	5	0	5	5	
	Mean	4	5	1	98%
Methyl alcohol	1	5	− 5	−10	
	2	25	− 5	−30	
	3	10	10	0	
	4	−10	0	10	
	5	−10	− 5	5	
	Mean	4	− 1	− 5	75%
Toluene	1	−10	−10	0	
	2	0	− 5	− 5	
	3	0	20	20	
	4	15	20	5	
	5	15	5	−10	
	Mean	4	6	2	95%

A further investigation of the subject is in progress, using air bubbles against quartz after the manner of Derjaguin,[6] who reports the presence of thick interfacial films on glass and mica in water. In view of the recent work of Tolansky,[7] any interferometric work on "smooth" mica cleavage planes must be viewed with suspicion, since variations in surface level of the order of several thousand angstroms may exist.

[1] W. G. Eversole and P. H. Lahr, J. Chem. Phys. **9**, 530 (1941).
[2] E.g., A. von Buzagh, *Colloid Systems* (Technical Press Ltd., London, 1937), pp. 153–4.
[3] J. J. Bikerman, J. Chem. Phys. **9**, 880 (1941).
[4] W. G. Eversole and P. H. Lahr, J. Chem. Phys. **9**, 686 (1941).
[5] U. R. Evans, Chem. Ind. **14**, 106 (1945); see also L. H. C. Tippell, *Methods of Statistics* (Williams and Norgatt Ltd., London, 1941), pp. 112–3.
[6] B. Derjaguin and M. Kussakov, Acta Physicochimica **10**, 25 (1939); B. Derjaguin and M. Kussakov, Acta Physicochimica **10**, 153 (1939).
[7] E.g., S. Tolansky, Proc. Roy. Soc. **A184**, 41 (1945); S. Tolansky, Proc. Roy. Soc. **A184**, 51 (1945).

Bond Hybridization in the Non-Tetrahedral Carbon Atom

JOHN E. KILPATRICK[1] AND RALPH SPITZER[2]
Department of Chemistry, University of California, Berkeley, California
June 17, 1946

INASMUCH as Duffey's calculations[3] lead to the prediction of 180° H−C−H angles in cyclobutane and cyclopropane (and possibly ethylene) which we do not think reasonable, we are presenting a somewhat similar calculation which we had made and which gives more reasonable results.

Duffey calculates s, p hybrids with maxima in the directions of the required bonds. However, considerably stronger bonds can be formed by dropping this requirement and assuming that bond strength is proportional to the value of the orbital in the desired direction, whether or not the maximum of the orbital lies in this direction.

The orbitals f_1 and f_2 were used to form the two carbon-carbon bonds whose angle is determined by the geometry of the molecule. The directions of the other two bonds are

taken in directions of the maxima of f_3 and f_4. With no loss in generality and a considerable gain in the simplicity of the equations, orbitals f_1 and f_2 can be chosen with their maxima in the xz plane, equally inclined to the z axis. By symmetry, f_3 and f_4 then lie in the yz plane, also equally inclined to the z axis.

Applying the usual normalization and orthogonality conditions we have:

$$f_1 = as + bp_z + (1/2)^{\frac{1}{2}} p_x, \tag{1}$$

$$f_2 = as + bp_z - (1/2)^{\frac{1}{2}} p_x, \tag{2}$$

$$f_3 = bs - ap_z + (1/2)^{\frac{1}{2}} p_y, \tag{3}$$

$$f_4 = bs - ap_z - (1/2)^{\frac{1}{2}} p_y, \tag{4}$$

$$b = +(\tfrac{1}{2} - a^2)^{\frac{1}{2}}. \tag{5}$$

We now determine the value of a (and b by Eq. (5)) so that f_1 will have the maximum value in a particular direction θ_0 in the xz plane by setting $df_1/da = 0$. This requires that

$$a = \left(\frac{1}{2 + 6\cos^2\theta_0}\right)^{\frac{1}{2}}, \tag{6}$$

$$b = \left(\frac{3\cos^2\theta}{2 + 6\cos^2\theta_0}\right)^{\frac{1}{2}}. \tag{7}$$

The angle θ_{34} between the bonds formed with the orbitals f_3 and f_4 is given by the expression:

$$\tan\theta_{34} = \frac{-2(1 + 3\cos^2\theta_0)^{\frac{1}{2}}}{3\cos^2\theta_0}. \tag{8}$$

We have calculated the H−C−H angle, θ_{34}, and bond strengths, f_{01} and f_{03}, for several values of $2\theta_0$, the C−C−C angle (Table I). Assuming bond energies proportional to

TABLE I.

$2\theta_0$ ($=\theta_{12}$)	Strength of bonds (1) and (2) f_{01}	θ_{34}	Strength of bonds (3) and (4) f_{03}
0°	1.414	126° 52′	1.982
60°	1.887	121° 58′	1.989
90°	1.984	115° 23′	1.995
108°	2.000	109° 58′	2.000
109° 28′	2.000	109° 28′	2.000
120°	1.996	105° 50′	1.998
180°	1.932	90°	1.732

square of bond strength and using[4] 59 and 87 kcal. for normal C−C and C−H bond energies, we obtain 10 and 2 kcal. as the strain energies per CH_2 group of cyclopropane and cyclobutane in fair agreement with experimental values of about 10 and 4[5] (estimated from cyclobutane derivatives). Probably about 2 kcal. should be added to the calculated values for torsional strain.[6] The energy calculation does not apply to ethylene because the bond is much shorter than it is in normal paraffins.

That the exterior angle in cyclopropane is not 180° as suggested by Duffey is shown conclusively by the large dipole moment of 1,1-dichlorocyclopropane.[7] Also, the calculation Duffey quotes from Herzberg[8] is incorrect. The correct C−C distance for 180° angle is 1.616A not 1.556A. The moment of inertia of cyclopropane is fitted, for example, by $r_{C-C} = 1.530$A (electron diffraction), $r_{C-H} = 1.070$, $\sphericalangle H-C-H = 125°$. No unique angle is obtained from one moment of inertia. Finally, Donohue *et al.*[9] find 120°±8° for ∢HCH in spiropentane. The electron diffraction of 1,1-dichlorocyclopropane would determine this angle.

In conclusion, it should be pointed out that the ideas of s,p hybridization and proportionality of energy to f^2 are approximations, and the agreement of these calculations with experiment is to a great extent fortuitous. For this reason, we did not attempt any further refinements such as simultaneous maximization of C−C and C−H bond energies.

[1] Research Associate for the American Petroleum Institute Research Project 44.
[2] National Research Fellow in chemistry.
[3] G. H. Duffey, J. Chem. Phys. **14**, 342 (1946).
[4] L. Pauling, *The Nature of the Chemical Bond* (Cornell University Press, Ithaca, New York, 1940).
[5] G. E. K. Branch and M. Calvin, *Theory of Organic Chemistry* (Prentice-Hall, Inc., New York, 1941), p. 279.
[6] K. S. Pitzer, Science **101**, 672 (1945).
[7] M. T. Rogers and J. D. Roberts, J. Am. Chem. Soc. **68**, 843 (1946).
[8] G. Herzberg, *Infra-Red and Raman Spectra of Polyatomic Molecules* (D. Van Nostrand, New York), p. 440. The C–C distance given for 120° is also incorrect.
[9] J. Donohue, G. L. Humphrey, and U. Schomaker, J. Am. Chem. Soc. **67**, 332 (1945).

Electronic Shifts at Moderate Temperatures in Metals of Group VIII

W. R. HAM* AND C. H. SAMANS**
American Optical Company, Southbridge, Massachusetts
May 31, 1946

FURTHER evidence has been secured, supplementing that offered some years ago for pure iron,[1] of what are believed to be specific electronic shifts in iron within ordinary temperature ranges. Similar series have also been established for all the other Group VIII metals by measurements of either the electrical resistance of pure or alloyed metal wires or of the electrolytic conductivity of glasses containing these metals. For all the metals, the temperatures of the discontinuities follow, within experimental limits, the simple Ritz formula:

$$T_k = ct[(1/n_0^2) - (1/n^2)],$$

where ct is a constant which is different for each metal; n_0 has the value 3 for Fe, Co, Ni, 4 for Ru, Rh, Pd, and 5 for Os, Ir, Pt; and n, for each metal, has the successive values n_0+1, n_0+2, $\cdots\ \infty$.

No change was found in the critical temperatures either with concentration or with the form of chemical combination. Hence the effect is believed to be a purely atomic phenomenon.

The fact that the Curie magnetic transition temperatures of Fe, Co, and Ni, all occur exactly at some definite term in the appropriate series indicates that the data may be of great importance in clarifying the theory of ferromagnetism.

Further details will be published shortly.

* Consulting physicist.
** Research metallurgist.
[1] C. B. Post and W. R. Ham, J. Chem. Phys. **5**, 913–919 (1937). W. R. Ham and W. L. Rast, Trans. A.S.M. **26**, 885–902 (1938).

On Steric Effects

TERRELL L. HILL
Department of Chemistry, University of Rochester, Rochester, New York
June 19, 1946

STERIC effects have long been recognized in both equilibrium and rate studies. Quantitative experimental data are now available in a number of instances.[1] However, on the theoretical side, it appears that only qualitative interpretations have been attempted. The purpose of this note is to suggest a very obvious and simple (but apparently new) semi-quantitative theoretical approach to the problem which might be found useful at least in some cases.

The forces involved in steric effects are well known: (1) groups or atoms (within a molecule) may repel each other if too close together (just as two gas molecules do for sufficiently small inter-molecular distances); (2) in order to decrease this interaction, the groups or atoms will tend to move apart, but this will generally require the stretching or bending of bonds with a related increase in energy. The final configuration will thus be the result of a compromise between the two types of force, and will be the configuration of minimum energy. The above simple argument (which can be generalized) applies when we may neglect entropy effects, all configurations but the one of lowest energy, polar effects, solvent effects, etc.

The suggestion to be made here is that it may sometimes prove worthwhile to attempt to formulate the above discussion quantitatively. For example, we might express approximately the steric energy, E^s, of a molecule as follows:

$$E^s = u_0\left(\frac{r_0}{r}\right)^{12} - 2u_0\left(\frac{r_0}{r}\right)^{6} + \tfrac{1}{2}k_s(l-l_0)^2 + \tfrac{1}{2}k_b(\theta-\theta_0)^2, \quad (1)$$

where additional terms are necessary if there is more than one pair of interacting groups, more than one bond being stretched, or more than one bond angle being bent. In Eq. (1), l is a bond distance, θ a bond angle, k_s and k_b are force constants, l_0 and θ_0 are the values of l and θ in the absence of steric effects, r is the distance between the two interacting groups, and $-u_0$ is the minimum value of the interaction energy (at $r=r_0$). Equation (1) assumes, as an approximation, that the Lennard-Jones form of the interaction potential is appropriate here and that Hooke's law holds (for large displacements in some cases).

The minimum value of E^s in Eq. (1) is desired. This is found using $r=r(l,\theta)$, $\partial E^s/\partial l=0$ and $\partial E^s/\partial\theta=0$. The constants u_0 and r_0 may be estimated from van der Waals constants and radii, or other data. The force constants are hypothetical force constants. They are not the force constants which might be determined experimentally, but rather those which would exist in the absence of steric effects. Hence, they must be estimated by analogy, guessed, or calculated backwards from experimental data.

Calculations of this kind might also be of interest from the point of view of studying (classically) polar and steric effects on molecular structure.[2]

The best type of equilibrium experimental data for comparison with theoretical calculations is of the sort obtained by Brown[1]: measurement of ΔH, ΔF, and ΔS for a series of gas phase reactions in which there is a systematic change in substituents. The procedure then is to calculate E^s for the reactants and products of the different reactions in the series (generally E^s may be taken as zero for some of these substances), and compare calculated values of $\Delta E_i{}^s$ (where i refers to the ith reaction in the series) with the deviations of ΔH_i from the values of ΔH_i which would be expected in the absence of steric effects (e.g., in the absence of steric effects, ΔH_i might be a linear function of i). A corresponding treatment of steric effects on reaction rates involves calculation of E^s for the reactants and the activated complexes in the series.

Sufficient preliminary equilibrium calculations have been made for the gas phase addition reaction between trimethylboron and the methylamines (and ammonia) to indicate that forces of the sort discussed here can give effects of the type and order of magnitude found experimentally by Brown. However, a discussion of results will be deferred until time is available to carry out more detailed and refined calculations (e.g., including polar effects).

Note added June 25, 1946: It has come to the author's attention that F. H. Westheimer has been developing independently a similar approach to this problem, with particular reference to reaction rates.

[1] See, for example, H. C. Brown and co-workers, Science **103**, 385 (1946); J. Am. Chem. Soc. **67**, 374, 378, 503, 1452, 1765 (1945).
[2] L. Pauling, *Nature of the Chemical Bond* (Cornell University Press, Ithaca, New York, 1945), pp. 78–80.

Nitrogen and Stearic Acid Adsorption by Supported and Unsupported Catalysts

HERMAN E. RIES, JR., MARVIN F. L. JOHNSON, AND JOHN S. MELIK
Research and Development Department, Sinclair Refining Company, East Chicago, Indiana
June 21, 1946

IT has been suggested earlier[1] that diatomaceous earth supports of low area (and relatively large pores) may be responsible for the high area small pore structure of certain supported catalysts. Considerable evidence supporting this viewpoint and bearing on the structure of supported catalysts has recently been obtained in these laboratories by means of nitrogen adsorption at low temperatures[2] and stearic acid adsorption from solution.[3] The following observations strongly indicate that the unsupported catalyst precipitated in the absence of diatomaceous earth forms finely-divided essentially non-porous particles, whereas the supported catalyst precipitated in the presence of the low area diatomaceous support develops a small pore structure of much greater area.

UNSUPPORTED CATALYST

The nitrogen and stearic acid areas of an unsupported catalyst, U,[4] are, respectively, 91 and 93 sq.m per g (ignited weight). This good agreement indicates that the large stearic acid molecules reach all the surface available to the smaller nitrogen molecules and that the particles

are effectively non-porous. With the great majority of similar materials studied in the range of this and higher areas the nitrogen values are greater than the stearic acid values by a factor of two or more. Furthermore the nitrogen adsorption-desorption isotherm for catalyst U in the 0.4 to 0.6 relative pressure region does not show the hysteresis effect characteristic of the high area supported catalyst and generally attributed to small pores.[5] Finally the small non-porous particle size required for an area of 91 sq.m per g is qualitatively confirmed by the extremely slow sedimentation rate in benzene observed in the stearic acid experiments. Relatively large pores are, of course, not excluded by the above observations.

CATALYST SUPPORTED ON DIATOMACEOUS EARTH

The nitrogen and stearic acid areas of the catalyst supported on diatomaceous earth, H−G,[4] are, respectively, 270 and 46 sq.m per g (ignited weight), or expressed more significantly as area per gram of catalyst material, approximately 516 and 90 sq. m per g (see Table I). The increase in nitrogen area over that of the unsupported material is more than fivefold. Since the larger stearic acid molecules are adsorbed to the same extent as on the unsupported catalyst they evidently reach practically none of the internal surface of the high area supported material. The development of fine pore structure in the supported catalyst is also demonstrated by the marked adsorption-desorption hysteresis effect observed with nitrogen in the 0.4 to 0.5 relative pressure region.[5]

TABLE I. Nitrogen and stearic acid adsorption by supported and unsupported catalysts.

	Area, sq.m/g		Nitrogen hysteresis (0.4 to 0.6 relative pressure)
	Nitrogen (BET)	Stearic acid	
U (unsupported)	91 (91)*	93 (93)	None
H−G (on diatomaceous earth)	270 (516)	46 (90)	Marked
T (on titanium dioxide)	72 (134)	45 (82)	None

* Values in parentheses are areas per gram of *catalyst material*. Catalyst material constitutes approximately fifty percent by weight of the supported samples. In computing these values the maximum possible contribution of the support is subtracted (although a considerable portion of the support surface is undoubtedly covered). The nitrogen and stearic acid areas of the diatomaceous earth are, respectively, 23 and 2 sq.m/g and for the titanium dioxide, 10 and 8 sq.m/g.

CATALYST SUPPORTED ON TITANIUM DIOXIDE

In sharp contrast to the results obtained with a diatomaceous earth support are those found for the same catalyst supported on non-porous titanium dioxide. The nitrogen and stearic areas of this supported catalyst, T,[4] are, respectively, 72 and 45 sq. m per g or 134 and 82 sq. m per g of catalyst material. No hysteresis is observed in the 0.4 to 0.6 relative pressure region of the nitrogen isotherm. Evidently the non-porous titanium dioxide support does not produce the high area fine pore structure obtained with the diatomaceous earth.

[1] Ries, Van Nordstrand, and Teter, Ind. Eng. Chem. **37**, 310 (1945).
[2] Brunauer, Emmett, and Teller, J. Am. Chem. Soc. **60**, 309 (1938).
[3] Harkins and Gans, J. Phys. Chem. **36**, 86 (1932).
[4] The unsupported catalyst, U, was prepared by the reation between sodium carbonate and a salt of a heavy metal whose oxide is readily reducible. The precipitation of the supported catalyst, H−G, was similarly performed in the presence of suspended diatomaceous earth. In the preparation of catalyst T, titanium dioxide was substituted for the diatomaceous earth. All catalysts were calcined at 350°C for two hours. Catalyst material constitutes approximately fifty percent by weight of the supported samples. The catalysts were prepared by Dr. Olson of these laboratories.
[5] Ries, Van Nordstrand, Johnson, and Bauermeister, J. Am. Chem. Soc. **67**, 1242 (1945).

The Interpretation of Pressure Dependence of Accommodation Coefficients

JOHN L. MORRISON
Department of Chemistry, University of Alberta, Edmonton, Alberta, Canada
June 24, 1946

IN a recent paper, Amdur[1] interprets the pressure dependence of the accommodation coefficients of several gases on platinum. He attributes the pressure dependence to simple Langmuir adsorption of the same gas as that of which the accommodation coefficient is being measured.

Probably this interpretation is the correct one for the gases H_2, D_2, N_2, CO, and O_2. However an alternative interpretation is possible for the inert gases He, Ne, A, Kr, and Xe.

In the paper giving the experimental results, Amdur, Jones, and Pearlman[2] report using neon of 99.9 percent purity. Thus in 0.1-mm pressure neon, there is impurity of 10^{-4}-mm pressure.

Morrison and Roberts,[3] using accommodation coefficient measurements, found that a clean tungsten surface adsorbs oxygen at pressures as low as 10^{-9} mm and becomes completely covered with molecular oxygen at a pressure of about 10^{-5} mm, always in the presence of neon at 0.1-mm pressure. Moreover, Roberts[4] found that clean tungsten adsorbs a saturated film of hydrogen at 4×10^{-4}-mm pressure in the presence of neon at 0.07-mm pressure.

Since the amount of impurity in each of Amdur's inert gases is directly proportional to the pressure of the inert gas, the adsorption of this impurity could account for the fitting of the Langmuir isotherm.

[1] I. Amdur, J. Chem. Phys. **14**, 339 (1946).
[2] I. Amdur, M. M. Jones, and H. Pearlman, J. Chem. Phys. **12**, 159 (1944).
[3] J. L. Morrison and J. K. Roberts, Proc. Roy. Soc. **A173**, 1 (1939).
[4] J. K. Roberts, Proc. Roy. Soc. **A152**, 445 (1935).